Concentration and Recovery of Rare Earth Elements from Eastern US Coal Refuse

Brendan Lloyd MacCormac

Thesis submitted to the faculty of the Virginia Polytechnic Institute and State University in partial fulfillment of the requirements for the degree of

Master of Science
In
Mining Engineering

Aaron Noble, Chair
Roe-Hoan Yoon
Gerald H. Luttrell

October 2nd 2020
Blacksburg, Virginia

Keywords: (Rare Earth Elements, Coal, Ion Exchange)

Concentration and Recovery of Rare Earth Elements from Eastern US Coal Refuse

Brendan Lloyd MacCormac

Academic Abstract

Recent studies funded by the US Department of energy have shown that coal and coal byproducts contain elevated contents of Rare Earth Elements (REEs), making them a potential resource for these critical materials. The approach employed in this research focused on the concentration and extraction of REEs from fine coal refuse derived from various preparation plants in the Appalachian coal basin of the United States.

Initial efforts in this research focused on the identification and characterization of REEs in various fine coal refuse streams from nine distinct industrial preparation plants in Appalachia. The average REE content in these materials was determined to be approximately 200 ppm, but the REE content showed a strong correlation to the aluminum content, suggesting that the REEs are closely associated with the clay minerals present in the refuse.

Given the relatively low REE concentrations, initial efforts sought to concentrate the REEs through decarbonization and dispersive liberation steps. In these tests, high-shear agitation in the presence of a polyelectrolyte, followed by sedimentation was able to isolate the REE-enriched fine clay particles from siliceous gangue minerals. Following the dispersive liberation step, all samples were found to have an REE content greater than 300 ppm, a benchmark used for many initial exploratory studies. In one case, the REE content was increased by more than 125%.

Subsequent extraction tests initially utilized a direct ion-exchange leaching approach with ammonium sulfate as lixiviant. In all cases, the simple ion-exchange leaching process failed to recover significant quantities of rare earth elements, ultimately suggesting that the REEs in fine coal waste may be passivated or bound in a colloidal phase. The approach that showed the most promise was strong alkaline pretreatment, followed by ion-exchange leaching with ammonium sulfate at pH 4. A combination of strong alkali and high-temperatures treatment successfully liberated the REEs, converting them to a form amenable to ion-exchange leaching. The highest REE recovery achieved with this method was determined to be 39%.

Lastly, bench-scale solvent extraction tests were used to further concentrate REEs in the leach solution and demonstrate that mixed rare earth concentrates can be successfully produced from fine coal refuse.

Concentration and Recovery of Rare Earth Elements from Eastern US Coal Refuse

Brendan Lloyd MacCormac

General Audience Abstract

Since the introduction of personal electronics, rare earth elements (REEs) have become essential raw materials for modern life. They are used in many common household goods such as cell phones, computers, and flat screen TVs. They are also vital components in various industrial, medical, and military applications. Currently, the majority of the world's supply is obtained from China, which has raised concerns on the vulnerability of the supply chain and the potential impacts of supply disruption on clean energy technologies. In light of this risk, the US Department of Energy has classified a number of REEs as critical elements and has subsequently funded research to investigate ways to diversify the supply chain through alternative resources.

The approach employed in this research seeks to extract and recover REEs from fine coal refuse. This industrial waste is a byproduct of the coal mining and beneficiation processes, which produce between 70 to 90 million tons a year (National Research Council (U.S.). Committee on Coal Waste Impoundments., 2002). By valorizing this waste material through REE recovery, mining companies will be incentivized to reprocess existing impoundments, ultimately promoting superior economic and environmental outcomes.

Despite their name, rare earths are not "rare" from the standpoint of raw abundance; however, their scarcity is derived from the complexity of the extraction and separation processes. In China, the majority of the heavy rare earth elements are produced from ion-exchangeable clays. These clays have REEs weakly attached to the surface, so that they can be readily recovered by washing them with a salt solution that remove the positively charged rare earth ions from surface. The technical approach employed in this project sought to replicate this process for the clay materials found in fine coal refuse. Additional steps were needed to properly concentrate, activate, and extract the REEs; however, the end-to-end processing tests confirmed that mixed rare earth concentrates can be produced from fine coal wastes consisting primarily clay minerals.

Acknowledgements

Firstly, I wish to thank God, my lord and savior Jesus Christ, and the Holy Spirit from whom I have drawn strength and inspiration to complete this work. I want to thank my family especially my parents for their efforts to instill in me the value of diligence, and the importance of education. I also wish to thank my loving and beautiful wife, Rebecca, for her unending support and encouragement when I thought the challenges were too great.

I also must thank my research advisor Dr. Aaron Noble who provided much guidance as to the direction of my work and provided help when I became discouraged. I also cannot overstate the contributions of Dr. Roe Hoan Yoon who could always find a new direction whenever it appeared the challenges were too great. Dr. Gerald Luttrell always provided clarity whenever my research would begin to drift off course. Finally, I thank Jonathan Angle, Mcalister Council-Troche, and Wesley Edge for their friendship and instrumental aid in my research.

This material is based upon work supported by the Department of Energy under Award Number DE-FE0031523.

Contents

Academic Abstract ii
General Audience Abstract iii
Acknowledgements iv
List of Figures vii
List of Tables ix
Chapter 1. Introduction 1
1.1. Background 1
1.2. Literature Review 4
1.2.1. Recovery of Rare Earth Elements from Mineral Resources 4
1.2.2. Recovery of Rare Earth Elements from Ion Adsorption Clays 7
1.2.3. Summary 15
1.3. Research Motivation and Objectives 16
1.4. Document Organization 16
Chapter 2. Sample Characterization and Techno-Economic Benchmarking 17
2.1 Introduction and Scope 17
2.2 Sample Identification and Sampling 17
2.3 Sample Characterization 20
2.1.1. Particle Size Analysis 20
2.1.2. Proximate and Sulfur Analysis 21
2.3.1 Release Analysis 22
2.3.2 Rare Earth Element Analysis 23
2.3.3 Major Metal Analysis 26
Chapter 3. Rare Earth Concentration via Dispersive Liberation 29
3.1. Introduction and Scope 29
3.2. Methods and Materials 29
3.3. Results and Discussion 31
3.4. Summary and Conclusions 41
Chapter 4. Rare Earth Extraction via Ion Exchange Leaching 42
4.1. Introduction and Scope 42
4.2. Materials and Methods 42
4.2.1. Materials 42
4.2.2. Leaching Experimental Protocols 44

4.2.3. Solvent Extraction Protocols 49
4.2.4. Data Analysis 50
4.3. Results and Discussion 50
4.3.1. Exploratory Tests 50
4.3.2. Kinetics Tests 53
4.3.3. Leaching Additives 57
4.3.4. Gas Purging 59
4.3.5. Chemical Pretreatment 63
4.3.6. Alkaline Pretreatment 64
4.3.7. Solvent Extraction 66
4.4. Summary and Conclusions 69
Chapter 5. Summary and Conclusions 70
5.1. Summary 70
5.2. Conclusions 71
5.3. Recommendations for future work 72
References 73

List of Figures

Figure 1. Structure of the edges of kaolinite crystals and the effects of pH on the charge after (Meunier, 2005) 8
Figure 2. Potential incorporation mechanisms for REEs on clay particles after Vobenkaul et al, 2015. 9
Figure 3. Comparison between Aluminum and REE content of coal from the USGS CoalQual Database samples after Bryan et al., 2015 14
Figure 4. Heap leach of REEs integrated with coal processing flowsheet after Honaker et al. 2018. 15
Figure 5. Process used to prepare coarse BLAM samples for study 18
Figure 6. BLAM sample particle size distributions. 20
Figure 7. Particle size distribution for various thickener underflow samples. 20
Figure 8. Denver D12 lab flotation cell. 22
Figure 9. Release analysis curves for all field samples. 22
Figure 10. Relationship between total REE and ash for both the current data set (red points) as well as data from a prior study that surveyed more than 20 preparation plants in the NAPP and CAPP coal basins (grey points) 24
Figure 11. Thermo Scientific Niton XL2 GOLDD in analysis cradle 26
Figure 12. Trendlines and coefficients of determination for the relationship between TREE content and the aluminum and silicon. 28
Figure 13. Dispersive liberation test results, left photograph is from initial feed solutions, right photograph is after 100 hours of settling. Treated material was mixed for 30 minutes with 10 lb/ton sodium silicate. 30
Figure 14. REE content (ash basis) in LWTUF before (67.15% ash) and after blunging (89.0% ash), as determined by lithium metaborate fusion. 31
Figure 15. LWTUF XRD spectra before and after dispersive liberation 32
Figure 16. SEM election backscatter images of lanthanide phosphate particles in dispersed LWTUF 34
Figure 17. EDS spectra comparison of the REE bearing particle pictured in Figure 16a (blue spectra) and the nearby clay particle (yellow spectra) 34
Figure 18. Major component elements of the two REE bearing particles shown in Figure 16 35
Figure 19. Mass balance of decarbonization and blunging process as performed on LTUF. 35
Figure 20. Relationship between Al (left panel) and Fe (right panel) content to REE content of decarbonization and blunging process product streams. 36
Figure 21. Size distribution data for LTUF as received, compared with both blunging products. 36
Figure 22. Relative enrichment of elements in blunged LTUF vs unblunged LTUF 37
Figure 23. REE distribution differences between CREC and LWTUF 39
Figure 24. Major elements in CREC sample. 39
Figure 25. XRD analysis results comparing CREC to a blunged LWTUF sample 40
Figure 26. Gas purge reductive ion exchange apparatus in operation. 46
Figure 27. (left) Branson sonicating bath, (right) Yamato Shaker table with rack. 48
Figure 28. Ion exchange leaching results for all particle sizes (-325 mesh, -80 mesh, -10 microns) and lixiviant doses (0.01 to 1M) categorized by lixiviant type. Sample: BLAM, leaching time: 1 hour, acid dose: 0.3mL of 2% by volume sulfuric. 52
Figure 29. Element-by-element extraction comparison for various lixiviants and doses. Sample: BLAM, leaching time: 1 hour, acid dose: 0.3 mL of 2% by volume sulfuric. 53

Figure 30. CMBTUF kinetic curve for the average of the 5 tests, the confidence intervals are displayed for each time interval. 54
Figure 31. Kinetic curve for ammonium sulfate ion-exchange for all samples as they were received 55
Figure 32. A comparison of the IX performance for MCMTUF and CMBTUF compared to the primary samples focused on during the earlier stages of the research. 55
Figure 33. A comparison of the REE content of MCMTUF and CMBTUF compared to the primary samples focused on during the project. 56
Figure 34. Molar ratio in solution assays taken from kinetic study on LWTUF, all results normalized to the concentration at 5 minutes. 59
Figure 35. Comparison between AS 0.5M ion exchange at pH 4 and the two stage acetate and SHMP leaching. Note the Y-axis is in PPM not percent recovery. 63
Figure 36. Differences in selected contaminants between AS and the two stage leaching process. 64
Figure 37. TREE extracted into the pregnant leach liquor solution (PLS, orange) over time after alkali pretreatment. 65
Figure 38. Total aluminum extracted during heated KOH and NaOH pretreatment tests. LWTUF sample. 65
Figure 39. Elemental breakdown of ion-exchangeable fractions extracted from LWTUF based on the lithium meta-borate fusion feed assay. 66
Figure 40. Solvent extraction process flowsheet 67
Figure 41. Element-by-element enrichment ratio of REEs for solvent extraction of BLAM leachate. 0.6M DEHPA and 0.4M TBP in kerosene. O:A = 1:1 extraction, 1:1 scrubbing with 1.0M HNO3, 20:1 stripping with 0.6M HNO3. 68
Figure 42. Element-by-element enrichment ratio of REEs for solvent extraction of BLAM leachate. 0.6M DEHPA and 0.4M TBP in kerosene. O:A = 1:1 extraction, 1:1 scrubbing with 1.0M HNO3, 20:1 stripping with 0.6M HNO3. 68

List of Tables

Table 1. Properties of rare earth elements and crustal abundance after Van Gosen, 2017 1
Table 2. Major global producers of rare earth oxides after Gamboji 2020. 2
Table 3. Ionic radius of select rare earth ions and common IX cations. 11
Table 4. Clay-rich samples acquired for analysis 17
Table 5. Proximate analysis and sulfur content results for selected samples. Note that a single BLAM sample was submitted. 21
Table 6 Rare earth content as determined by ICP-MS 25
Table 7. Major sample constituents determined by XRF 27
Table 8. Summary Results on Impact of Decarbonization and Blunging Process to REE Concentration. 38
Table 9. Leaching test summary 42
Table 10. Reagent abbreviations 43
Table 11. Experimental Parameters for Initial Ion Exchange Leaching Tests 51
Table 12. Summarized Extraction Data from Ion Exchange Leaching Tests 51
Table 13. Test series summary for organic acid combinations and reducing agents and their leaching performance on LWTUF, the best extractions from each series is highlighted. 58
Table 14. Extraction tests with decanted blunged LTUF pellets 61
Table 15. Extraction tests with blunged LTUF slurry 62
Table 16. Extraction tests with decanted blunged LTUF pellets 62
Table 17. Second stage extraction tests with decanted blunged LTUF pellets 62

Chapter 1. Introduction

1.1. Background

Rare Earth Elements (REEs) were discovered centuries ago but have become vital components in many modern electronics. Given their paramount importance in clean energy and defense applications, the supply of these elements has become a topic of national and global concern. The first rare earth mineral was discovered in 1787 by Carl Arrhenius in Ytterby, Sweden, and the final element of the series, promethium, was isolated in 1947 (Gupta & Krishnamurthy, 1992). The lanthanum to lutetium series exhibits a trend whereby the ionic radius decreases as the atomic mass increases. The phenomenon is referred to as the *lanthanide contraction* and is the result of the unique properties of the 4*f* orbitals, which reduce the size of the electron shell as the orbitals fill (Housecroft & Sharpe, 2012). Though there are properties in common between all REEs such as oxidation states and electron configurations, they are often divided into light and heavy classifications based on their relative position on the periodic table (Table 1).

Table 1. Properties of rare earth elements and crustal abundance after Van Gosen, 2017

Element	Symbol	Atomic number	Atomic radius	Crustal abundance
Light REEs				
Lanthanum	La	57	116	39
Cerium	Ce	58	114	66.5
Praseodymium	Pr	59	113	9.2
Neodymium	Nd	60	111	41.5
Samarium	Sm	62	108	7.05
Europium	Eu	63	107	2
Gadolinium	Gd	64	105	6.2
Heavy REEs				
Terbium	Tb	65	104	1.2
Dysprosium	Dy	66	103	5.2
Holmium	Ho	67	102	1.3
Erbium	Er	68	100	3.5
Thulium	Tm	69	99	0.52
Ytterbium	Yb	70	99	3.2
Lutetium	Lu	71	98	0.8
Yttrium	Y	39	93	33

Though called “rare” many of the LREEs have relatively high crustal abundances, for example, cerium is roughly as common as copper. The reason for the nomenclature is the paucity of economically viable ores. As of 2020 there were approximately 120 million tons of global REE reserves (Table 2).

Table 2. Major global producers of rare earth oxides after Gamboji 2020.

	Mine Production		
	2018	2019	Reserves
United States	18,000	26,000	1,400,000
Australia	21,000	21,000	3,300,000
Burma	19,000	22,000	NA
China	120,000	132,000	44,000,000
India	2,900	3,000	6,900,000
Madagascar	2,000	2,000	NA
Russia	2,700	2,700	12,000,000
Other countries	3,700	4,300	48,320,000
Total	189,000	213,000	115,920,000

In the last two decades, the phrase “rare earth elements” has become a common sight in popular press headlines usually accompanied by discussions of supply chain vulnerabilities. REEs have many vital high technology applications. Many emerging green technologies rely on rare earth elements for batteries, magnets, and advanced light weight alloys (Long et al., 2012). For example, according to Alonso et al the permanent magnet generators contained in wind energy turbines require significant quantities of Nd and Dy for the large high-strength permanent magnets necessary for their operation. In addition, many other REEs have found occasional use in high strength magnet development including holmium, which is the most magnetic naturally occurring element. yttrium is particularly versatile and has a myriad of useful applications from strengthening aluminum alloys, to anti-cancer drugs, LED phosphors, laser crystals, and even superconductors. Scandium is extensively used in exotic aerospace aluminum alloys as it provides the greatest strengthening effect per percent mass and greatly improves weldability. Despite being one of the costliest of the REEs, scandium has seen use in the scandium-aluminum alloy frames of mass-produced aircraft such as the Russian Mig-29. As these emerging technologies mature and are more widely adopted, the demand for these critical elements will continue to increase (Alonso et al., 2012). Rare earth elements also have uses in more traditional but vital industrial sectors, specifically in petroleum where rare earth oxides are used in fluid cracking catalysts, which break down heavy oils to create lighter products (Akah, 2017). The

addition of rare earths to these catalysts increases their resilience to destruction by certain metals, such as vanadium (Gallezot et al., 1989). Though all REEs have important applications, only a few REEs (Y, Nd, Eu, Tb, Dy) were identified by the US Department of Energy as critical based on future projections and recommendations were made to diversify suppliers as the majority originate from a single polity (Bauer et al., 2011).

The rare earth minerals make up the majority of the rare earth bearing ores in the world. Monazite and xenotime are both examples of REE-phosphate minerals while bastnäesite is the most common REE bearing fluoro-carbonate. Monazite and bastnäesite primarily contain LREEs while xenotime is predominantly a source of yttrium and HREEs (Pradip & Fuerstenau, 1991). Currently, the majority of the world's rare earth elements demands are met by the People's Republic of China, which produces the majority as a coproduct from the massive Bayan Obo iron deposit (Drew et al., 1990). This deposit is considered the largest rare earth minerals deposit in the world containing reserves in excess of 48 million tons of rare earth minerals (Drew et al., 1990). Another lucrative source of REEs in China is the laterite ion-exchangeable clays or (IX-clays). While these materials are low in overall REE concentration, they are highly enriched in HREEs and Yttrium and benefit from amenability to a simple extraction process.

The laterite IX-clays are the product of intense weathering of granite plutons (Bao & Zhao, 2008; Hu et al., 2017; Xiao et al., 2015). The clay resulting from this weathering process has a negatively charged basal surface caused by isomorphic substitution within the alumino-silicate matrix (Meunier, 2005). The negative surface charge attracts cations to the surface, particularly the REEs with a high charge density caused by the lanthanide contraction. This geochemical configuration leads to the selective enrichment of weakly bonded HREEs creating ideal conditions for relatively inexpensive ion-exchange methods to achieve high extraction efficiencies. The high extraction efficiency of Chinese IX-clay mining methods allows for the exploitation of resources with concentrations of REEs as low as 0.05% (G. A. Moldoveanu & Papangelakis, 2016).

The advantageous economics of these IX-clay resources led to China supplying 95% of the world's rare earth oxide (REO) demand in the last decade (Bauer et al., 2011). This monopolistic supply for a resource so critical for the modern world is worrying due to the potential for disruption due to natural disasters, political unrest, or geopolitical reasons. Previously, China has implemented an export quota on REOs leading to a 1500% increase in

prices (Hatch, 2012). Another concern is the relative opacity of the rare earth metals market when compared to more traditional metals that are openly traded. The majority of rare earth metal trades are conducted through bilateral contracts at negotiated rates, this lack of transparency has resulted in disruptively volatile prices (Bauer et al., 2011). The volatility of REE valuation is a major issue as it incurs significant risk to developing new REE mining projects. This economic risk is especially great with new rare earth mineral type deposits that necessitate extensive up-front capital expenditure in comminution and acid leaching or alkaline cracking circuits. The vulnerability of the REE supply and the high risk involved in developing new mineral deposits has led to a push to explore alternative REE sources and a revisiting of old deposits that have already been developed. For example, the Mountain Pass mine, a significant supplier of REEs during the last century has been reactivated in 2018 and is responsible for the increasing US production since then (Gambogi, 2018, 2020). Unfortunately, Mountain Pass, like many other known potential resources, is a bastnäesite deposit that contains high levels of low value cerium and lanthanum, but little in the way of critical and HREEs (Seredin & Dai, 2012). The lack of critical REEs in traditional rare earth mineral (REM) deposits has led to increased funding in investigations of alternative sources that are rich in HREEs such as those located in coal byproducts and coal combustion ash.

The coal byproducts, especially waste products, are of particular interest due to their already reduced particle size and increased concentration caused by the coal cleaning process. Additionally, the presence of significant tonnages of coal associated waste products in impoundments throughout the US could present future sources of REEs if they can be recovered.

1.2. Literature Review

1.2.1. *Recovery of Rare Earth Elements from Mineral Resources*

As mentioned above, the major traditional rare earth mineral resources in the world are the Chinese Bayan Obo complex, US-based Mountain Pass mine, and Mount Weld in Australia. The mine sites require extensive processing circuits to recover the valuable REEs contained within the ores. To illustrate the intricacies of processing two different types of rare earth minerals, overviews of the Bayan Obo and Mountain Pass mines are described below.

The Bayan Obo ore body is a unique mixture of approximately 170 different minerals including: fluorite, hematite, magnetite, tantalo-niobates, rare earth carbonates and phosphates

(Chang, 1995). The complex geology of this ore body requires a variety of flotation techniques to isolate each salable product. Gupta and Krishnamurthy provide a detailed description of the methods used process the ore mined from Bayan Obo. Per their work the ore is mined using a traditional drill blast load haul cycle and the blasted ore is crushed to 90% passing 74 μm**.** The crushed ore is then subjected to flotation with tall oil and a sodium silicate depressant to isolate the iron bearing minerals, niobium oxides, and silicates into the tailing stream for additional processing. To affect a more selective flotation, the tall oil is removed by use of a de-sliming thickener designed to remove particles under 5 μm. The following flotation step uses sodium silicate and sodium fluorosilicate to depress the barite, calcite, and fluorite in the slurry while a hydroxamic acid collector is used to float the rare earth minerals. The pH for this flotation is controlled by sodium carbonate to a range of 5-6. After this roughing stage either a cleaning stage is performed or high intensity magnetic separation, which result in a bastnäesite and monazite concentrate with a total recovery of 61% at a grade of 68% and 36% rare earth oxide (REO) respectively (Gupta & Krishnamurthy, 1992).

The flowsheet by Gupta and Krishnamurty further describes the chemical processes used to produce a salable product. These chemical processes for extracting REEs from monazite are energy intensive and are performed in industry either by acid treatment or alkali cracking. Acid treatment begins with the dissolution of the monazite concentrate in concentrated sulfuric acid at over 200°C and is followed by one of three techniques: stepwise neutralization, double sulfate precipitation, and sodium oxalate precipitation. Alkali cracking uses 70% sodium hydroxide solution at 140°C to displace the phosphate associated with the heavy metals and REEs. The slurry is filtered and the solution is evaporated to create tri-sodium phosphate as a marketable byproduct. The solid residue is then dissolved using strong mineral acids then the thorium and REE laden PLS is processed similarly to the acid treatment products. Thorium is both difficult to separate from REEs in the PLS and hazardous to dispose of. Fortunately, the geology of the Bayan Obo deposit is such that the thorium content of the monazite is only 0.26%. Both the caustic and acid treatments require the neutralization followed by re-acidification of the PLS and all methods but double sulfate precipitation make use of solvent extraction (Gupta & Krishnamurthy, 1992; Houot et al., 1991). Double sulfate precipitation requires sulfuric acid and sodium sulfate salts to precipitate alkali metals and is commonly used in recycling of NiMH batteries to recover cobalt, nickel, and to a more limited extent LREEs.

Gupta and Krishnamurthy also detail the processes used at Mountain Pass which has a number of differences from the Bayan Obo mine. Mountain Pass mine contains a high grade bastnäesite (7% REE) ore that similarly to the Bayan Obo deposit is mined using the traditional drill blast load haul method in an open pit configuration. The mined ore is ground to 80% passing 150 μm and is preconditioned in 6 stages with high temperature steam at each stage combined with the incremental addition of first sodium carbonate for pH control and fluorosilicate, second ammonium lignin sulfonate, and finally tall oil. The conditioned ore is then sent as a 35% solids slurry to a flotation circuit consisting of one rougher stage and 4 cleaner stages. The first stage cleaner tailings are rerouted to a scavenger stage and the scavenger concentrate is reground and mixed with the feed to the rougher. The concentrate from the flotation circuit is 60% REO with a recovery of approximately 70%. This concentrate is leached at a pH of 1 filtered, dried, and calcined to produce an up to 90% REO product for REE separation (Gupta & Krishnamurthy, 1992; Houot et al., 1991).

Solvent extraction (SX) is a technique used to fractionate the different rare earths and major contaminants into different product streams. SX uses an acidic aqueous phase and an organic phase to separate the rare earths between the two based on their tendency to form complexes with the extractant dissolved in the organic phase versus the solubility of the rare earths in the aqueous phase (Gupta & Krishnamurthy, 1992). The major advantage of this process is the ability to separate individual elements based on their affinity with the aqueous phase vs organic phase and the ability to process feed solutions with very high concentrations of ions. The extractants are often too viscous and are dissolved in a diluent, the most effective diluent has been found to be kerosene. Some of the commonly used phosphorus based extractants are D2EHPA for chloride or nitrate based aqueous systems, TBP for nitrate, EHEHPA for sulfate or chloride (Gupta & Krishnamurthy, 1992; Kao et al., 2006; Kumari et al., 2015; Xie et al., 2014). Many additional extractants exist that are under trade names, which use amines as the functional group for complexing with the REE bearing ions. The most common is TBP and the mechanism for REE extraction from a nitric solution is shown in the equation below (Preston et al., 1996):

$$[RE^{3+}]_{aq} + [3(HA)_2]_{org} \rightarrow [RE(A)_3(HA)_3]_{org} + 3[H^+]_{aq}$$

According to Gupta and Krishnamurthy there are many variations in SX-based on the feed and the required product but the most common steps are extraction, scrubbing, stripping, and saponification. Each stage is typically defined by the organic to aqueous ratio (O:A) and the pH or molarity of the acid. Specific ratios, acid strengths and other engineering details are difficult to find in open literature. But the general trend through the course of an SX circuit is an increasing O:A ratio and increasing acid molarity. The purpose of the extraction phase is to recover as many of the REE ions as possible into the organic phase. For recovery to occur the acidity of the aqueous phase will be low relative to later stages that will cause the majority of the cations in solution to form complexes with the extractant in the organic phase. The scrubbing phase is used to remove the impurities that were in the initial feed. To do this the organic is mixed with an aqueous phase of higher acidity than the extraction aqueous phase. This mixing process will remove cations that have weaker bonds with the extractant and as lanthanides have high charge densities they are preferentially bonded to the phosphate or organic acid group in the extractant. A stripping phase is designed to remove the REEs from the organic phase. This separation stage has a comparatively high O:A ratio and the aqueous phase acid is significantly stronger than the scrubbing stage. These conditions will create an aqueous phase product that is has high concentrations of REE ions. After stripping the organic phase is acid washed and undergoes saponification by a strong alkali to remove any remaining cations and allow reuse of organic phase. This stage is necessary due to the high cost and large volumes of extractant required for large scale solvent extraction operations. Additionally, the aqueous phase from the extraction is often recycled back into leaching operations to improve the water balance and reuse the residual acidity (Gupta & Krishnamurthy, 1992; Xie et al., 2014).

1.2.2. *Recovery of Rare Earth Elements from Ion Adsorption Clays*

While mineral-based deposits supply the majority of light REEs, heavy REEs are found in abundance in ion exchangeable clays, most notably the laterite clay deposits in the Jiangxi province of China. This unique type of deposit has significant economic advantages due to its geology.

The primary constituents of IX-clays are illite and kaolinite (Papangelakis & Moldoveanu, 2014). Both clays are non-expanding phyllosilicates, but kaolinite has a single tetrahedral sheet bonded to an octahedral sheet (1:1) and illite crystals have an octahedral sheet

between two tetrahedral sheets (2:1). According to Meunier These crystal arrangements result in differing modes of aggregation, though both illite and kaolinite form “books” or stacks of crystals, the illite crystals maintain a small cation rich interlayer that kaolinite does not possess. Though both kaolinite and illite are among the lowest cation exchange capacity (CEC) clays they still retain charges on the exposed basal surfaces and edges of the crystals (Meunier, 2005). During the process of forming these minerals, part of the Si^{4+} and Al^{3+} ions in the cross-linked polyhedral are isomorphically substituted by cations of lower formal charges, *e.g.*, Al^{3+} for Si^{4+} and Fe^{2+} for Al^{3+}, causing the basal surfaces of the clay mineral particles to be negatively charged when they are submersed in aqueous media. While the exchangeable sites on the edges of the crystals are from interrupted bonds, these sites are responsible for the anion exchange capacity of the clay mineral (Meunier, 2005). The exchangeable sites on the edge of the crystals are pH dependent where at high pH they sites are neutralized while at acidic pH aluminol and silanol groups are hydrated and behave as Lewis acids (Figure 1).

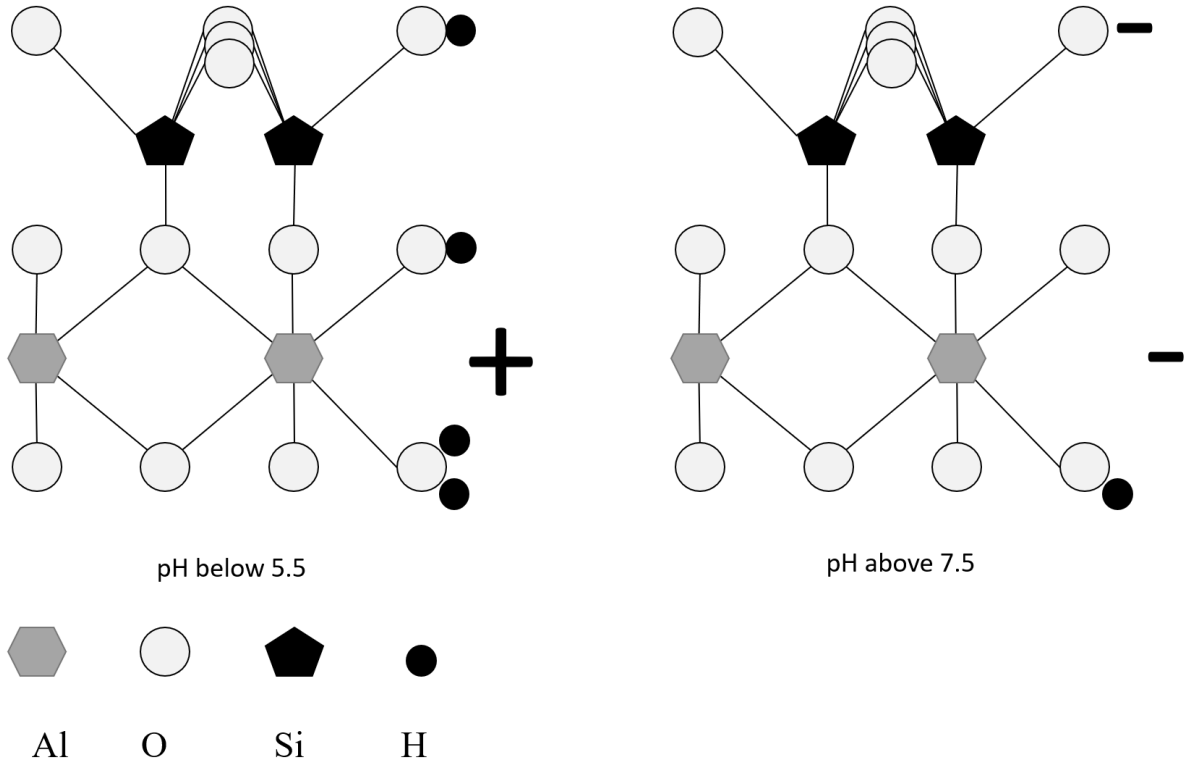

Figure 1. Structure of the edges of kaolinite crystals and the effects of pH on the charge after (Meunier, 2005)

Kaolinite is often the result of weathering of biotite in volcanic ash falls or feldspar in the case of granite (Rebertus et al., 1986). The weathering process for biotite is the result of acidic rainwaters leaching the iron and magnesium, which causes the change in color from black to

grey/white. Alteration of feldspar depends on the form, plagioclase or orthoclase, where one is the result of the acidity while the other forms due to the dissolved carbon dioxide both are provided by rainwater (Bohor & Triplehorn, 1993). The chemical process of orthoclase (Land, 1984) and plagioclase (Siebert et al., 1984) feldspar formation is shown below:

Orthoclase Feldspar

$$2KAlSi_3O_8 + 2CO_2 + 11H_2O = 2K^+ + Al_2Si_2O_5(OH)_4 + 4H_4SiO_4 + 2HCO_3^-$$

Plagioclase Feldspar

$$2NaAlSi_3O_8 \bullet CaAl_2Si_2O_8 + 4H^+ + 2H_2O = 2Al_2Si_2O_5(OH)_4 + 4SiO_2 + 2Na^+ + Ca^{2+}$$

Kaolinite crystals can also be formed from alumino-silicate gels that grow by Ostwald ripening (Steefel & Van Cappellen, 1990).

Ion exchangeable clays, despite what the name implies, contain varying proportions of different phases of rare earth elements (Figure 2). The primary phase is the ion-exchangeable (IX) phase; this phase includes the species what are extractable at mildly acidic conditions with a monovalent salt. Generally, HREEs and yttrium are enriched in this phase as compared to cerium and lanthanum. The REEs presence on clay particles is explained by electrostatic attraction due to the negatively charged basal surfaces of the clay and the positively charged REE ions followed by physisorption (Georgiana A. Moldoveanu & Papangelakis, 2012). Experimental data has shown that LREEs are more preferentially adsorbed to the clay surfaces and are found in higher levels closer to the surface of laterite bodies while HREEs are found in the lower clay layers of southern Chinese IX-clay deposits (Xiao et al., 2016; Yang et al., 2019). These weakly adsorbed REE ions are known as the ion-exchangeable phase, in some cases these ions are so weakly adsorbed that they can be removed by the addition of salt water. These REEs are still present due to the low ionic strength of the groundwater in that region of China (Coppin et

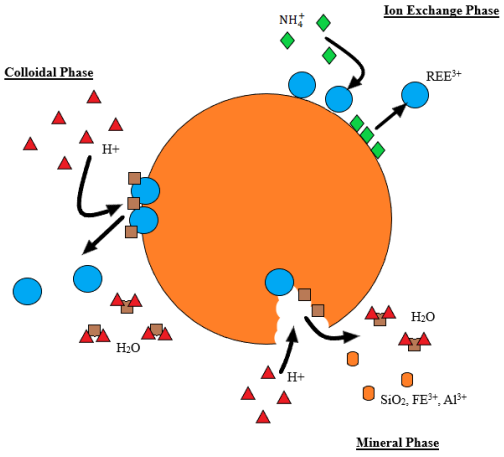

Figure 2. Potential incorporation mechanisms for REEs on clay particles after Vobenkaul et al, 2015.

al., 2002; Harter & Naidu, 2001). The difference in REE fractionation by depth is likely caused by the variations in kaolinite structure and soil pH through the soil column (Yang et al., 2019). Based on data from Malaysian deposits of similar lateritic types the LREE/HREE fractionation is linked to the extent of weathering (Sulaiman, 1991). In some examples of Chinese laterite, significant amounts of the more valuable HREEs are in water soluble/ion-exchangeable form, in some cases as high as 21% of the Dysprosium and 72-90% of the Yttrium (Chi et al., 2005).The colloidal phase is distinct from the ion-exchangeable phase as the rare earth elements are in the form of oxides and hydroxides. The colloidal phase occurs in limited amounts in Chinese examples of IX clays as the natural conditions are too acidic, in clays that exist in more alkaline conditions this phase is more prevalent (G. A. Moldoveanu & Papangelakis, 2016). This phase, though not ion-exchangeable, is leachable under acidic conditions. Additionally, recent work has shown that reducing organic acids can increase the solubility of the limited quantities of colloidal phase present in Chinese rare earth clays (Fuguo et al., 2018). The last major phase of occurrence is the mineral phase that includes REEs substituted into the aluminosilicate matrix of the clays and microscopic rare earth minerals. One mineral positively identified in Chinese IX clays is rhabdophane; a hydrated rare earth phosphate (Chang, 1995).

The kinetics of ion exchange is relatively rapid in batch leaching studies, usually requiring less than 5 minutes to reach equilibrium using monovalent sulfate salts at pH 5 (G. A. Moldoveanu & Papangelakis, 2016). This process is possible due to the high enthalpies of hydration for REE ions that favor partitioning into solution over monovalent cations like ammonium or lithium, which have an order of magnitude lower hydration enthalpies (Table 3).

Table 3. Ionic radius of select rare earth ions and common IX cations.

Cation	Ionic radius (Å)	Hydration Energy (kJ/mol)
La^{3+}	1.06	-3285
Ce^{3+}	1.03	-3340
Pr^{3+}	1.01	-3384
Nd^{3+}	0.99	-3420
Pm^{3+}	0.98	-3445
Sm^{3+}	0.96	-3465
Eu^{3+}	0.95	-3508
Gd^{3+}	0.94	-3522
Tb^{3+}	0.92	-3553
Dy^{3+}	0.91	-3577
Ho^{3+}	0.89	-3621
Er^{3+}	0.88	-3647
Tm^{3+}	0.87	-3668
Yb^{3+}	0.86	-3715
Lu^{3+}	0.85	-3668
Li^{+}	0.68	-520
Na^{+}	0.95	-406
NH_4^{+}	1.48	-322
Cs^{+}	1.69	-276

The enthalpy of hydration or hydration energy is the determining variable for the exchange of physiosorbed ions into the aqueous phase (Teppen & Miller, 2006). The more negative hydration energy of the lanthanides is readily displaced by the less strongly hydrated monovalent cations as demonstrated in the reaction below (Zhang et al., 2015**)**:

$$[Al_2Si_2O_5(OH)_4]_a \cdot bRE^{3+}(s) + 3bNH_4{}^{+}(aq) = [Al_2Si_2O_5(OH)_4]_a \cdot (NH_4^{+})_{3b}(s) + bRE^{3+}(aq)$$

Though the hydration energy for the HREEs is more negative and therefore should be the most easily extracted, the reduced ionic radius due to the lanthanide contraction effect cause these ions to be more strongly adsorbed (Coppin et al., 2002). Additionally, as the atomic number increases in the lanthanide series so too does the propensity of the ion to hydrolyze (Bentouhami et al., 2004). A hydrolyzed ion is considered chemisorbed to the surface and is incapable of being recovered by ion-exchange.

A significant body of research has been produced on the subject of IX rare earths and lanthanide chemistry. Much of the early work in lanthanide separation was a byproduct of the nuclear industry's research into uranium enrichment and expanded from there into practical applications of the techniques used in uranium enrichment to mineral processing. More recently, efforts have been directed towards researching the origin and chemistry of Chinese rare earth

clays due to their high concentrations of HREEs. Previous work on Chinese ion-exchange rare earth clay has focused on: ion selectivity, environmental sensitivity, and optimization (Qiu et al., 2018). A major issue in processing IX pregnant leach solutions is the number of cationic contaminants present. Therefore, lixiviant and pH control are vital to increase the selectivity of the exchange process, as the pH drops below 4 the solubility of aluminum rapidly increases and consumes reagents (Ran et al., 2017; Wang et al., 2017; Yang et al., 2019).

With regard to the environmental effects of IX leaching, the most economically viable lixiviant, ammonium sulfate, is a source of nitrogen pollution, and as much IX extraction is performed in situ in China there is a potential for significant impact on the water quality near mine sites. This combined with efforts by the Chinese government to improve environmental quality has led to investigations into magnesium sulfate and ferrous sulfate as alternative lixiviants (Chen et al., 2018; Fuguo et al., 2018; Xiao et al., 2015). In order to increase the efficiency of the alternative lixiviants, organic acids were used as reducing/complexing agents which had the added benefit of accessing colloidal phase REEs (Shan et al., 2002). Further work was conducted with a variety of organic acids focusing not only on the acid's ability to form complexes with rare-earth ions but also their effect on the surface charge of the clay particles. The results showed that at a mildly acidic pH (3-6), organic acids enhance the extraction of the ion-exchangeable phase of REEs; however, the mechanism was dependent on concentration of the organic acid. At lower concentrations, increases in extraction efficiency were primarily caused by the modification to the zeta potential of the clay induced by the organic acids. Alternatively, the coordination of organic acids with rare-earth ions was the primary contributing factor at high concentrations. In both cases, the kinetics of the IX reaction was increased (Wang et al., 2017). Tests were conducted using several organic acids (tartaric, malic, acetic, and citric); however, citric acid demonstrated the best ability to prevent reabsorption of REE ions to the clay surfaces (Shan et al., 2002).The presence of trace quantities of rare earths in coal and the associated partings and strata is well documented (Dai et al., 2016; Hower et al., 1999, 2016; Ward, 2002). In general, these concentrations were previously considered inconsequential; however, increased demand for REEs and concerns about supply chains have prompted considerable investment in utilization of coal and coal-related waste products as sources of REEs. The origin of these REEs in coal come in a wide variety of forms depending on the geology of each coal basin. Specifically, four different processes have the potential to introduce REEs to coal: surface water

additions (Terrigenous), meteoric groundwater, volcanic ash (tuffaceous), and hydrothermal type processes. These geological phenomena can occur at different stages of coal formation and some coals with elevated levels of REEs have gone through more than one of these processes (Hower et al., 2016; Seredin & Dai, 2012). These alterations lead to different phases of REEs in the seam, the tuffaceous additions come in the form of monazite, zircon, and apatite while meteoric groundwater and hydrothermal processes generate the authigenic carbonates and oxides among others. Frequently, the REE mineralizations of the tuffaceous form are found in "tonsteins" (German for claystone) (Lyons, 1992). Of these different forms, the most prevalent in the high REE coals is the authigenic type mineralization (Seredin & Dai, 2012).

REEs also have an affinity for carboxylic acid groups, these are often found in lower rank coals such as lignite due to the incomplete coalification of the organic matter. The complexes formed by HREEs with the carboxylic acid groups, usually in the form of humic or fulvic acids, are stronger than those formed with LREEs (Laudal et al., 2018).

Investigations into the environmental impacts of the trace elements contained in coal fly ash from power plants has revealed the rare earth content of various coals around the United States (Franus et al., 2015; Hower et al., 2018; Mayfield & Lewis, 2013; Scott et al., 2015). Initial investigations into recovery of these rare earth elements focused on fly ash from coal power plants (King et al., 2018). The more successful of these projects required strong alkaline or oxidizing reagents to break down the vitreous encapsulating material around the rare earth oxides combined with strongly acidic leaching solutions to recover REEs (Taggart et al., 2018). Despite the high concentrations of rare earths contained within the coal fly ash, the aggressive chemical treatments required to efficiently extract them are both expensive and are potential environmental hazards. Therefore, additional work has been done focusing on extracting the rare earths from coal products before their combustion. The identification of rare earth phosphate mineral grains in coal samples that contain fire clay tonsteins in Eastern Kentucky have drawn attention to that region as the REE content of the fly ash produced from this region's coal were reported to have REE contents up to 4000 ppm (Bohor & Triplehorn, 1993; Chehreh Chelgani & Hower, 2018; Hower et al., 2016; Lyons, 1992). This tonstein occurs mostly in western Kentucky but extends into Tennessee, Virginia, and West Virginia as well. This tonstein is characterized by its elevated kaolinite content, between 60-95%, and the documented presence of monazite. Elevated aluminum content in coal samples is also correlated with increased REE

contents indicating a relationship between mineral content and REE content **(**Figure 3**)** (Bryan et al., 2015).

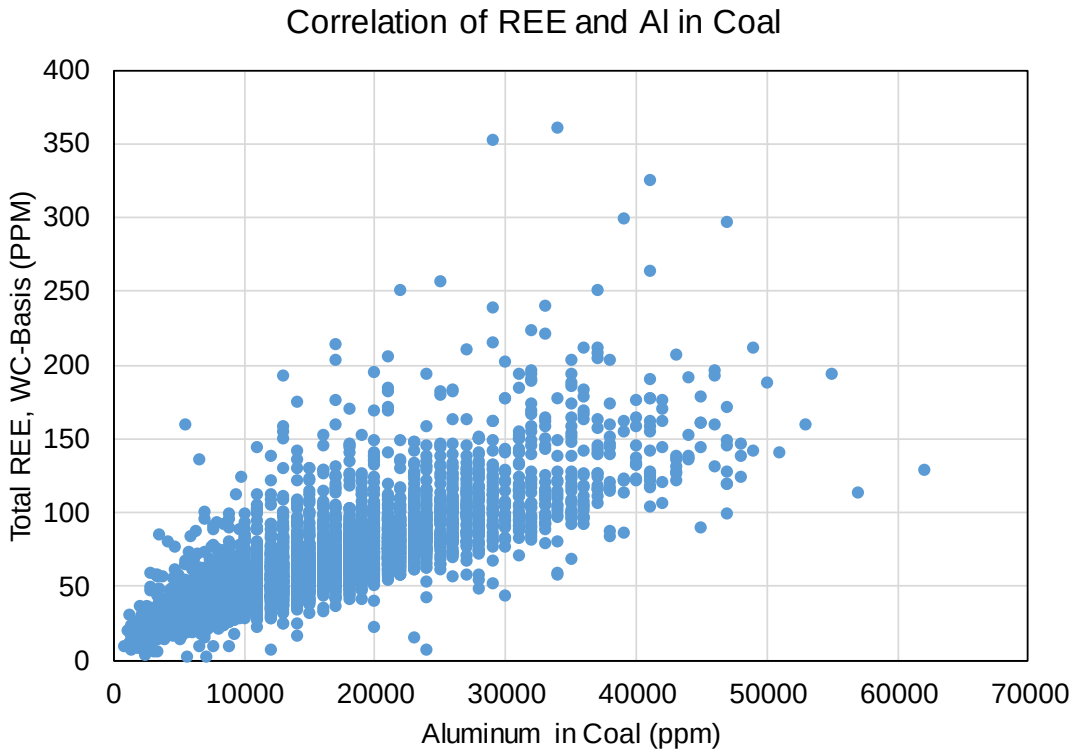

Figure 3. Comparison between Aluminum and REE content of coal from the USGS CoalQual Database samples after Bryan et al., 2015

Based on characterization research done on US coals, recent investigations have focused on processing coarse refuse samples from the REE rich fire clay by testing various surface chemistry based and physical separation techniques (Zhang et al., 2018). One example of a developed processing flowsheet developed uses a heap leach process on coarse refuse produced from conventional physical and chemical separation techniques already in use in coal processing (Figure 4).

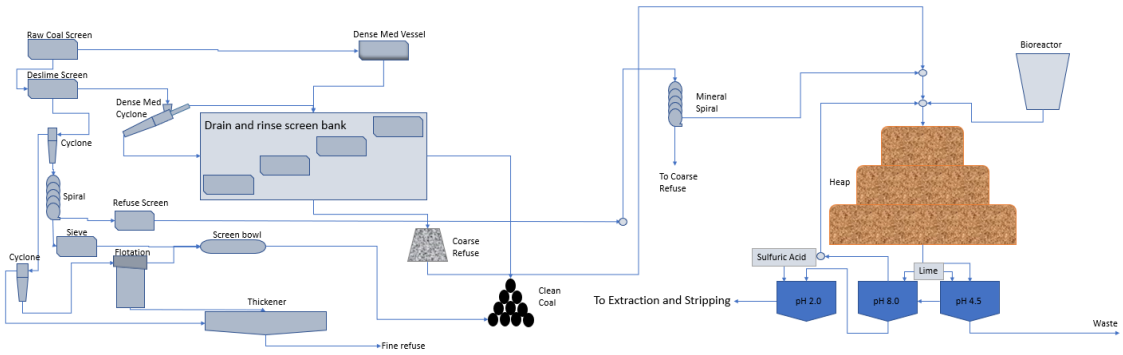

Figure 4. Heap leach of REEs integrated with coal processing flowsheet after Honaker et al. 2018.

As of 2015, multiple sites have been discovered along the Blue Ridge Mountains in Virginia that contain REE rich granite plutons have undergone similar weather processes as the Chinese REE clays (Foley & Ayuso, 2015). Additionally, hydrothermally altered felsic bulk rock in South Carolina has resulted in kaolin deposits that contain up to 400 ppm REEs. These discoveries indicate that the clay minerals bearing REEs are present near the Appalachian Mountains. Therefore, there is potential that weathering of similar felsic igneous plutons could result in coal associated REE deposits. In the hopes that some quantity of the REEs present in coal are associated with the clay minerals, researchers in the US have attempted to adapt Chinese IX techniques for coal associated feed stocks from Pennsylvania in the hopes of replicating their success (Rozelle et al., 2016). Research into coal associated REEs in the United States has not been limited to east coast coals, additional work has been conducted on lower grade coals in the west. The Institute for Energy Studies at the University of North Dakota has successfully extracted organically associated REEs from lignite samples using dilute acids to recover between 80 to 90% from low rank coals.

1.2.3. *Summary*

Given the existing literature on the REE supply chain and alternative sources of REEs, the following summarized conclusions are derived:

- REEs are important to society, but supply is monopolistic and diversification would reduce vulnerability.
- REEs from IX clays are much easier/cheaper to extract than mineral phase REEs
- Coal/byproducts may be a good source, but REE mode of occurrence can vary widely by source.

- Substantial flowsheet development work has been done for coarse refuse, fly ash, and western coals.
- Only limited work has been done to develop a process flowsheet for REE extraction from fine coal refuse which offers much potential due to the already reduced size and presence of clay which may host ion-exchangeable phases of REEs.

1.3. Research Motivation and Objectives

Based on previous work done on coal and coal related waste products, the current investigation will focus on flowsheet development for the recovery of REEs from thickener underflows and coal products with finely disseminated ash. The objectives of the research are twofold:

1. Identify and characterize nature of rare earth elements in fine coal refuse products from Appalachian coal preparation plants.
2. Develop a process to concentrate, extract, and recover these elements while exploiting the unique technical and economic advantages peculiar to REEs derived from fine waste resources.

1.4. Document Organization

The main body of this thesis is organized into 5 major chapters, each signifying a different stage of flowsheet development.

Chapter 1 includes a literature review on the state of the art and explains the objectives and motivation of the research

Chapter 2 presents the identification and characterization of samples and the creation of a basic economic model to create a benchmark for feasibility.

Chapter 3 contains the development of a REE preconcentration and clay isolation technique known as dispersive liberation.

Chapter 4 covers the REE leaching and ion-exchange experiments methods and results.

Chapter 5 summarizes the body of work and provides recommendations for future work.

Chapter 2. Sample Characterization and Techno-Economic Benchmarking

2.1 Introduction and Scope

For the purposes of this investigation into REE recovery from coal byproducts, a selection of samples was made from mine sites from a variety of locations in the eastern US. The samples were characterized in order to determine REE contents and to identify presence of other elements that could be correlated to REE content or amenability to various methods of recovery. In order to determine the feasibility of recovering the REEs from the acquired samples a basic techno-economic analysis was performed to create a benchmark for recovery and lixiviant costs.

2.2 Sample Identification and Sampling

During the course of this investigation 8 samples were acquired and to simplify the organization and labelling sample codes were created for each. The samples are all thickener underflows with the exception being BLAM which is a secondary cyclone product (Table 4). The thickener underflow samples were collected using standard sampling protocols, typically via sampling ports after the thickener pump discharge. All new samples with the exception of LWTUF were collected in 5-gallon buckets, producing a total dry sample weight of approximately 5 kg.

Table 4. Clay-rich samples acquired for analysis

Sample Code	County	State	Date Sampled	Plant Stream
BLAM	Raleigh County	West Virginia	December 2017	Secondary Cyclone Product
LWTUF	Perry County	Kentucky	January 2018	Thickener Underflow
TCATUF	Wise Country	Virginia	March 2018	Thickener Underflow (Plant Blend A)
TCBTUF	Wise Country	Virginia	March 2018	Thickener Underflow (Plant Blend B)
MCPTUF	Dickenson County	Virginia	March 2018	Thickener Underflow (Plant Blend P)
MCMTUF	Dickenson County	Virginia	March 2018	Thickener Underflow (Plant Blend M)
CMBTUF	Green Country	Pennsylvania	March 2018	Thickener Underflow
ALA	Tuscaloosa County	Alabama	June 2018	Thickener Underflow

The secondary cyclone product sample (BLAM) was ground by a combination of jaw, cone, and plate grinding to reduce the size below 80 mesh. Further size reduction was performed by attrition milling for 25 minutes to produce the -325 mesh product and 75 minutes to produce the ultrafine or -10 micron class. The crushing was performed for two purposes: first to reduce the size to be comparable to the thickener underflow samples and secondly to determine at which size liberation of the associated clay mineral matter.

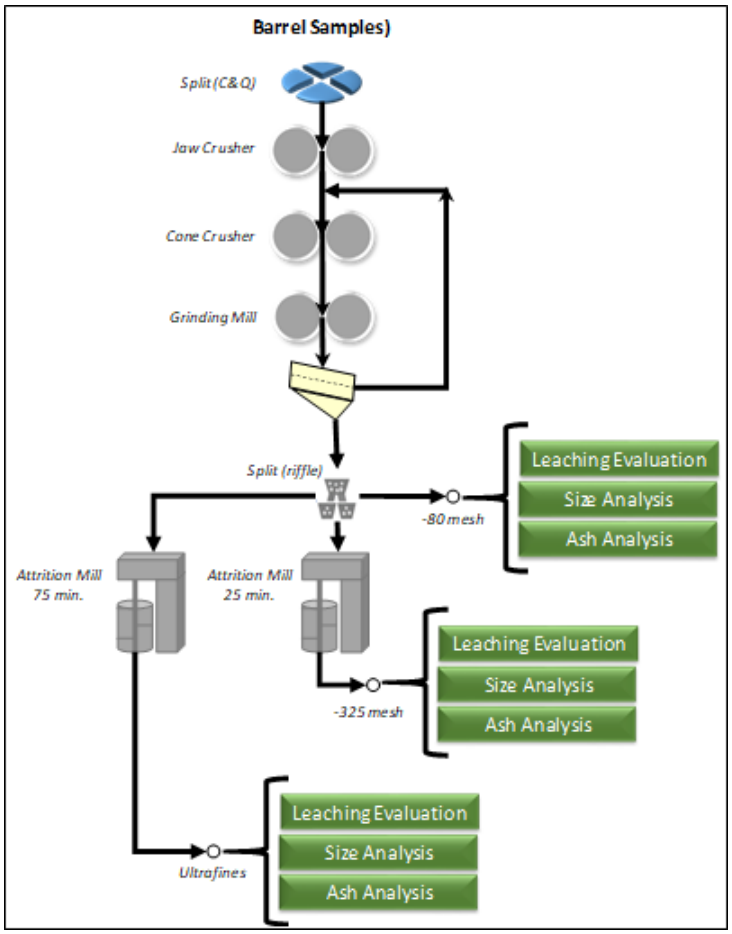

Figure 5. Process used to prepare coarse BLAM samples for study

All thickener samples were initially received wet in 5 gallon buckets with the exception of LWTUF which was received in a barrel. For the 5 gallon buckets, each sample was allowed to settle, decanted, then vacuum filtered, and finally placed in stainless steel pans and dried at 60 degrees Celsius for 18 hours. Barrel samples were split by transferring the slurry to a tank and

vigorously mixing the slurry while pumping it through a centrifugal pump. Splits were taken from the recirculating slurry from the pump outlet and collected into a bucket. After two weeks of drying in an oven at 60 degrees Celsius, the resulting solid material was combined, agitated, and then split in accordance with ASTM D2013M-12.

2.3 Sample Characterization

2.1.1. *Particle Size Analysis*

The particle size distributions were determined using a Microtrac S3500 laser diffraction particle size analyzer. Size measurements were conducted by mixing 1 gram of solids with approximately 100 ml of distilled water and 0.5 ml of Triton-X surfactant to counteract the hydrophobicity of the coal. Data from the particle size analysis is included in Figure 6 and Figure 7.

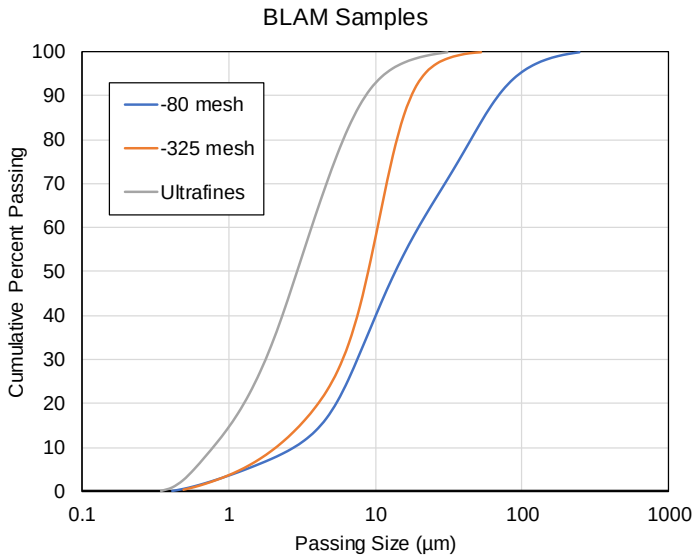

Figure 6. BLAM sample particle size distributions.

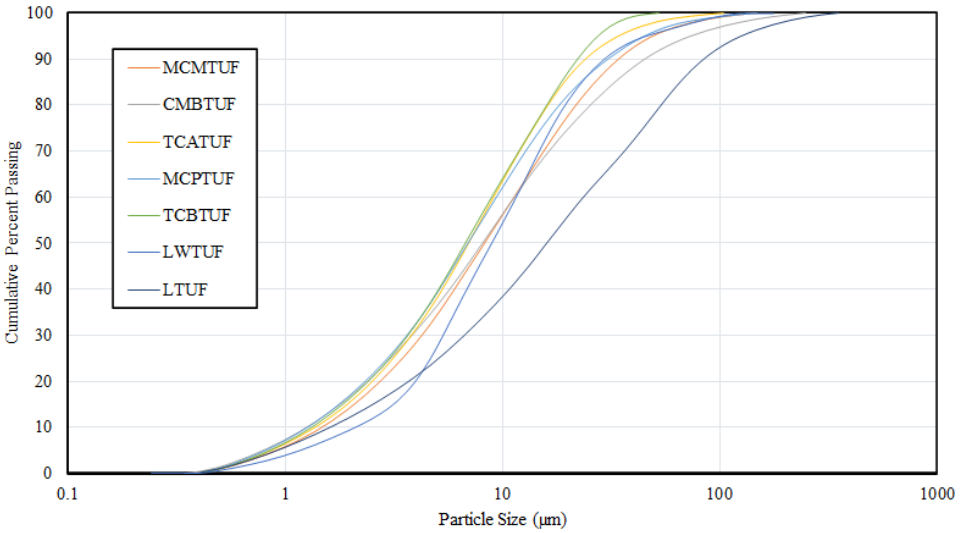

Figure 7. Particle size distribution for various thickener underflow samples.

The various thickener underflows we received have D80s between 18 and 25 microns while the -80 mesh BLAM sample has a D80 of approximately 50 microns as shown in Figure 7. The samples all have top sizes between 50 to 250.

2.1.2. *Proximate and Sulfur Analysis*

For proximate analysis, a LECO TGA701 Thermogravimetric analyzer was used in accordance with ASTM D7582MA to obtain the moisture and ash content. Approximately one gram of sample was used in all cases, and each analysis was repeated on no fewer than three representative splits. The sulfur content of the samples was determined by Precision Testing Laboratory Incorporated, an ISO-9001 compliant laboratory in Beckley, West Virginia. Results from these analyses are shown in Table 5. The thickener underflows contained similar levels of coal with CMBTUF containing the highest proportion of volatile material while MCPTUF contained the least. Additionally, the -325 BLAM sample has a much higher value for moisture than the other BLAM samples, which is surprising as the -10 micron sample has gone through an identical procedure. It appears that the -325 mesh BLAM sample was not allowed to air dry as long as the -10 micron sample after attrition milling.

Table 5. Proximate analysis and sulfur content results for selected samples. Note that a single BLAM sample was submitted.

Sample	Ash (%)	Moisture (%)	Dry Ash (%)	Dry Sulfur (%)
BLAM -80 mesh	26.19 ± 0.22	0.51 ± 0.06	26.33 ± 0.20	
BLAM -325 mesh	18.65 ± 0.11	18.84 ± 0.57	22.98 ± .02	0.84
BLAM -10 micron	21.46 ± 0.48	3.16 ± 2.46	22.16 ± 0.08	
CMBTUF	48.58 ± 0.07	4.19 ± 0.28	48.91 ± 0.08	0.39
LWTUF barrel #1	64.62 ± 0.08	1.08 ± 0.19	67.24 ± 0.18	1.35
MCMTUF	59.96 ± 0.92	4.17 ± 0.16	60.01 ± 0.28	0.35
MCPTUF	74.06 ± 0.17	4.09 ± 0.15	74.36 ± 0.18	0.47
TCATUF	72.27 ± 0.18	4.23 ± 0.15	72.54 ± 0.17	0.48
TCBTUF	60.64 ± 0.26	4.11 ± 0.15	60.95 ± 0.26	0.51

2.3.1 Release Analysis

Release analysis tests were performed with a Denver D12 laboratory flotation machine (**Error! Reference source not found.**) in a 2 liter cell agitated at 1,000 RPM. MIBC (dosed at 0 .75 lb/ton) was used as the frothing agent, while kerosene (dosed at 0.65 lb/ton) was used as a collector. The release analysis procedure first used five sequential rougher stages, recleaning the concentrate in each stage to produce a final combined tailings product. The concentrate from this rougher stage was then processed in a cleaner stage, with froth concentrate products recovered at 30 seconds, 60 seconds, 120 seconds, 240 seconds, and complete froth exhaustion. A second tailings product was also produced from the cleaning stage.

The results of the release analysis are shown graphically in Figure 9**Error! Reference source not found.** for the crushed BLAM sample as well as the six other thickener underflow samples. This data shows that most of the thickener underflow froth products are < 10% ash, with the associated yield varying from <20% (MCPTUF) to nearly 50% (CMBTUF). CMBTUF in particular contains significant quantities of sub five percent ash coal and would likely benefit from further decarbonization to further concentrate REE.

Figure 8. Denver D12 lab flotation cell.

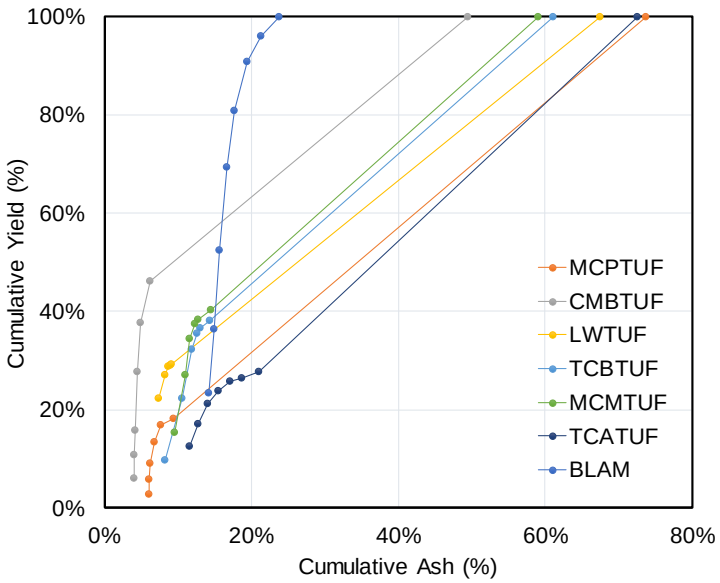

Figure 9. Release analysis curves for all field samples.

2.3.2 Rare Earth Element Analysis

The REE content of each sample was determined by the ICP-MS toxicology laboratory at the Virginia Tech School of Veterinary Medicine. The analytical procedure used a microwave-assisted aqua regia digestion procedure followed by ICP-MS finish. This method was found to produce results similar to that of complete digestion with HF. The total rare earth element content (TREE) of each sample is shown in Table 6. Note that all assays are given on a whole sample basis unless otherwise stated.

All samples have a similar distribution of REEs, with the only major distinction being the total REE content that varies from 157 PPM (CMBTUF) to 245 PPM (LWTUF). With respect to the distribution between heavy and lights, all samples are consistent, with approximately 77% to 80% of the total being classified as light (i.e. La – Eu) and 20% to 23% being classified as heavy (i.e. Gd – Lu, Y, Sc). The scandium content averages approximately 5% of the total REEs.

The relationship between total REE versus ash content roughly follows a linear trend with higher ash contents correlating to a higher REE content. Figure 10 shows the ash/REE relationship for both the current data set (red points) as well as data from a prior study (Luttrell et al., 2019) that surveyed more than 20 preparation plants in the north and central Appalachian coal basins (grey points). Five of the six thickener underflow samples (i.e. those at the higher ash contents: LWTUF, MCMTUF, MCPTUF, TCATUF, TCBTUF) fall slightly above the background data set, and thus, the REE content may be considered "above average" for the corresponding ash content. As has been noted in prior reports, the BLAM sample (26% ash, 180 PPM REE) is truly anomalous, as the REE content is approximately twice as high as the background data at that same ash content. Lastly, the MCMTUF sample (49% ash, 157 PPM REE) falls in line with the background data.

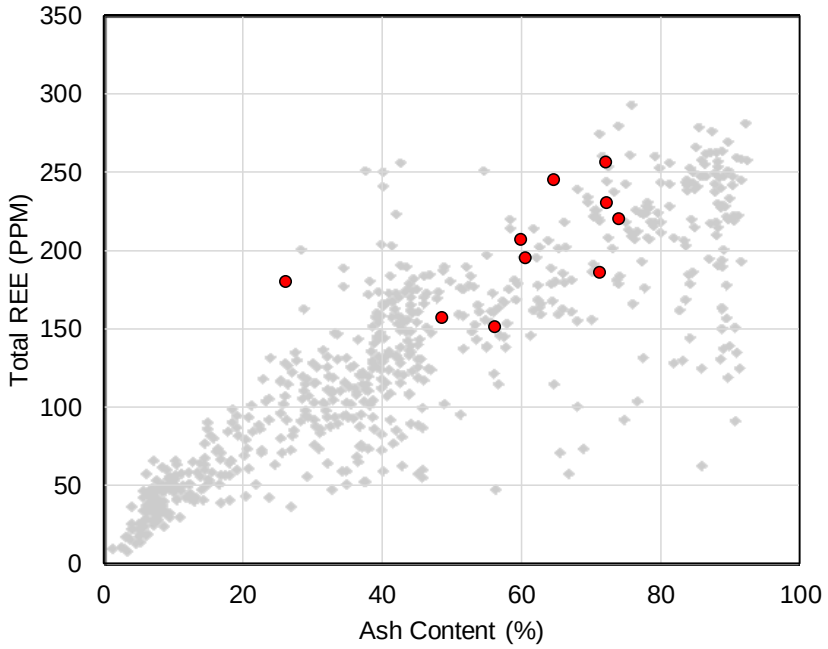

Figure 10. Relationship between total REE and ash for both the current data set (red points) as well as data from a prior study that surveyed more than 20 preparation plants in the NAPP and CAPP coal basins (grey points)

Table 6 Rare earth content as determined by ICP-MS

REE	BLAM	CMBTUF	LWTUF	MCMTUF	MCPTUF	TCATUF	TCBTUF	LTUF	ALA
Sc (PPM)	6.87	9.67	9.68	11.12	10.98	11.30	9.34	6.55	2.97
Y (PPM)	19.85	12.47	21.69	21.13	18.42	19.54	16.62	11.42	24.84
La (PPM)	31.49	28.36	44.30	36.24	40.31	41.44	34.66	28.67	32.00
Ce (PPM)	64.65	58.21	91.39	73.18	81.32	84.93	70.66	58.08	68.59
Pr (PPM)	7.42	6.71	10.75	8.54	9.53	10.02	8.37	6.55	7.16
Nd (PPM)	28.26	25.25	40.63	32.51	36.09	38.12	32.60	24.80	26.08
Sm (PPM)	5.46	4.99	7.61	6.24	6.74	7.26	6.95	4.67	5.28
Eu (PPM)	1.09	0.89	1.23	1.23	1.33	1.31	1.24	0.89	1.08
Gd (PPM)	5.22	4.16	6.52	5.69	5.52	6.02	5.70	3.55	5.13
Tb (PPM)	0.75	0.53	0.88	0.81	0.76	0.81	0.70	0.48	0.77
Dy (PPM)	4.06	2.79	4.81	4.44	4.07	4.35	3.70	2.58	4.97
Ho (PPM)	0.79	0.50	0.89	0.86	0.77	0.82	0.69	0.47	0.94
Er (PPM)	2.04	1.35	2.40	2.33	2.08	2.20	1.86	1.24	2.68
Tm (PPM)	0.29	0.18	0.34	0.32	0.29	0.31	0.26	0.17	0.37
Yb (PPM)	1.65	1.12	2.08	1.97	1.79	1.87	1.60	0.98	2.58
Lu (PPM)	0.24	0.16	0.29	0.28	0.25	0.27	0.23	0.13	0.40
Total REE (PPM)	180.10	157.33	245.49	206.89	220.25	230.56	195.16	151.23	185.84

2.3.3 Major Metal Analysis

Other major elemental constituents were determined by X-ray fluorescence (XRF). Samples were first pressed into a pellet using a 14-ton bottle jack press with a mold, and then analyzed using a Thermo Scientific XL-2 GOLDD handheld XRF (Figure 11). X-ray scans were conducted for 60 seconds, and each pellet was analyzed three separate times at different locations. The results from the three repeat analyses were averaged, and the datum for the five primary constituent elements are shown in **Error! Reference source not found.**. The XRF r esults show that LWTUF, TCATUF, and MCPTUF have the highest Al and Si content relative to the others, with the Al content exceeding 10% and the Si content exceeding 25% for these three samples.

Figure 11. Thermo Scientific Niton XL2 GOLDD in analysis cradle

Each pellet was irradiated three separate times for a minute each and the results for five of the primary constituent elements from the three runs were averaged (Table 7).

Table 7. Major sample constituents determined by XRF

Sample Code	Al (%)	Si (%)	S (%)	Ti (%)	Fe (%)
BLAM	3.99 ± 0.15	11.87 ± 0.16	2.72 ± 0.05	1.16 ± 0.03	1.32 ± 0.02
MCMVTUF	8.53 ± 0.15	20.85 ± 0.20	1.06 ± 0.03	0.54 ± 0.02	3.60 ± 0.04
TCATUF	10.34 ± 0.33	24.79 ± 0.13	0.94 ± 0.07	0.22 ± 0.08	4.28 ± 0.06
TCBTUF	8.60 ± 0.08	21.54 ± 0.35	1.06 ± 0.05	0.47 ± 0.05	3.84 ± 0.08
CMBTUF	7.72 ± 0.12	19.93 ± 0.28	2.74 ± 0.11	0.74 ± 0.03	1.96 ± 0.02
LWTUF	11.58 ± 0.17	25.88 ± 0.37	1.03 ± 0.01	0.75 ± 0.02	4.19 ± 0.05
MCPTUF	11.76 ± 0.34	27.05 ± 0.20	0.57 ±0.02	0.43 ± 0.08	5.20 ± 0.08

Based on the XRF results LWTUF, TCATUF, and MCPTUF have the highest aluminum and silicon content. Elevated aluminum content is correlated (r=0.85) with an increased level of clay minerals (Jozanikohan et al., 2016). Additionally, TCATUF, LWTUF, and MCPTUF have the highest TREE levels of the seven samples, which indicate that the lanthanides are associated with the ash producing minerals within coals (Hower et al., 1999). The correlations between the major elements and the TREE content of each sample are shown in Figure 12Figure 12. Note that BLAM was excluded from these plots as the XRF results for it are dissimilar. One hypothesis for the difference in the BLAM results is from the high levels of volatile matter present in the BLAM sample as compared to the others.

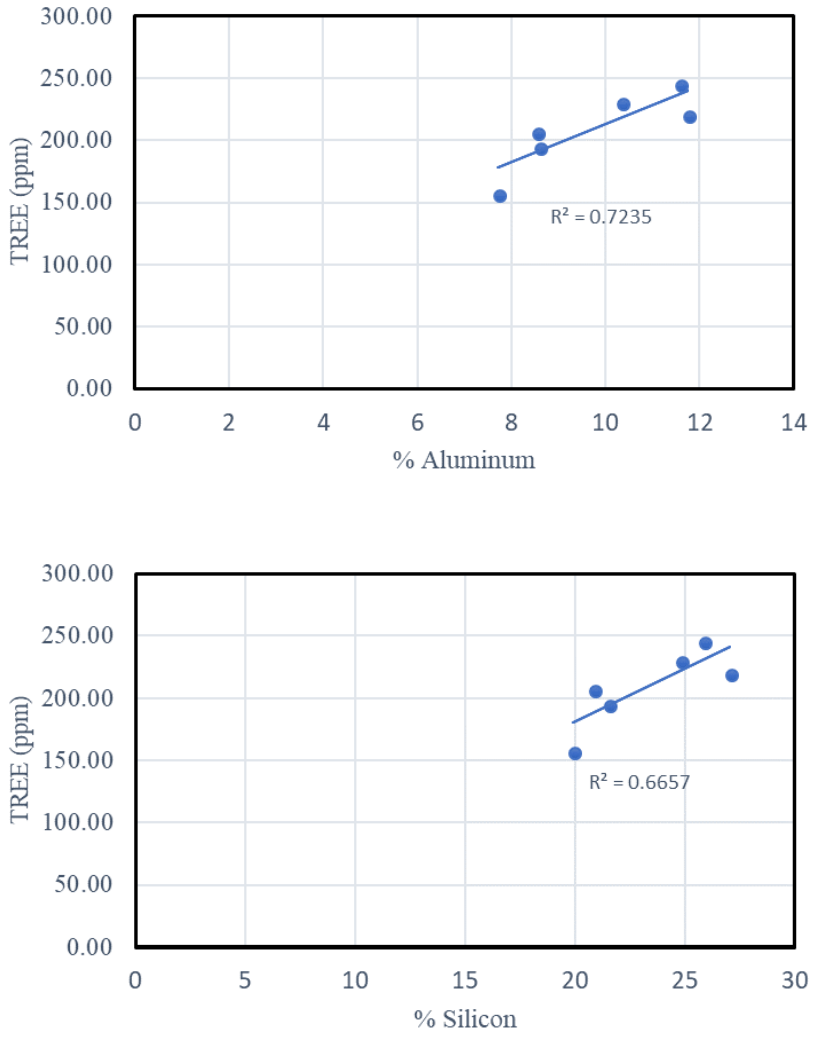

Figure 12. Trendlines and coefficients of determination for the relationship between TREE content and the aluminum and silicon.

Chapter 3. Rare Earth Concentration via Dispersive Liberation

3.1. Introduction and Scope

Existing literature indicates an association between the IX REE phases and clay minerals contained within the samples. Clay minerals, due to their surface charges, tend to agglomerate or create “books” that can entrap IX REEs within preventing efficient extraction. The clay production industry has a dispersive liberation technique (known as blunging) that was created as a conditioning stage before flotation for the removal of impurities from pigment kaolinite (Shi & Yordan, 1997). This dispersion technique uses a high percent solids slurry with a strong dispersant and violently mixes them in a high temperature environment. The potential advantages of this clay concentration process before IX are twofold: first due to the pH requirements for effective IX to occur removing minerals such as calcium carbonate or other carbonaceous gangue will limit the consumption of acid and second the high shear conditions used in this process are capable of de-booking clay particles which increases the exposed surface area accelerating the leaching process.

3.2. Methods and Materials

An initial test was performed on the LWTUF sample to ascertain whether it was effective at dispersing a thickener underflow. For this test, water was added to approximately 45 grams of LWTUF sample until the slurry was 50% solids and 0.225 grams of sodium silicate was added as the dispersant. The slurry was vigorously mixed in a warring commercial blender for a total of 30 minutes. The blending time was split into 5-minute intervals with 10 minutes of cool down time allowed for the motor to cool. The temperature increase from the friction of blending such a thick slurry was sufficient and additional heat was not added to the experiment. After dispersion the blunged slurry was added to a settling cylinder and the volume was brought to 842 mL with tap water to bring the water content to 95% by weight. Another settling cylinder was filled with a slurry consisting of the unblunged LWTUF material and diluted to the same water content. Both cylinders were shaken then allowed to settle for 100 hours. The speed at which each settled was visually compared to determine the effectiveness of the process. At the end of the 100-hour observation period, the unblunged sample had completely settled while the cylinder with the blunged sample was still cloudy (Figure 13).

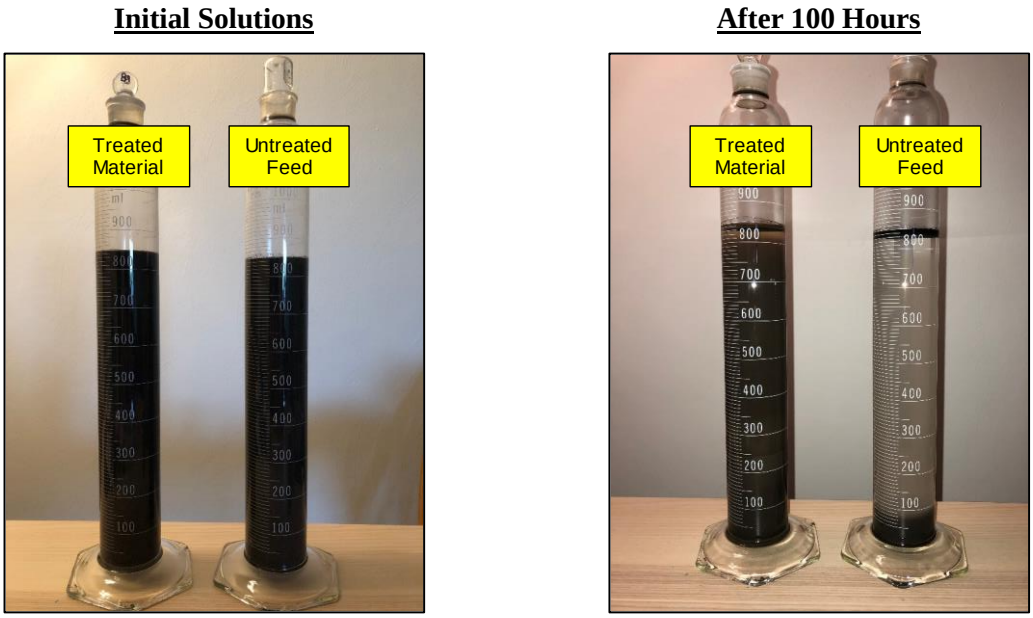

Figure 13. Dispersive liberation test results, left photograph is from initial feed solutions, right photograph is after 100 hours of settling. Treated material was mixed for 30 minutes with 10 lb/ton sodium silicate.

In a second proof-of-concept test, the dispersive liberation process was assessed to determine if the isolation of clays led to an increase of the REE content of the feed material. One sample of LWTUF was prepared by first removing the coal through froth flotation. Flotation was conducted to exhaustion in a 2 liter laboratory Denver flotation cell using MIBC as a frother. The clay-rich tailings from this process were then subjected to dispersive liberation at 60% solids using 10 lb/ton sodium silicate at elevated temperature. The product of this process was then placed in a settling column similar to the columns used in Figure 13. After 11 hours of settling, the suspended solids were decanted from the column, filtered, and dried. A sample of this material was then recovered for digestion and ICP-MS analysis. In later tests, the long settling tests were replaced by wet screening using various size fine sieves.

Following the proof-of-concept tests, efforts were expanded to critically assess the full deportment of REEs during the decarbonization and blunging process. In this experiment, the LTUF sample was evaluated, given its relatively low as-received REE content (154 ppm). For this test, flotation was performed twice in a 6 liter laboratory cell, in a method similar to ASTM D5114/D5114M. The flotation time was fixed at 13 minutes based on an initial flotation trial run with LTUF. Two flotations were performed to generate enough tailings solids to efficiently blunge. After completion, the flotation tailings were then dewatered by centrifugation. The pellets were removed from the centrifuge tubes, mixed, analyzed by TGA, weighed, and placed

within the blunging cell. Based on the initial moisture content, water was added to reach a solids content of 35% by weight. Following dilution, the blunging vessel was then placed under a modified overhead press with a serrated mixing blade and agitated at 800 RPM for 4 hours. After agitation, the blunged material was settled and classified in the same manner as discussed in previously. All process streams were then sampled and analyzed for REEs and major gangue elements via ICP-MS. Laser particle size analysis was also conducted to confirm the size separation imparted by the settling process.

3.3. Results and Discussion

The element-by-element results for this blunged sample as well as the analysis of the as-received LWTUF material are shown in Figure 14. These data indicate that the decarbonization and dispersive liberation processes provide a significant increase to the sample REE concentration. In total, the REE concentration was improved from 250 ppm to 366 ppm, an improvement of over 46%. The increase is particularly noted for Sc, as well as the LREEs, La – Nd.

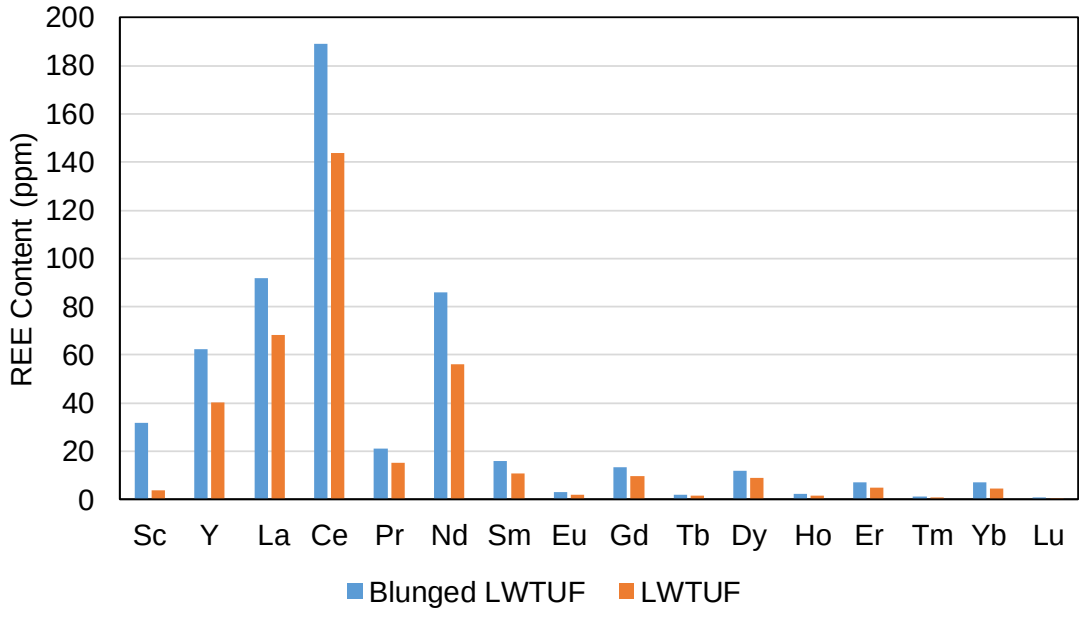

Figure 14. REE content (ash basis) in LWTUF before (67.15% ash) and after blunging (89.0% ash), as determined by lithium metaborate fusion.

Given the effectiveness of dispersive liberation on improving the rare earth concentration in a feedstock, further characterization work was performed on the final fine concentrate product. Specifically, XRD and SEM-EDS were used to determine mineralogy and morphology of the product material. The mineralogical results from XRD are shown in Figure 15. This figure contains stacked XRD spectra for the blunged LWTUF sample as well as the as the as-received LWTUF. The most notable change between the blunged and as-received sample was the sharp decrease in the strength of the silica peak. This data thus confirms that kaolinite and muscovite present in the feed are concentrated during the blunging process by the elimination of silica.

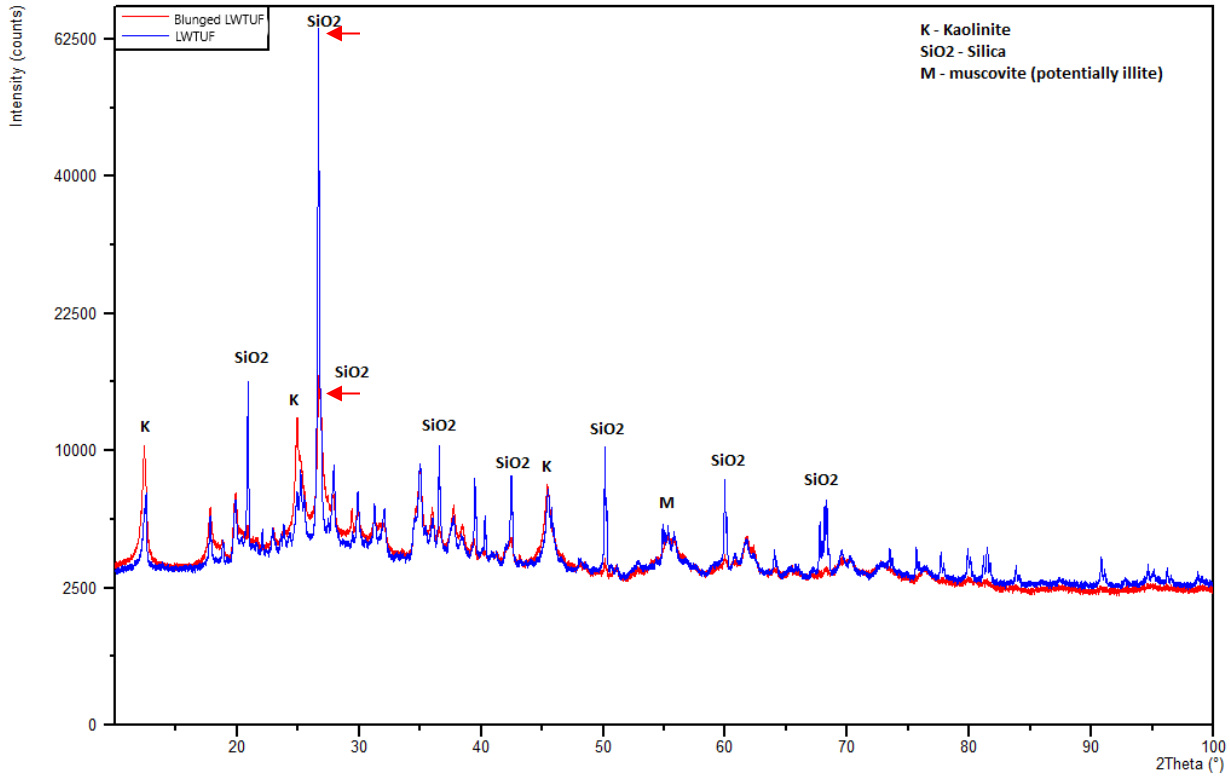

Figure 15. LWTUF XRD spectra before and after dispersive liberation

In a separate blunging test using LWTUF, the products were analyzed by SEM-EDS to ensure effective liberation of rare earth bearing minerals and clay delamination. All SEM-EDS was performed on an FEI Quanta 600F and the spectra were analyzed using the Bruker Espirit software package. The sample was sputter coated with palladium and platinum to a thickness of 7 nm. The images were taken in electron backscatter mode as this highlighted the higher density rare earth bearing particles against the clay minerals. As shown in Figure 16a liberated particles

of rare earth phosphates (circled in red, see spectra in Figure 17) were present in the sample. Note that all compositions determined by EDS are considered semi-quantitative.

Also of note in Figure 16 is the clay agglomerate in the top left corner indicating that the clay is not fully dispersed, illustrating that more aggressive methods of dispersion may be necessary. Figure 16b below shows an example of an incompletely liberated particle of rare earth phosphate surrounded by a clay matrix; additionally, the surrounding particles appear to be agglomerations of clay particles, further indicating incomplete dispersion. During SEM-EDS analysus all REE bearing particles encountered were less than 6 μm across, which indicates that separation based on a finer particle size cut may further concentrate REEs.

Over the duration of SEM-EDS analysis, 30 different particles were analyzed for a variety of elements, and only particles containing phosphorous contained detectable concentrations of REEs. The phosphorous to TREE ratio was highly variable, ranging from 1.1 to 3.7. This may indicate different phases of occurrence or the presence of zircon, which has peak overlap with phosphorous and was detected in non-phosphorous bearing minerals. Additionally, this variability could also be from material close to the point chosen for analysis, as the EDS in point mode acquires data from an approximately μm^3 area. Figure 18 compares the major components in the two particles pictured in Figure 16, as the particle in Figure 16b is not fully liberated. The additional aluminum and silicon detected may be the result of the surrounding minerals or could indicate that the REE-phosphate is associated with clay minerals. It is conceivable that REE-phosphate could form on the cationic edges of the clay particles possibly in the form of rhabdophane.

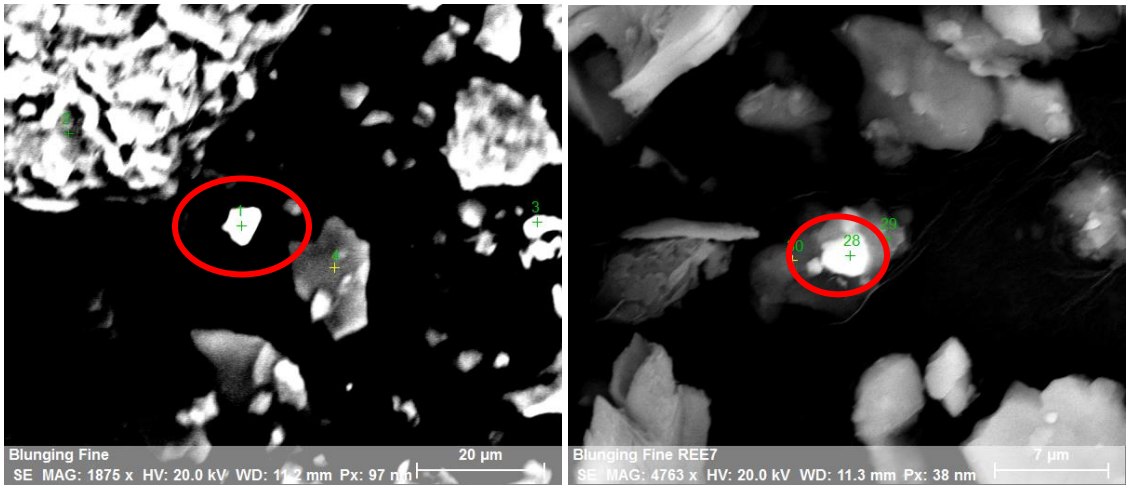

(a) (b)

Figure 16. SEM election backscatter images of lanthanide phosphate particles in dispersed LWTUF

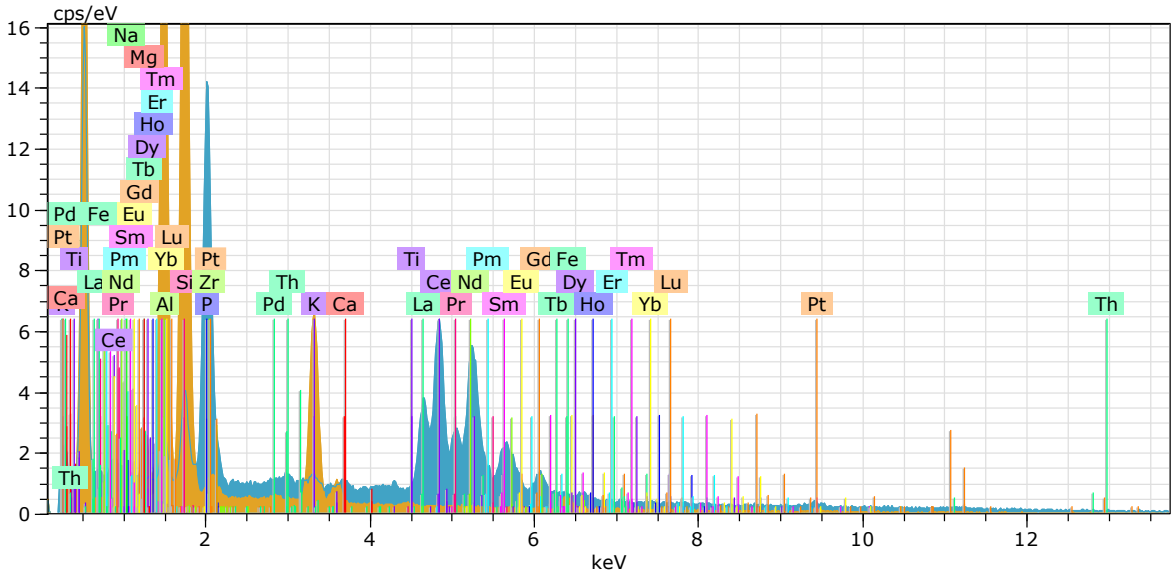

Figure 17. EDS spectra comparison of the REE bearing particle pictured in Figure 16a (blue spectra) and the nearby clay particle (yellow spectra)

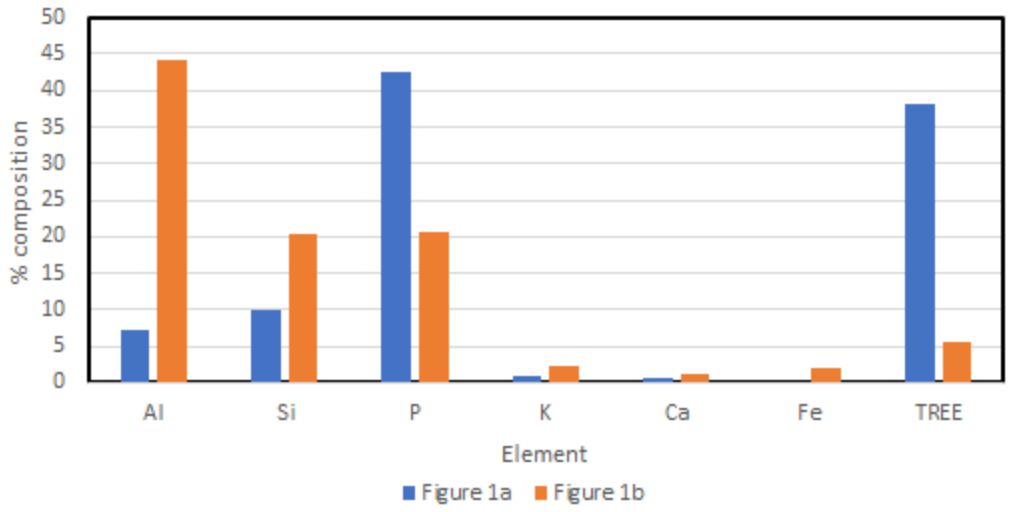

Figure 18. Major component elements of the two REE bearing particles shown in Figure 16

The results from the mass balance assessment are shown in Figure 19, and Figure 20 shows correlations between major element content (Al and Fe) and REE content for each endpoint sample generated during the experiment. Based on this data, the recovery of REEs through the circuit to the fine blunging concentrate is 19.6%. The low recovery is due to the significant mass of relatively high-grade material left in the tailings from the blunging process. Most notable from the data acquired during the mass balance calculation is the strong relationship between the Al content and REE content of the various circuit products. An inverse relationship was observed for Fe vs. REEs.

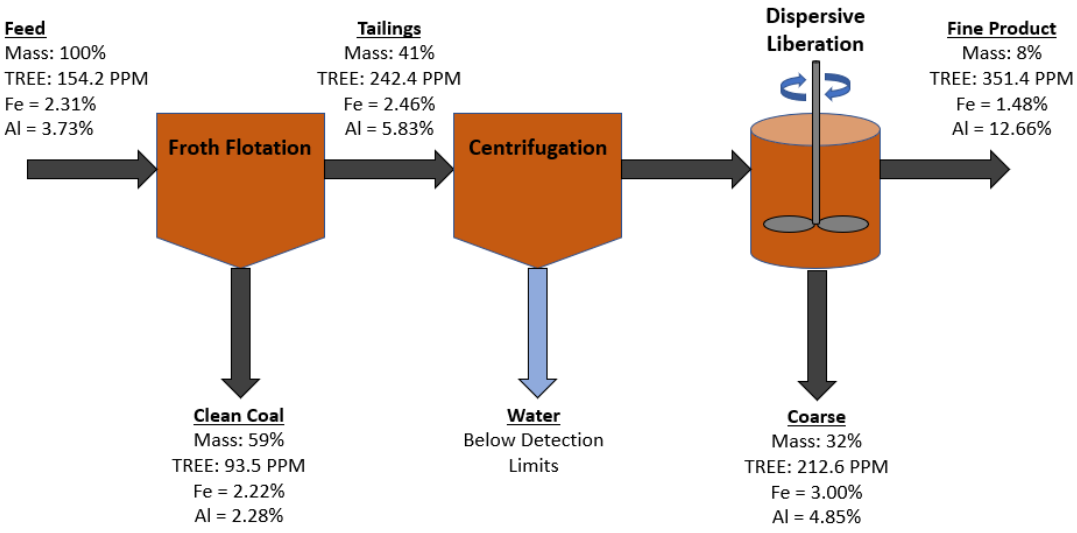

Figure 19. Mass balance of decarbonization and blunging process as performed on LTUF.

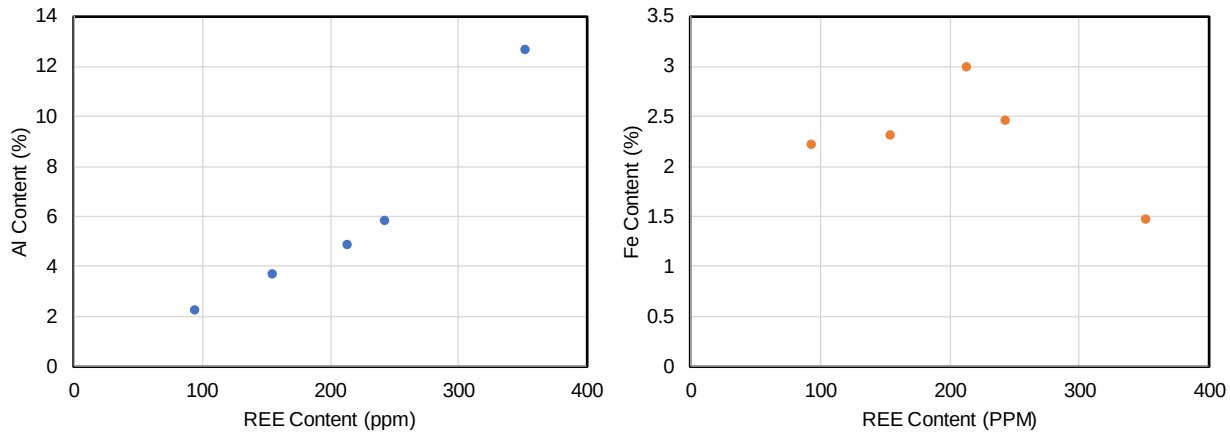

Figure 20. Relationship between Al (left panel) and Fe (right panel) content to REE content of decarbonization and blunging process product streams.

The particle size distribution for the final products of blunging were determined by laser diffraction using a Microtrac S3500. This data is shown in Figure 21. The LTUF concentrate produced from the blunging process has a D50 of 1.474 µm and a top size of 9.4 µm. Approximately 87% of the particles in the concentrate are less than the target top size of 5 µm. The tailings from blunging resulted in an 8.22 µm D50 and a top size of 277.9 µm. Based on these results, the 11-hour settling time used after blunging is sufficient. The fine particle size (Figure 21), the increased aluminum content (Figure 19), and the XRD spectra (Figure 15) indicate that the process is concentrating kaolinite by removal of salicaceous gangue.

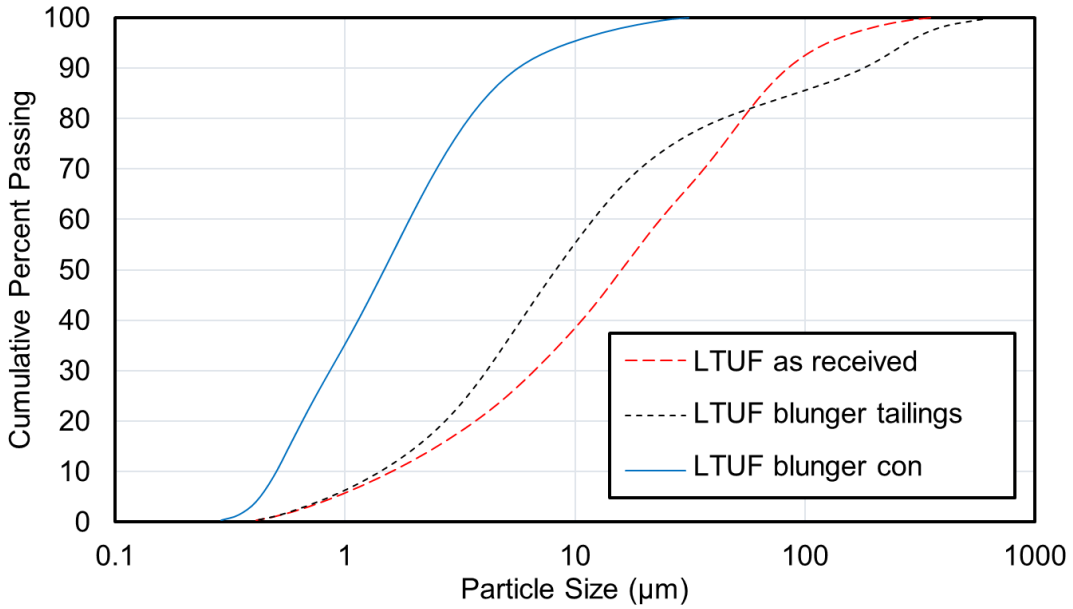

Figure 21. Size distribution data for LTUF as received, compared with both blunging products.

Assays of the LTUF thickener underflow indicate a feed grade of 151.2 ppm, which is significantly lower than other feedstocks such as LWTUF; however, the concentrate produced by blunging has a grade of 349.8 ppm, a total concentration ratio of 2.31x. Element-by-element concentration ratios for the LTUF blunged product relative to the original feed are shown in Figure 22. Nearly every element is enriched by at least a factor of 2, with the highest concentration ratio being Sc at 2.84.

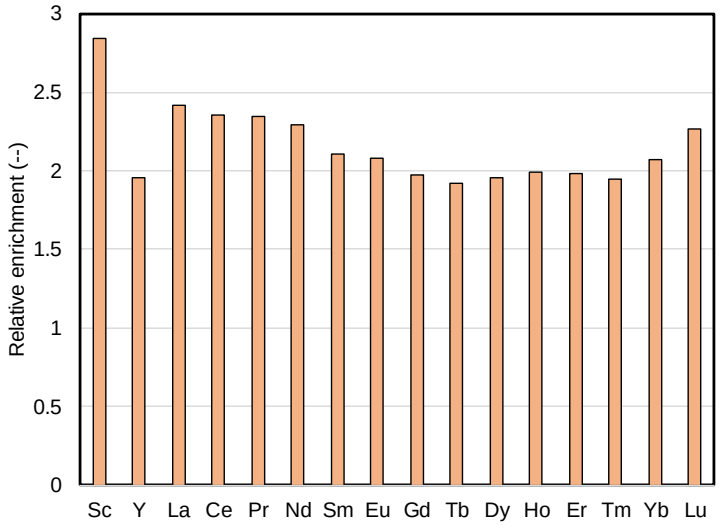

Figure 22. Relative enrichment of elements in blunged LTUF vs unblunged LTUF

As part of a parametric test program, several samples including LWTUF, MCMTUF, TCBTUF, and LTUF were evaluated to determine the REE increase imparted to the feed material through the blunging process. These results are shown in Table 8. All samples have shown a notable increase in REE concentration after blunging, exceeding 24% in all cases. Nevertheless, the LTUF sample has produced the best result to date with a 131.8% improvement after blunging.

Table 8. Summary Results on Impact of Decarbonization and Blunging Process to REE Concentration.

Sample ID	Original TREE (ppm)	After Blunging TREE (ppm)	% Increase
LWTUF S1	250	366	46.4
LWTUF S2	257	371	44.3
LWTUF S3	257	389	51.6
MCMTUF	207	274	32.6
TCBTUF	195	253	29.7
LTUF	151	350	131.8

In an attempt to identify geochemical differences between isolated clay from coal wastes and ion-exchangeable clays we sought out a source for rare earth bearing ion-exchangeable clay from China. After receiving the Chinese rare earth clay (CREC), we conducted a microwave based aqua regia assay to determine the rare earth and major element content.

When compared to other samples used throughout the project it has significantly higher levels of Yttrium and HREEs (Figure 23). The relatively low levels of lanthanum and cerium also would suggest a low quantity of mineral phase REEs. The major mineral components of the CREC was compared to a blunged LWTUF sample and it was noted to have a significantly lower amount of all measured major component cations (Figure 24). Unlike LWTUF, both sodium and calcium were below limits of quantification for the ICP-MS, this dearth of potentially competing cations and/or carbonate bearing cations in part explains the high extractability of the REEs associated with the CREC. Additionally, an approximately 1 gram sample of CREC was placed in 25 mL of deionized water and the pH of the solution rapidly dropped to 4.

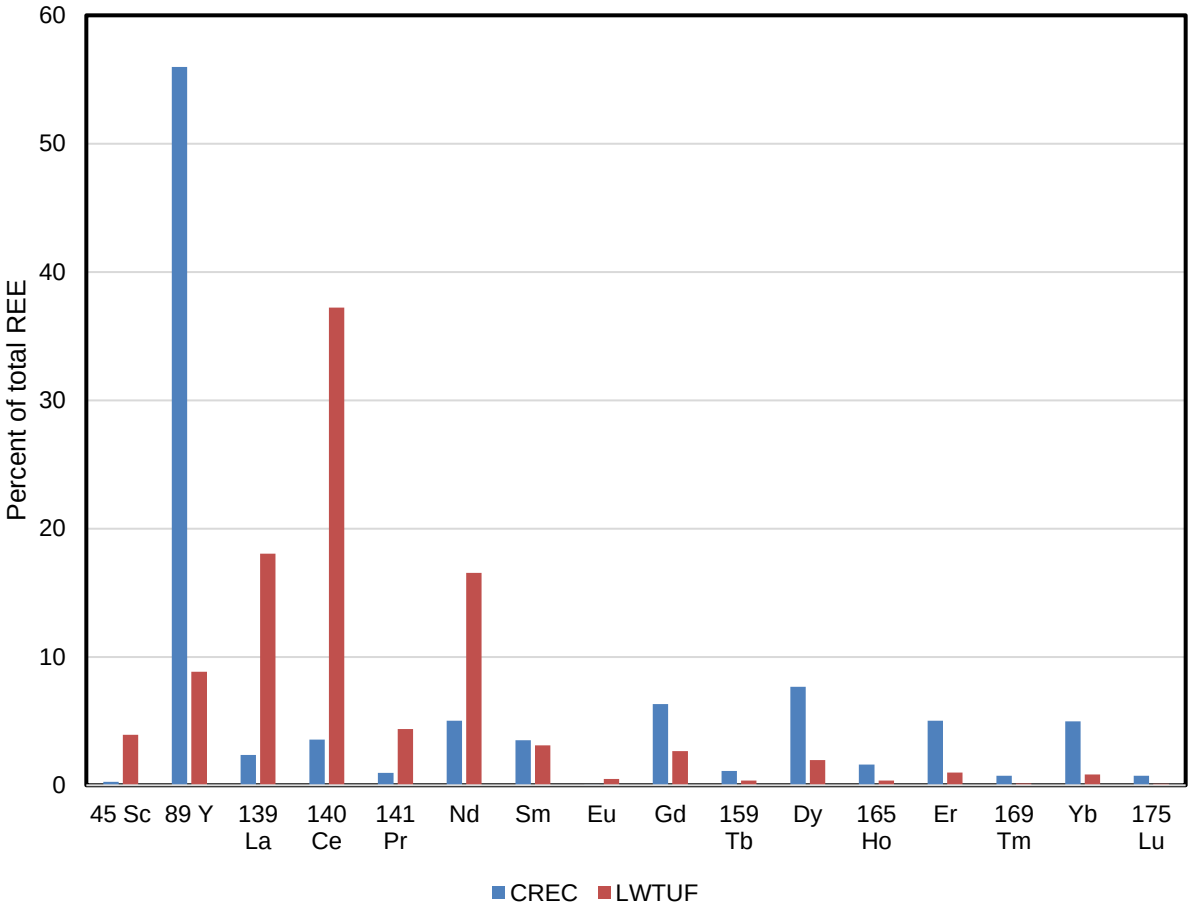

Figure 23. REE distribution differences between CREC and LWTUF

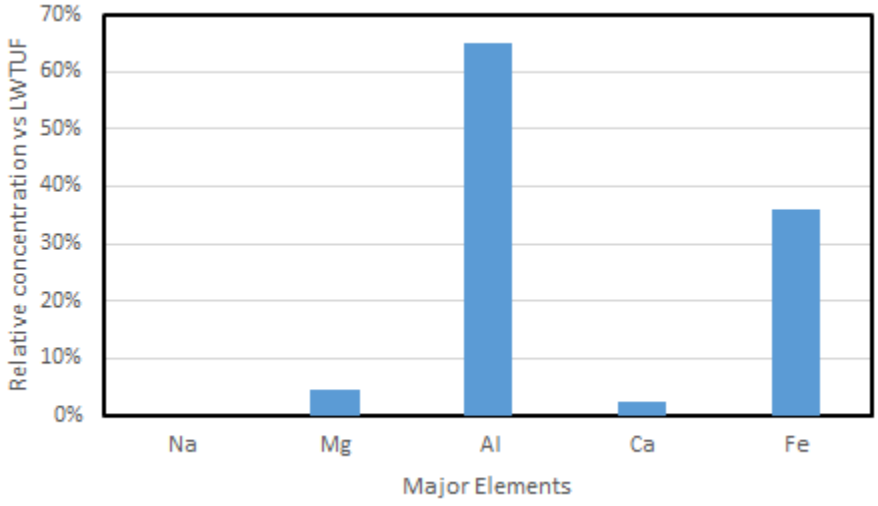

Figure 24. Major elements in CREC sample.

XRD analysis was also performed on the Chinese clay by the Virginia Tech Materials Science Department for comparison with a sample of LWTUF that had undergone dispersion and has a D_{50} of 5 μm (Figure 25). The LWTUF sample was chosen for the comparison as it was the primary focus of the project at the time due to its measured high level of contained REEs. The purpose of dispersing the LWTUF sample was to attempt to isolate the clay from the sample to directly compare with the Chinese clay. The results show a significant difference between the two samples, specifically microcline was positively identified in the CREC while there is little evidence of its presence in the LWTUF sample. Though clay is a significant portion of each sample the presence of the microcline indicates a difference in the parent rock of the sediment and/or the samples are in different stages of weathering. Typically, when a granite weathers the feldspar and muscovite readily erode ultimately resulting in siliceous sands and clay particulates.

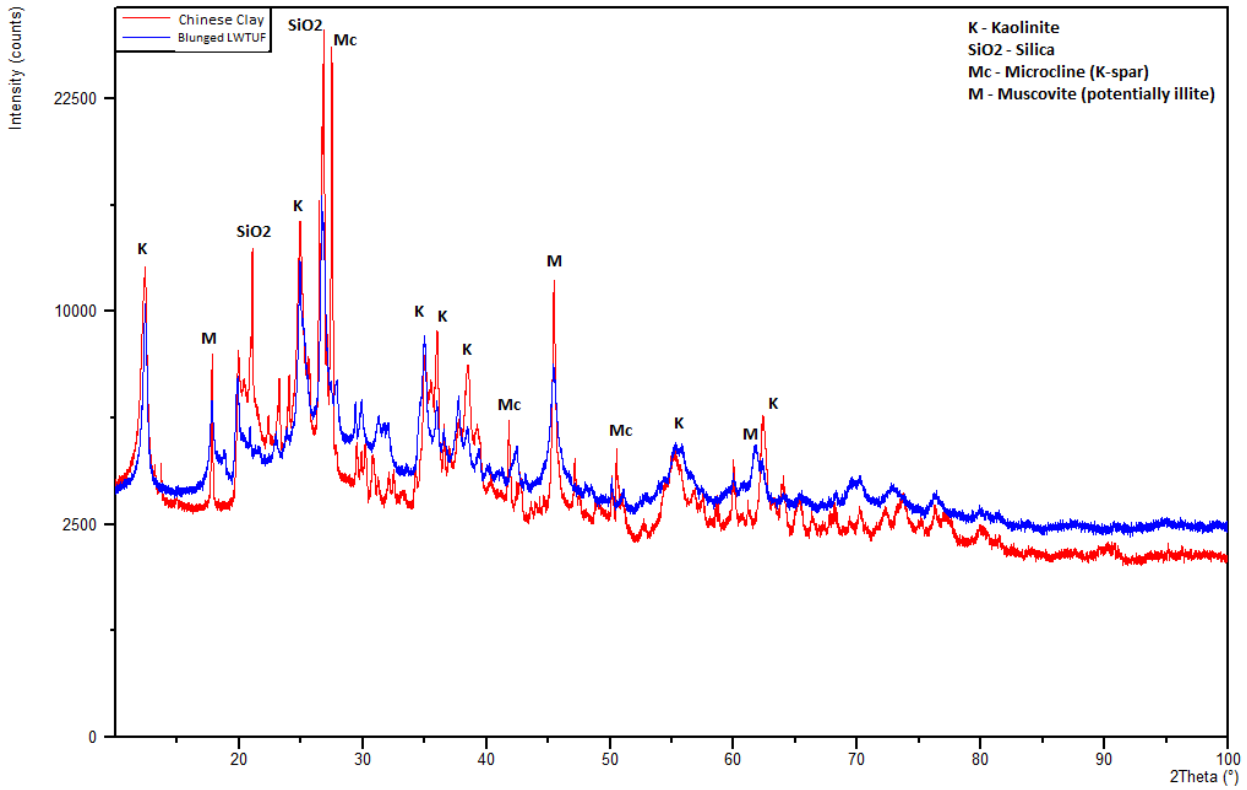

Figure 25. XRD analysis results comparing CREC to a blunged LWTUF sample

Though both LWTUF and CREC contain these sand and clay particles the presence of microcline, a potassium rich feldspar, in the CREC while the LWTUF contains only silica, illite,

and kaolinite. Instead the LWTUF sample contains significant quantities of sodium and calcium which indicates that any detrital clays parent granite's feldspar component consisted of plagioclase feldspar. Alternatively, the origin of the significant calcium and sodium could be due to groundwater infiltration from the overlying strata in the coal seam which includes calcium rich limestone. This geochemical difference between these samples provides some insight into why the two behave so differently during IX leaching processes and deserves further study.

3.4. Summary and Conclusions

From the experimental work in this chapter, three key conclusions are derived:

- The dispersive liberation or "blunging" process successfully concentrated the ultra-fine clay materials in the thickener underflow samples evaluated in this project. This finding was confirmed by both particle size analysis and XRD.
- In all cases, the dispersion concentrate had an increased REE concentration relative to that of the feed material. In the case of LTUR, the REE content more than doubled.
- SEM-EDS of LWTUF samples did confirm the presence of REE-phosphate formations associated with the clay particles.

Chapter 4. Rare Earth Extraction via Ion Exchange Leaching

4.1. Introduction and Scope

Ion exchange leaching also known as salt exchange is a commonly used method of recovering rare earth elements that are adsorbed onto the surface of clays found in Chinese laterite deposits. The process has gone through multiple generations of improvement with the original process using sodium chloride and currently ammonium sulfate is the most commonly used lixiviant. Though ion exchange leaching of Chinese clays is well documented, recently efforts have been made to adapt this process to other feedstocks. Specifically, clay bearing coal products and by-products have been an area of increased investigation (Rozelle et al., 2016). Efforts in this section were focused identifying the mode of REE occurrence and maximizing recovery. A short summary of the experiments conducted is listed in Table 9 illustrating the direction and narrowing focus of research. The leaching approaches began with the use of salt exchange but evolved towards more aggressive techniques capable of accessing mineral phase REEs.

Table 9. Leaching test summary

Samples	No. of Runs	Experimental Tract
All	123	Benchmarking and Novel lixiviants
LWTUF	38	Leaching additives
LWTUF and LTUF	34	Gas purged reductive leaching
ALA	4	Acetate and pyrophosphate
LWTUF	15	alkaline pretreatment

4.2. Materials and Methods

4.2.1. *Materials*

Several chemical reagents were used throughout the various test series. The primary leaching lixiviants include ammonium sulfate (AS, 99.0% purity, Sigma Aldrich),

aminomethylpropanol (AMP, >95%, Sigma Aldrich), and Tetraethylammonium Chloride (TEAC, >98%, Sigma Aldirch). For pH adjustment, both sulfuric acid (95%-98%, Sigma Aldrich), hydrochloric acid (37%, Sigma Aldrich), and sodium hydroxide (>98%, Sigma Aldrich) were used in the various trials.

Some of the latter trials during the period used chelating agents and reducing agents as potential leaching modifiers. The chelation agents evaluated in the current reporting period include: ascorbic acid (AA), citric acid (CA), ethylenediamine tetraacetic acid (EDTA), isoascorbic acid (IAA), nitriloacetic acid (NTA), sodium tripolyphosphate (TPP), and oxalic acid (OA). The reducing agents included: L-ascorbic acid (AA), sodium dithionite (DT), and hydroxylamine hydrochloride (HA). AA is included on both lists as it can function as either a reducing agent or a chelation agent. All chelating and reducing agents were supplied by Fisher Scientific. Table 10 summarizes many of the reagents used in testing.

Table 10. Reagent abbreviations

Abbreviation	Description
AA	Ascorbic acid
ACDB	Ammonium citrate dibasic
AMP	2-amino-2-methyl-1-propanol
AS	Ammonium sulfate
DAH	1-Dodecylamine hydrochloride
EtOH	Ethanol
H2O2	Hydrogen peroxide
H2SO4	Sulfuric acid
HA	Hydroxylamine hydrochloride
HCl	Hydrochloric acid
HTAC	Hexadecyltrimethylammonium chloride
KOH	Potassium hydroxide
MeOH	Methanol
NaOH	Sodium hydroxide
OA	Oxalic acid
TEAC	Tetraethylammonium chloride
TMAC	Tetramethylammonium chloride

During the following series of tests, the samples described in Chapter 2 subsection 2 were used. Different testing series focused on different samples. Frequently, the LWTUF sample was used due to the large supply and reported high REE content.

4.2.2. *Leaching Experimental Protocols*

General

All elemental analysis was performed at the Virginia Tech Veterinary Medicine Laboratory on an Aglient ICP-MS. This included method development for microwave digestion of solids in aqua-regia. Solids were also dissolved for analysis by lithium metaborate fusion using a method developed by other researchers at Virginia Tech. Results from all REE assays are presented on a whole sample basis.

Exploratory Tests

Each product was then air-dried and pulverized into a powder. 5 grams of each size class was then placed in 125 mL Erlenmeyer flasks and mixed with 10 mL of lixiviant solution of a specified concentration with the pH adjusted by the addition of 0.3 mL of 2% (v/v) sulfuric acid. The flasks were shaken for 1 hour and the solutions were decanted into a vacuum filter using 413 filter paper and washed with 1L of deionized water. The solids were then dried at 60 degrees Celsius overnight and weighed to indicate weight loss. The dried samples were then digested by microwave-assisted aqua-regia and the digestion solution was analyzed by ICP-MS. Notably, the aqua-regia digestion was incomplete and solid still remained after the process but the procedure should still indicate the remaining acid leachable (colloidal) and ion-exchangeable REE phases within the solid.

Kinetic Tests

A 0.5-gram aliquot of each sample was placed in a disposable plastic beaker with a disposable PTFE stir bar and was mixed with 25.0 mL of fresh 0.5 M/l ammonium sulfate solution. The pH was adjusted to 4.0 ± 0.3 by 2.5% v/v HCl in a 10 mL burette. 0.25 mL Samples were taken at recorded time intervals with 1.0 mL graduated syringes and then filtered by leur lock 0.22 μm syringe filters into 4.75 mL solutions of 2.0% HNO_3 and 0.5% HCl for ICP-MS analysis. The time, pH, and titrant volume were recorded every time a sample was taken.

Leaching Additives

A new experimental protocol was developed to increase throughput and minimize potential sources of experimental error. The modified procedure borrows from the work conducted by Wang et al., 2017. Distinguishing features of the modified procedure include:

· The LWTUF sample for this experiment was split as a slurry and vacuum filtered into a large cake. The cake was not oven dried further to assess any potential chemical alteration of the material associated with additional heating.

· Disposable polypropylene containers were used in place of Erlenmeyer flasks as the leaching vessels. The modification will eliminate the time needed to prepare clean glassware and reduce the potential for cross contamination.

· The liquid-to-solid ratio was increased from 2:1 to 10:1, thereby allowing a higher extraction efficiency and less pH adjustment.

· The total extraction time was increased from 1 hour to 2 hours.

· Recovery was determined by directly analyzing the REE content of the leach liquor, rather than by the loss in REEs between the initial and final solids. By analyzing both the leach liquor and the residual solids, a complete balance can be determined to ensure experimental accuracy. The lack of vacuum filtration reduces the potential for loss of sub 5-micron solids through the filter membrane. Also, the solid is never transferred between containers reducing loses due to adherence to the walls of the vessel. Additionally, the leach liquor analysis removed the variability inherent to the incomplete aqua-regia digestions performed on each solid sample. As a side benefit this new process also significantly increased the throughput for analysis as microwave digestion was a time consuming and laborious process.

Gas Purging

Based on the promising results of reducing agents a new experimental apparatus was assembled to provide greater control of the oxidation/reduction potential in the vessel during the leaching process. The most significant modification from the prior apparatus is that the new system has an air-sealed reaction vessel with an inlet where inert gas can be pumped into the

reactor **(**Figure 26). Prior results have suggested that open-air mixing causes excessive consumption of the reducing agent, which in turn results in low recovery. The oxygen-purged reactor should eliminate these side reactions. In addition, other key features of the new system include: a sealed titration cell, an inlet for a pH meter, potentiostat electrodes, and a gas outlet tube. The potentiostat is a PAR 283A using a platinum electrode combined with a saturated calomel reference electrode. The gas outlet tube bubbles directly into a water filled spouted vacuum filter flask to visually confirm that the apparatus is effectively sealed.

Figure 26. Gas purge reductive ion exchange apparatus in operation.

Specific attention was given to recovering all the solids to obtain a more accurate number for the mass loss. The procedure was modified by adding an additional step where the water used for cleaning the cell and magnetic stir bar was collected, centrifuged, and decanted. The pellet was then dried in an oven and weighed. This pellet weight was added back to the total mass of the sample. The mass loss during the first test may have been the result of a spill or excessive material stuck to the interior of the cell. The replicate tests had minimal variation in the results and the assay values between them were within ±10%.

The standard leaching test procedure was slightly modified for the gas-purged tests. During these tests, 40 mL of deionized water is first added to the titration cell with a small Teflon stir bar. The cell was then sealed by using modified rubber stoppers or electrical tape. To ensure that all dissolved oxygen was removed from the solution, the deionized water was

agitated at 300 RPM while the inert gas was purged through the solution for 10 minutes. After the initial purge, 4 grams of sample were added to the solution by quickly removing the pH electrode and pouring the sample through the port before resealing the system. Next, the pH was adjusted by using dilute sulfuric acid, though pH adjustment was not needed in all tests. Likewise, the slurry potential was monitored, and reducing agents were added to the solution until the slurry potential was below -0.6 V (SCE). Depending on the buffering capacity of the specific reducing agent, additional sulfuric acid occasionally needed reduce the pH to an acceptable set point.

After the desired pH and potential were achieved, the slurry was initially conditions for one hour. Following that period, ammonium sulfate was added to the solution (0.5 M), and the leaching reaction was conducted for a second hour. Following the two-hour sequence, the samples were centrifuged for 10 minutes at 5,000 RPM. The supernatant was collected for analysis, while the solids were dried, weighed, digested, and analyzed via ICP-MS. For kinetics studies samples were drawn at predetermined times by pipette, centrifuged at 5000 gravities for 10 minutes and decanted into a sterile 15 mL polypropylene centrifuge tube. The solution was then acidified and analyzed by ICP-MS.

The initial tests were performed on the use of gas purging and dissolved gas as a lixiviant. Previous experiments with neutral gasses were performed at standard temperature and pressure. In order to increase the concentration of gas in solution a commercial carbonator was acquired and modified for use with the experiment. The carbonator was run at 80 psi and deionized water was used as the solvent. At this pressure, the expected concentration of gas is 5.44 times higher than in the earlier gas purged cell tests. In order to allow adequate time for the gas to fully dissolve, the carbonator was filled with water and gas pressure was applied for one hour before use. The usage of dissolved gas in extractions requires additional steps to limit the loss of pressure during long duration tests. Instead of extractions being performed in open air or purged cells, they were done in 15 mL polypropylene centrifuge tubes which were tightly sealed and wrapped in parafilm. Otherwise, the methodology was the same as used for the exploration of alternate ammonium compounds with some modifications. All LTUF samples were kept in slurry form and added wet to the tubes, although in certain cases the slurry was centrifuged and the supernatant decanted. After the addition of reagents, the sealed centrifuge tube was sonicated

in a Branson 1510 cleaning bath at 40 kHz for 5 minutes to help disperse the pellet into the solution (Figure 27 left). After sonication the sample tubes were vigorously shaken by hand to ensure dispersion and then secured in a holding rack and placed on a Yamato SA320 shaker table for the duration of the experiment (Figure 27 right).

Figure 27. (left) Branson sonicating bath, (right) Yamato Shaker table with rack.

Chemical Pretreatment

For this test, the ALA sample was used. A representative sample was first decarbonized by agglomeration with pentane and stored wet. Before the extraction was performed, the sample was dispersed and screened to produce a clay-rich blunged concentrate. For this particular experiment, the sample was agitated by a high-speed overhead disperser at 12,000 RPM. The dispersant used for this experiment was sodium hexametaphosphate (SHMP), the same lixiviant used in the final stage of extraction, albeit at a significantly lower dose of 0.004 M. All steps were performed in a 50 mL polypropylene tube. After agitation, 0.5 M sodium acetate was added to the solution, and the pH was adjusted to 5.0 by addition of glacial acetic acid (25% v/v). The mixture was then shaken for 14 hours. After shaking, aliquots of the slurry were pipetted into two 15 mL tubes, centrifuged, and decanted. SHMP stock solution was then added to each 15 mL tube to a final volume of 10 mL, and the pH was adjusted to approximately 10.5 with 5.0 M NaOH. The slurry was then re-dispersed, as the acidic pH will cause the clays to coagulate.

Alkaline Pretreatment

Section specific methods for the chemical/alkaline pretreatment procedure are as follows: 0.5 g of the decarbonized and blunged LWTUF sample (~ 375 TREE) was weighed into a modified Teflon (PTFE-TFM) microwave digestion vessel. 10 mL of the 50% (w/v) KOH or NaOH was added before swirling, shaking, and then running the microwave program methodology. The samples were microwaved according to EPA 3052, which uses a temperature ramp that takes 10 minutes to reach 180 °C, and then holds at 180 °C for 10 minutes before cooling to 70 °C for safe handling after the run has completed. The vessels were removed from the microwave carousel to allow them to further cool in a fume hood before proceeding. Once cooled, the vessels were vigorously shaken before decanting into fresh 15 mL polypropylene centrifuge tubes. The microwaved samples were then centrifuged briefly to pelletize the sample and the supernatant was decanted. The pellet was then washed by adding 10 mL of 18 M-Ohm water, followed by brief vortexing and additional shaking to break up the pellet. This material was then again centrifuged to a pellet, and the wash water was decanted. Next, 25 mL of freshly prepared 0.5 M ammonium sulfate was used to rinse the microwaved and washed pellet directly into an acid washed 50 mL PTFE beaker. A disposable PTFE stir bar was used to stir the sample, and the pH was monitored via a calomel pH meter that had been calibrated using fresh buffer solutions at pH 4 and 7. The pH was adjusted via titration with 10% (v/v) HCl, and samples were taken at various pH points to analyze for REE content in the leach liquor via ICP-MS. During the test, 250 µL samples were taken at each point using disposable polypropylene graduated 1 mL syringes. These aliquots were filtered through 0.22 µm PVDF syringe filters directly into 4.75 mL of 2% (w/v) HNO3 + 0.5% (w/v) HCl solution (5 mL; 20x dilution total) for direct ICP-MS analysis of the leach liquor.

4.2.3. *Solvent Extraction Protocols*

Following the leaching tests, a series of solvent extraction tests were conducted to confirm that high purity REE oxides can be successfully produced from the resulting leach solutions. For this experiment, the BLAM sample was selected as the representative feedstock, as it contains the highest REE content on an ash basis. To prepare the stock leach solution, BLAM was roasted in a muffle furnace in air for 10 hours. The resulting ash was leached with 1 molar nitric acid in a stirred 2 liter flask at a liquid to solid ratio of 10:1 for 24 hours. The

leachate was separated from the ash by centrifugation and the pH was increased to 1.54 by addition of ammonia hydroxide.

Solvent extraction was conducted in three stages: extraction, scrubbing, and stripping. All stages were performed in glass 500 mL separatory funnels and were shaken by a Yamato orbital shaker for 15 minutes at max speed. The solvent used in these tests was kerosene with 0.6M of Bis(2-ethylhexyl) phosphate (DEHPA) and 0.4M n-butyl phosphate (TBP) as an extractant and modifier, respectively. At the end of each stage the spent aqueous phase was removed, and the aqueous phase for the next stage was measured by graduated cylinder and added to the solvent.

The ammonium hydroxide used for this was fisher chemical brand and was certified ACS plus. The TBP came from fisher chemical as well. The concentrated nitric acid used in this process was similarly received from fisher chemical and was certified ACS plus. The DEHPA was purchased from Alfa Aesar and was 95% pure. Assays were only performed on the aqueous phase. All assays were conducted by ICP-MS.

4.2.4. *Data Analysis*

Raw data from the ICP-MS was in parts per billion (nanograms per mL) and for the purposes of simplicity these values were converted to micrograms per gram of sample (PPM). In the cases of a fusion assay these values were then normalized to the whole mass of the sample before ignition for fusion. Extraction recovery was then calculated by comparing the aqueous assay of the leaching solution to the initial REE solids assay.

4.3. Results and Discussion

4.3.1. *Exploratory Tests*

Three different size classes of BLAM sample were evaluated as the BLAM sample is a bulk coal sample and the liberation size for the clay particles within the coal matrix is unknown. Additionally, alternative amine salts were selected to compare with the traditional IX lixiviant, ammonium sulfate. These alternative amines contain long carbon chains which are hydrophobic and should increase the potential of these compounds to adsorb to the clay surface and displace the REE ions (Table 11).

Table 11. Experimental Parameters for Initial Ion Exchange Leaching Tests

Parameter	Test Parameters
Sample	BLAM
Particle Size	-80 mesh, -325 mesh, -10 microns
Leaching Time	1 hour
Acid Dose	0.3 mL of 2% by volume Sulfuric Acid
Lixiviant and Dose	AS: Ammonium Sulfate (0.5M, 1M) TMAC: Tetramethylammonium Chloride (0.5M, 1M) DAH: Dodecylamine Hydrochloride (0.01M, 0.05M) HTAC: Hexadecyltrimethyammonium Chloride (0.01M, 0.05M) TEAC: Tetraethylammonium Chloride (0.5M, 1M)
Modifiers/Pretreatment	None

.

Table 12. Summarized Extraction Data from Ion Exchange Leaching Tests

Parameter	Extraction Efficiency (%)				
	AS	DAH	TMAC	HTAC	TEAC
High Dose	1 M	0.05 M	1 M	0.05 M	1 M
-80 mesh	7.21	7.43	2.02	1.72	8.98
-325 mesh	7.65	5.95	21.81	19.76	10.18
-10 microns	20.75	n.t.	17.99	n.t	14.65
Low Dose	0.5 M	0.01 M	0.5 M	0.01 M	0.5 M
-80 mesh	0.00	0.49	5.12	21.97	14.37
-325 mesh	n.t	12.91	15.60	11.87	17.29
-10 microns	16.12	9.16	17.73	n.t	n.t

n.t. = not tested

As shown in Table 12 BLAM performed best with 1 molar ammonium sulfate after grinding below 10 microns. For the LREEs the trend is true that the smaller the particle size the more efficient the extraction. For many of the heavy elements the -80 mesh sample performed better than the -325 sample.

The results from this initial test series were difficult to interpret. This may be due to significant error during the assay process, experimental error, or variability in the samples. To improve the reproducibility of later tests a new procedure for testing was developed.
If all the initial test results are combined into a single data set, we can confirm that a reduction in particle size does lead to an improvement in recovery (Error! Reference source not found.). The m ost significant improvement occurs between the -80 mesh and -325 mesh data sets, this is more pronounced if the highest value from the -80 mesh data set is excluded.

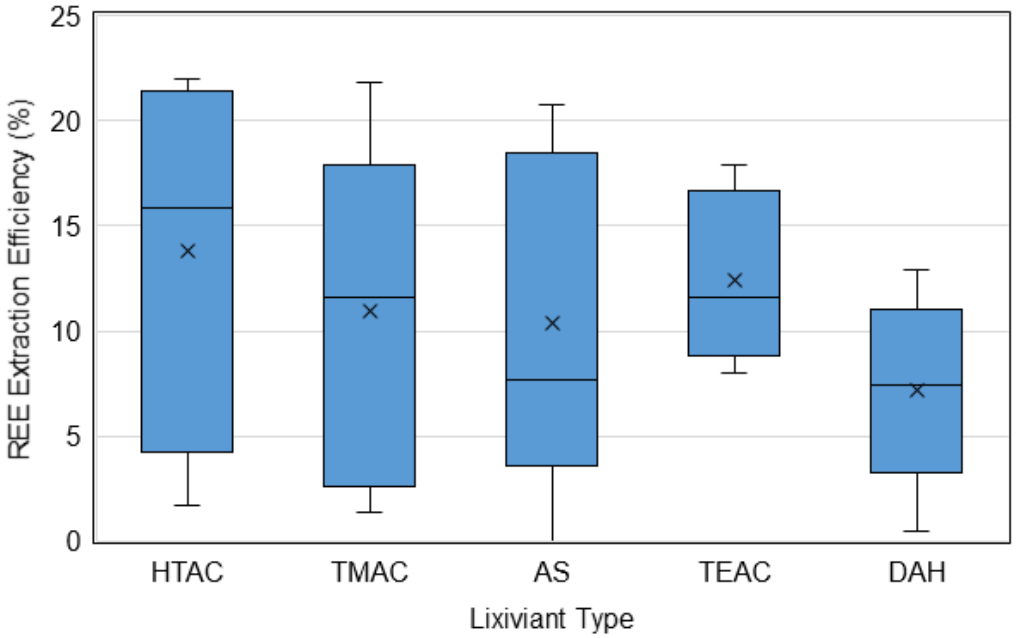

Figure 28. Ion exchange leaching results for all particle sizes (-325 mesh, -80 mesh, -10 microns) and lixiviant doses (0.01 to 1M) categorized by lixiviant type. Sample: BLAM, leaching time: 1 hour, acid dose: 0.3mL of 2% by volume sulfuric.

Figure 29 shows a comparison of the IX extraction efficiency on an element-by-element basis for each lixiviant. Moreover, the specific lixiviant dose shown in Figure 29 corresponds to the best result achieved with the respective lixiviant. As such, this data provides for a fair comparison between the various lixiviants. Unfortunately, ammonium sulfate did not perform well at this test condition, as the median extraction efficiency was only 7.65% at the 1.0 M dose. This particular reagent required finer grind sizes to produce the high extraction efficiency values exceeding 20%. Note that all lixiviants with the exception of DAH performed similarly in this testing. Based on this result ammonium sulfate was selected as the lixiviant to use in further exploratory testing. Interestingly, the data in Figure 29 shows that the differences between ammonium sulfate and the other lixiviants is more noted for the heavy REEs rather than the light

REES. TMAC and HTAC performed very well in extracting heavy REEs, with some recoveries approaching 25%. Unfortunately, the scandium recovery was notable low (<15%) in all cases.

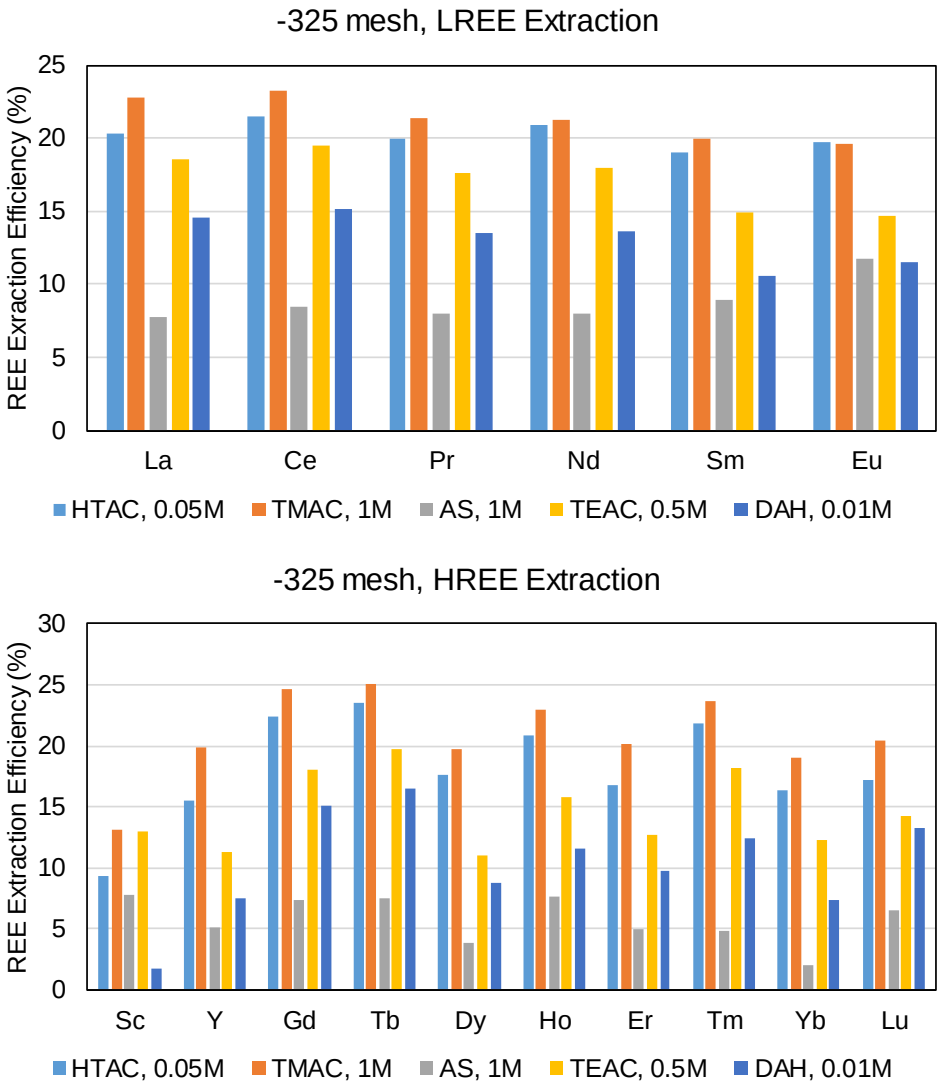

Figure 29. Element-by-element extraction comparison for various lixiviants and doses. Sample: BLAM, leaching time: 1 hour, acid dose: 0.3 mL of 2% by volume sulfuric.

4.3.2. *Kinetics Tests*

A major feature of the ion-exchange reaction is rapid kinetics (Georgiana A. Moldoveanu & Papangelakis, 2013). Therefore, kinetic tests were performed on each sample using a standard ion-exchange lixiviant. To verify the precision of the kinetic testing methods 5 replicates were performed and the CMBTUF sample was randomly chosen. During replicate 4, the burette began leaking titrant into the solution after the 45-minute time point while during replicate 2 the 45

minute time point had a failure in the syringe filter causing solids to be injected into the dilution which prevented ICP-MS analysis from being conducted. Additionally, the first time point on replicate two had a result that was abnormally high and based on the interquartile range was determined to be an outlier. In Figure 30 the individual data points are displayed in green while the averages of each time point group are shown in black.

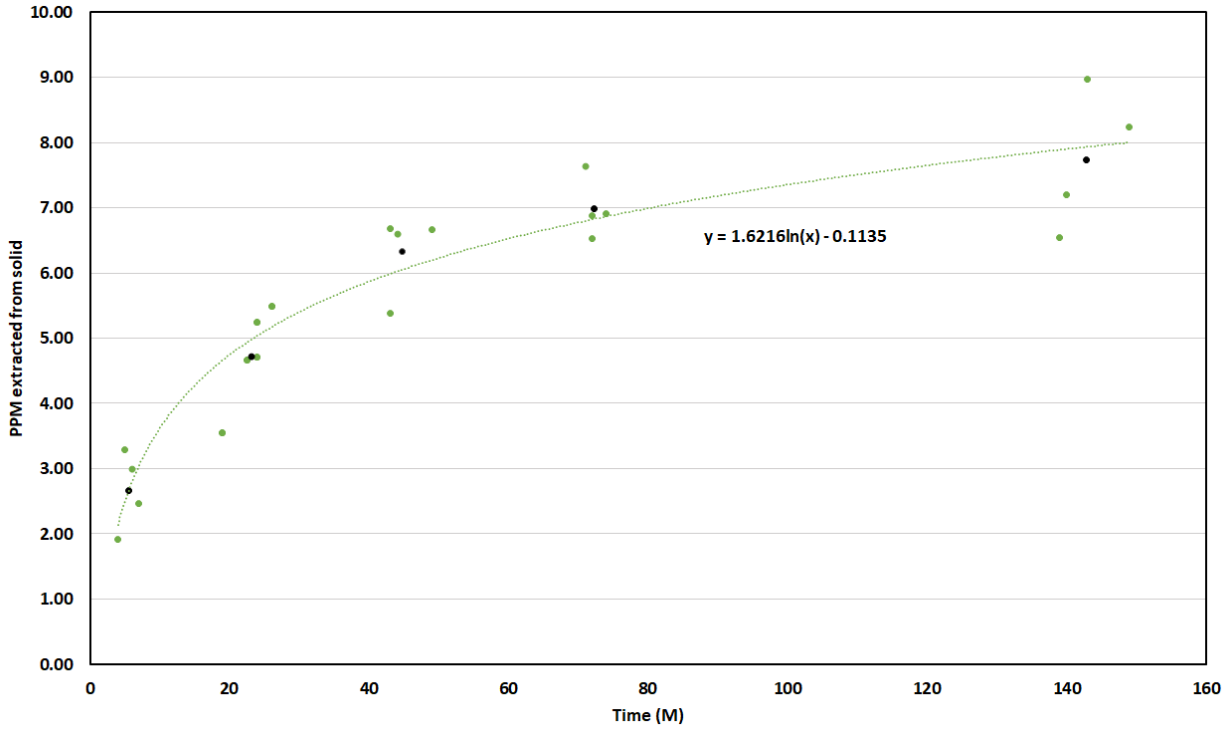

Figure 30. CMBTUF kinetic curve for the average of the 5 tests, the confidence intervals are displayed for each time interval.

Though some degree of the variation between values for each time point can be attributed to the difference in the times between each test the results should give a conservative estimate of the accuracy of the kinetic curves created. Based on the kinetic data collected and the error, the samples can be broken up into three groups: high IX with MCMTUF and CMBTUF, middle IX which includes the remaining thickener underflows with the exception of LTUF, and low IX with the lower ash content coal samples, and LTUF. The lower ash content coals may perform worse due to their hydrophobicity but LTUF's low extraction indicates that it has a low IX phase REEs.

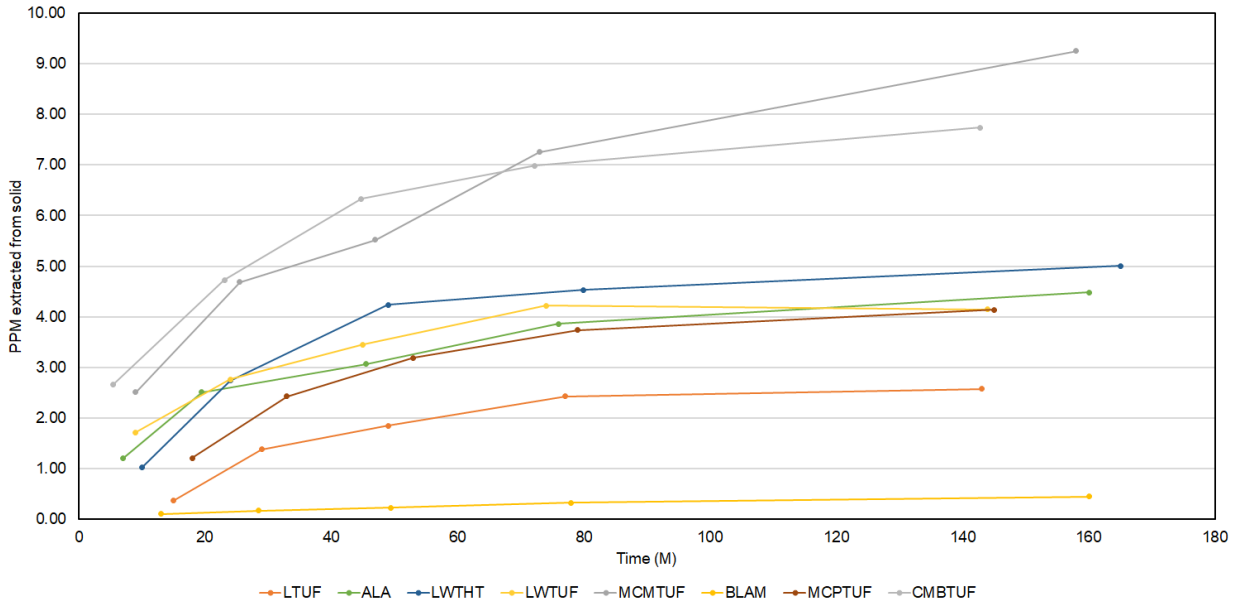

Figure 31. Kinetic curve for ammonium sulfate ion-exchange for all samples as they were received

MCMTUF and CMBTUF had the highest extraction from ammonium sulfate and though they are not significantly different in their final total REE extraction value there is a significant difference in the specific elements extracted (Figure 32).

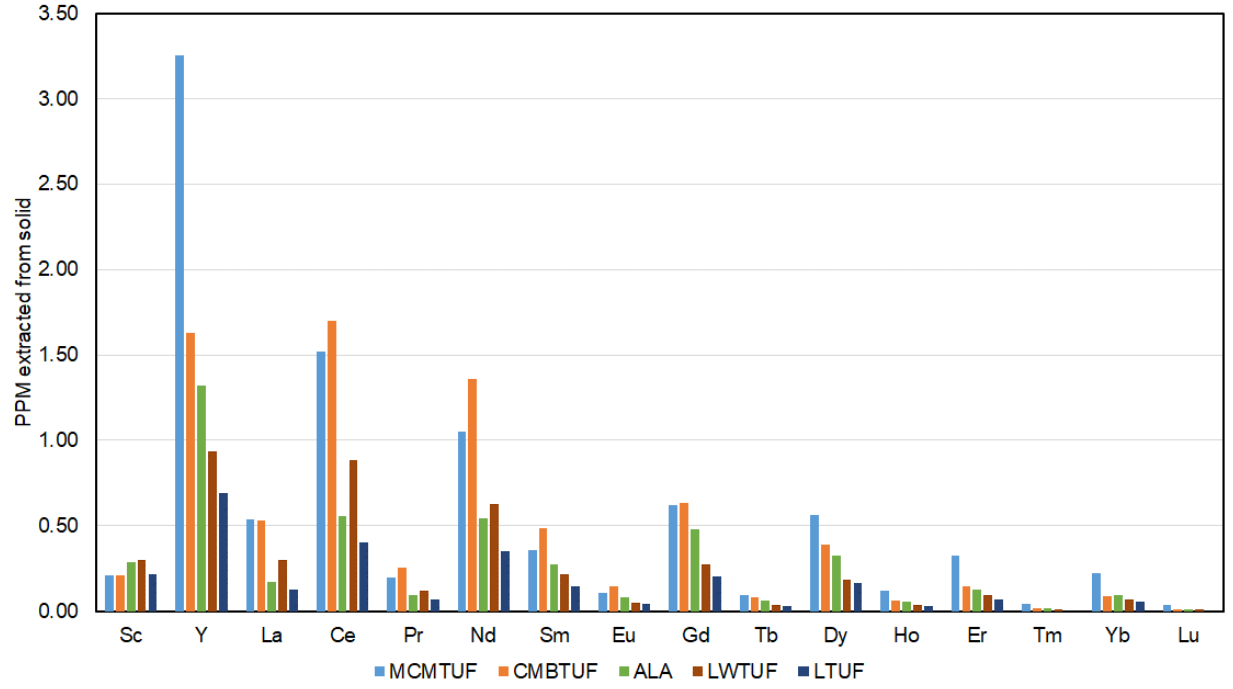

Figure 32. A comparison of the IX performance for MCMTUF and CMBTUF compared to the primary samples focused on during the earlier stages of the research.

The elements extracted from MCMTUF show a distribution approaching the traditional heavy rare earth rich ion exchange clay. This is very pronounced in the difference in exchangeable yttrium, erbium, and ytterbium compared to any of the other tested samples. Additionally, MCMTUF had the highest dissolved calcium in the leach liquor while consuming the second highest amount of acid (1.85mL).

The enhanced extraction observed with the MCMTUF sample occurred despite its similar distribution of REEs as compared to the more heavily investigated LTUF and LWTUF (Figure 33).

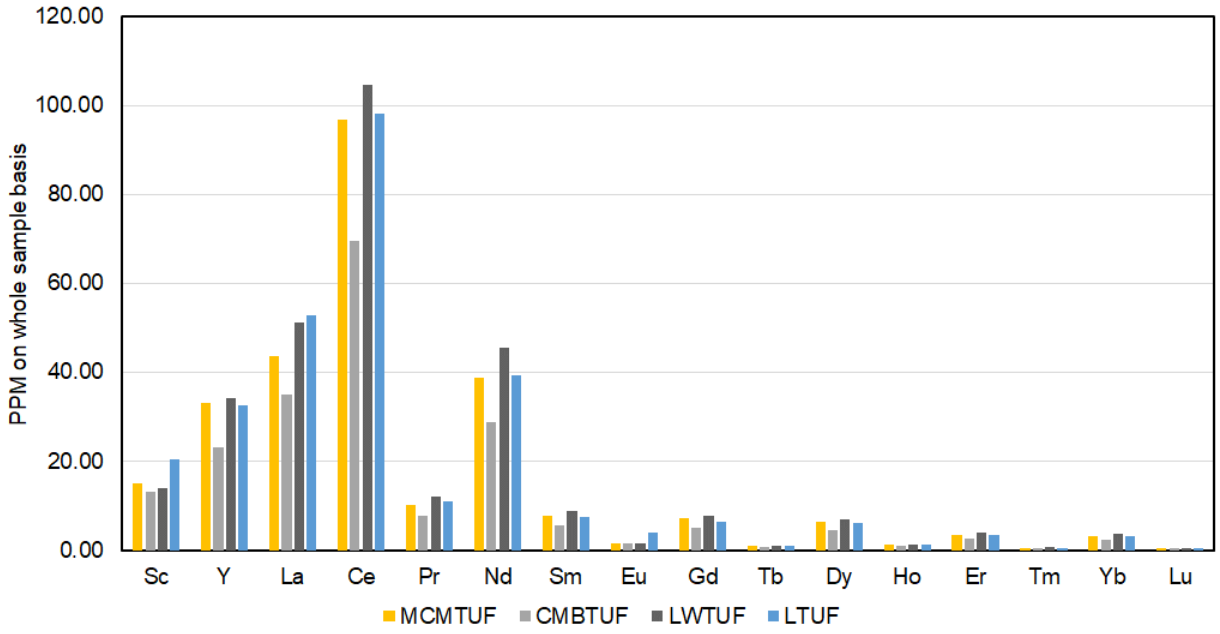

Figure 33. A comparison of the REE content of MCMTUF and CMBTUF compared to the primary samples focused on during the project.

This result could be due to similar mineralogy but the reason for the improved recovery from MCMTUF is not readily apparent. One potential reason could be differences in post depositional environment. One hypothesis is that the increased calcium content in the MCMTUF sample indicates that higher levels of carbonate minerals which would have acted as a buffer preventing acidic ground water from leaching the adsorbed REE species.

4.3.3. *Leaching Additives*

Various studies in the literature have shown that REEs may be bound in iron-oxyhydroxides colloids in ground water systems (Andersson et al., 2006; Ingri et al., 2000). One way to approach to improve the leaching characteristics of these species involves using reducing agents to reduce the iron into a more soluble species. Moreover, chelating agents may also be used increase the kinetics of this process by complexing with the leached iron. This approached, termed Enhanced Reductive Ion Exchange (ERIX) leaching, may be suitable for coal-based REE leaching if the REE species are indeed bound in iron colloids.

The initial tests runs were performed with 0.5M ammonium sulfate (AS) in addition to various concentrations of chelating and reducing agents ranging from 10 mM to 0.5M, depending on the specific reagent. The initial screening tests were conducted at a pH of 3 for 2 hours of leaching time, and a follow-on set of screening tests were conducted at a lower pH of 2. Additional tests were then conducted at both pH 3 and pH 2 for longer durations of 18, 20, and 132 hours. Not all combinations of reagents, pH values, and leaching durations were evaluated, as the individual test series were designed to provide specific information and evaluate ideas derived from prior tests. The results from the 57 screening tests are shown in Table 13**,** note that all PPM values are with respect to amount extracted from the solid unless otherwise noted (e.g. solution concentration or extraction into PLS). Refer to Table 6 for sample rare earth contents.

Table 13. Test series summary for organic acid combinations and reducing agents and their leaching performance on LWTUF, the best extractions from each series is highlighted.

Leaching Lixiviants	TREE Extracted (ppm)				
	pH = 2			pH = 3	
	2 hours	20 hours	132 hours	2 hours	18 hours
H2O	0.72	--	--	0.02	0.67
0.5M AS	11.27	14.17	15.13	2.08	2.16
0.5M AS + 5mM CA	--	--	--	5.07	--
0.5M AS + 5mM OA	--	--	--	2.50	--
0.5M AS + 5mM AA	--	--	--	2.41	--
0.5M AS + 5mM EDTA	--	--	--	5.05	--
0.25M AA	--	3.79	--	--	--
0.25M CA	--	11.34	--	--	--
0.25M AA + 0.25M CA	--	12.47	--	--	--
0.5M AS + 0.25M AA + 0.25M CA	--	13.63	--	--	--
0.5M AS + 10mM DT (DT Solution)	--	--	--	3.99	--
0.5M AS + 100mM DT (DT Solution)	--	--	--	3.24	--
10mM DT (solution)	--	--	--	0.20	0.42
0.5M AS + 10mM DT (DT Powder)	--	--	--	3.53	--
0.5M AS + 100mM DT (DT Powder)	--	--	--	2.36	--
10mM DT (DT Powder)	--	--	--	0.85	0.83
0.5M AS + 10mM DT + 5mM CA	11.26	--	--	6.41	--
0.5M AS + 10mM DT + 5mM OA	0.50	--	--	4.36	--
0.5M AS + 10mM DT + 5mM AA	11.74	--	--	3.79	--
0.5M AS + 10mM DT + 5mM EDTA	11.33	--	--	5.75	--
0.5M AS + 10mM DT + 50mM CA	11.12	--	--	6.41	--
0.5M AS + 10mM DT + 50mM OA	0.86	--	--	0.77	--
0.5M AS + 10mM DT + 50mM AA	12.56	--	--	7.27	--
0.5M AS + 10mM DT + 50mM EDTA	11.57	--	--	5.92	--
0.5M AS + 10mM DT + 250mM CA	11.95	--	--	--	--
0.5M AS + 10mM DT + 250mM OA	2.95	--	--	--	--
0.5M AS + 10mM DT + 250mM AA	12.09	--	--	--	--
0.5M AS + 10mM DT + 250mM EDTA	10.00	--	--	--	--
0.5M AS + 100mM DT + 5mM CA	--	--	--	3.43	8.65
0.5M AS + 100mM DT + 5mM OA	--	--	--	0.55	0.72
0.5M AS + 100mM DT + 50mM CA	--	--	--	5.84	3.72
0.5M AS + 100mM DT + 50mM CA + 10% EtOH	--	--	--	3.87	--
0.5M AS + 100mM DT + 50mM EDTA	--	--	--	--	5.06
0.5M AS + 50mM HA	11.28	--	--	--	--
0.5M AS + 50mM HA + 50mM CA	11.61	--	--	--	--
0.5M AS + 0.5M HA	--	--	14.23	--	--
0.5M AS + 0.5M HA + 0.25M CA		--	16.00	--	--
0.5M AS + 0.5M HA + 0.25M AA	--	--	17.79	--	--

Notes: Total feed concentration = 221.3 ppm; Highlight = maximum value in each column

CA = Citric acid
OA = Oxalic acid
AA = Ascorbic acid
EtOH = Ethanol
EDTA = Ethylenediaminetetraacetic acid
DT = Sodium dithionite
AS = Ammonium sulfate
HA = hydroxylamine hydrochloride

While the overall extraction efficiencies for all tests are quite low (<5%), it should be noted that no attempt was made to optimize the process or determine the best conditions for leaching. Instead, the intent was to identify trends to determine if a particular combination of

reagents provides a significant benefit above standard AS leaching. For the pH = 3 test series, the best extraction was found when using 0.5M AS + 10mM DT + 50mM AA. The REE mass extracted by this method (7.27 ppm) is approximately 3.5 times the amount extracted using AS alone. The same reagent combination also provided the highest extraction efficiency in the pH = 2 leaching group; however, this value (12.56 ppm) was only marginally higher than the AS alone. At these lower pH values, DT quickly oxidized, which was evident from the rapid color change of the solution after the addition of the DT stock. In addition, the results at pH = 2 are more closely grouped, indicating that increased acid dose may be overwhelming the contribution from the various lixiviants. The longer duration tests of 18 and 20 hours also indicated that at least one combination of reducing and chelating agents outperformed AS alone. For example, at 18 hours of leaching time and a pH of 3, 0.5M AS + 100mM DT + 5mM CA extracted 4 times the REE mass when compared to AS alone (8.65 ppm vs. 2.16 ppm). While the overall extraction efficiency is low, these results are promising and may provide further evidence that the colloidal phase is a significant component of REEs in coal.

4.3.4. *Gas Purging*

A kinetic test was performed on the LWTUF sample using a combined CO_2 and N_2 gas with a sodium borohydride/sodium bisulfate reducing agent and ammonium citrate as the lixiviants Figure 34.

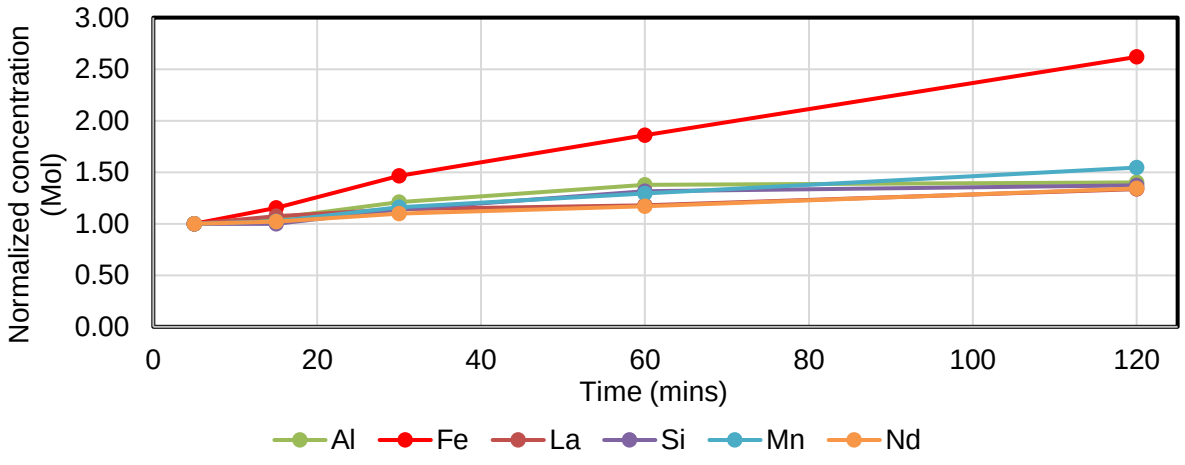

Figure 34. Molar ratio in solution assays taken from kinetic study on LWTUF, all results normalized to the concentration at 5 minutes.

The results of the test indicate that primarily iron and manganese are being extracted from the sample and that the reaction is still continuing after two hours. The high iron extraction is due to the reducing environment and acidic conditions which result in high iron hydroxide solubility. Additionally, aluminum and lanthanum have a directly related extraction performance.

The first series was run on decanted centrifuge pellets of blunged LTUF solids. This test had a series of three ammonium sulfate tests with carbon dioxide at ascending pH's from 3 to 5 determined by litmus paper and adjusted with 1M HCl. Unexpectedly, the pH 5 test, which required no addition of acid, performed the best. Of all the ammonium compounds tested the AS and ACDB test with carbonation performed the best with a recovery of 2.03%. It should be noted that the 2M HCl even over a period of 68 hours only succeeded in extracting approximately 5% of the TREE in LTUF which indicates that the majority of the samples REE content is not colloidal phase (Table 14).

Table 14. Extraction tests with decanted blunged LTUF pellets

Leaching Lixiviants	Duration (hrs)	Recovery (%)
H2O	68	0.66
Carbonated Water	68	0.00
1M AS	68	0.00
1M AS	68	0.04
1M AS	68	0.96
0.5M AS + Carbonated Water + 0.5M ACDB	68	2.03
0.5M HCl	68	3.30
0.8M HCl	68	4.37
2M HCl	68	4.97
1M AS	68	0.00
1M ACDB	68	1.81
0.5M HCl	68	3.37
0.8M HCl	68	4.32
2M HCl	68	4.74
Blunging slurry water	68	2.77
H2O	22	0.00
0.1M ACDB	22	0.08
0.5M ACDB	22	0.09
1M ACDB	22	0.08
0.3M AMP + 0.6M MeOH	22	0.00
0.01M DAH + 1.2M MeOH	22	0.00
3M AMP + 6M MeOH	22	0.00
1M AS	22	0.06
0.3M AMP + 0.6M MeOH + 5% HCl	22	0.23
0.01M DAH + 1.2M MeOH + 5% HCl	22	0.22
3M AMP + 6M MeOH + 5% HCl	22	0.19

Based on the results of this test series, carbonic acid and bicarbonate does not appear to improve the recovery of lanthanides by itself. When combined with ammonium compounds it does outperform ammonium sulfate alone which could be attributed to the increased acidity provided by the carbonic acid.

The second series used the blunged LTUF slurry without any dewatering. The blunging slurry water sample received no added reagents and contained more REEs and higher levels of aluminum and silica than all other samples including the acid leaching tests. This could indicate that the blunging process is extracting the exchangeable REEs. Additionally, the blunging slurry water had only 14.7% of the iron that was present in the 0.5M acid leaching test while extracting only 17.8% less REE (Table 15). The blunging slurry water was second only to acid leaching in

recovery. This could be due to the dispersion process releasing a small amount of sub-micron rare earth mineral particles into solution.

Table 15. Extraction tests with blunged LTUF slurry

Leaching Lixiviants	Sc (ppm)	Y (ppm)	La (ppm)	Ce (ppm)	Pr (ppm)	Nd (ppm)	Sm (ppm)	Eu (ppm)	Gd (ppm)	Tb (ppm)	Dy (ppm)	Ho (ppm)	Er (ppm)	Tm (ppm)	Yb (ppm)	Lu (ppm)	TREE (ppm)
1M AS	ND	ND	ND	ND	ND	ND	ND	ND	ND	ND	ND	ND	ND	ND	ND	ND	0.00
1M ACDB	1.49	1.94	ND	0.21	0.07	0.62	0.32	0.11	0.53	0.08	0.44	0.08	0.20	0.03	0.16	0.02	6.32
0.5M HCl	2.06	3.05	0.32	1.44	0.22	1.33	0.52	0.15	0.76	0.13	0.77	0.15	0.41	0.06	0.37	0.05	11.79
0.8M HCl	2.79	3.59	0.56	2.07	0.32	1.76	0.64	0.18	0.91	0.15	0.91	0.18	0.49	0.07	0.42	0.06	15.11
2M HCl	3.23	3.66	0.73	2.50	0.35	1.89	0.69	0.19	0.95	0.16	0.94	0.18	0.50	0.07	0.45	0.07	16.57
Blunging slurry water	1.06	0.56	1.77	3.57	0.38	1.53	0.25	0.05	0.18	0.02	0.12	0.03	0.07	ND	0.08	ND	9.68

The third series of tests was performed for only 22 hours and made use of other lixiviants investigated during earlier quarters and ACDB. Once again, the ACDB tests showed increased extraction vs AS. This decrease in REE in the solution after 30 minutes to an hour is noted in previous work and is likely due to hydrolysis of the lanthanide ions. ACDB appears to prevent REE ions from precipitating likely due to the chelating effects of dibasic citrate (Table 16).

Table 16. Extraction tests with decanted blunged LTUF pellets

Leaching Lixiviants	Sc (ppm)	Y (ppm)	La (ppm)	Ce (ppm)	Pr (ppm)	Nd (ppm)	Sm (ppm)	Eu (ppm)	Gd (ppm)	Tb (ppm)	Dy (ppm)	Ho (ppm)	Er (ppm)	Tm (ppm)	Yb (ppm)	Lu (ppm)	TREE (ppm)
H2O	ND	ND	ND	ND	ND	ND	ND	ND	ND	ND	ND	ND	ND	ND	ND	ND	0.00
0.1M ACDB	0.07	0.07	0.01	0.03	0.00	0.03	0.01	0.00	0.02	0.00	0.02	0.00	0.01	0.00	0.01	ND	0.28
0.5M ACDB	0.08	0.08	0.01	0.03	0.01	0.03	0.01	0.00	0.02	0.00	0.02	0.00	0.01	0.00	0.01	0.00	0.32
1M ACDB	0.08	0.07	0.01	0.03	0.01	0.03	0.01	0.00	0.02	0.00	0.02	0.00	0.01	0.00	0.01	ND	0.30
0.3M AMP + 0.6M MeOH	ND	ND	ND	ND	ND	ND	ND	ND	ND	ND	ND	ND	ND	ND	ND	ND	0.00
0.01M DAH + 1.2M MeOH	ND	ND	ND	ND	ND	ND	ND	ND	ND	ND	ND	ND	ND	ND	ND	ND	0.00
3M AMP + 6M MeOH	ND	ND	ND	ND	ND	ND	ND	ND	ND	ND	ND	ND	ND	ND	ND	ND	0.00
1M AS	0.01	0.07	0.00	0.02	0.00	0.03	0.01	0.00	0.02	0.00	0.02	0.00	0.01	0.00	0.01	ND	0.22

The final series of tests took the pellet from the previous AMP and DAH tests and leached them with 1.6M HCl for an additional 22 hours. This was done to see if the alkaline AMP and DAH solutions had converted the REEs into an acid extractable hydroxide form (Table 17).

Table 17. Second stage extraction tests with decanted blunged LTUF pellets

Leaching Lixiviants	Sc (ppm)	Y (ppm)	La (ppm)	Ce (ppm)	Pr (ppm)	Nd (ppm)	Sm (ppm)	Eu (ppm)	Gd (ppm)	Tb (ppm)	Dy (ppm)	Ho (ppm)	Er (ppm)	Tm (ppm)	Yb (ppm)	Lu (ppm)	TREE (ppm)
0.3M AMP + 0.6M MeOH + 5% HCl	0.16	0.15	0.04	0.13	0.02	0.10	0.03	0.01	0.05	0.01	0.04	0.01	0.02	0.00	0.02	0.00	0.80
0.01M DAH + 1.2M MeOH + 5% HCl	0.15	0.15	0.03	0.11	0.02	0.09	0.03	0.01	0.05	0.01	0.04	0.01	0.02	0.00	0.02	0.00	0.76
3M AMP + 6M MeOH + 5% HCl	0.12	0.13	0.03	0.11	0.02	0.08	0.03	0.01	0.04	0.01	0.04	0.01	0.02	0.00	0.02	0.00	0.65

The results of these tests on LTUF show that it is an inferior feedstock as compared to LWTUF as the best result with acid leaching on LTUF extracts less than 5% of the TREE over 68 hours while standard IX with AS can extract 7.4% of the TREE content in LWTUF in 19 hours. The LTUF sample may be reacting differently to the dispersive liberation process than

LWTUF. This is supported by the results in Table 15 on the blunging slurry water which contains elevated amounts of REEs. These results also indicate that carbon dioxide inhibits the extraction of REEs by ammonium sulfate.

4.3.5. *Chemical Pretreatment*

Based the prior results, the sodium acetate and acetic acid remove significant levels of calcium and magnesium from the solid, 4382 and 371 ppm, respectively. Calcium and magnesium are present in significant levels in the ALA sample as well as others; these ions also act as hard acids and likely inhibit the extraction of lanthanides by competing for ligands and lixiviants. The polyphosphate leaching stage is able to more effectively extract the middleweight REEs, especially neodymium, as compared to leaching with AS at 0.5 M (Figure 35). Additionally, the two-stage extraction is more selective in which cations are released from the solid (Figure 36). The reduction in the amount of iron and aluminum in solution is likely due to precipitation as hydroxides at the elevated pH. Considering iron contamination is a major concern for downstream processes, reducing iron content in the leach solution is an important factor.

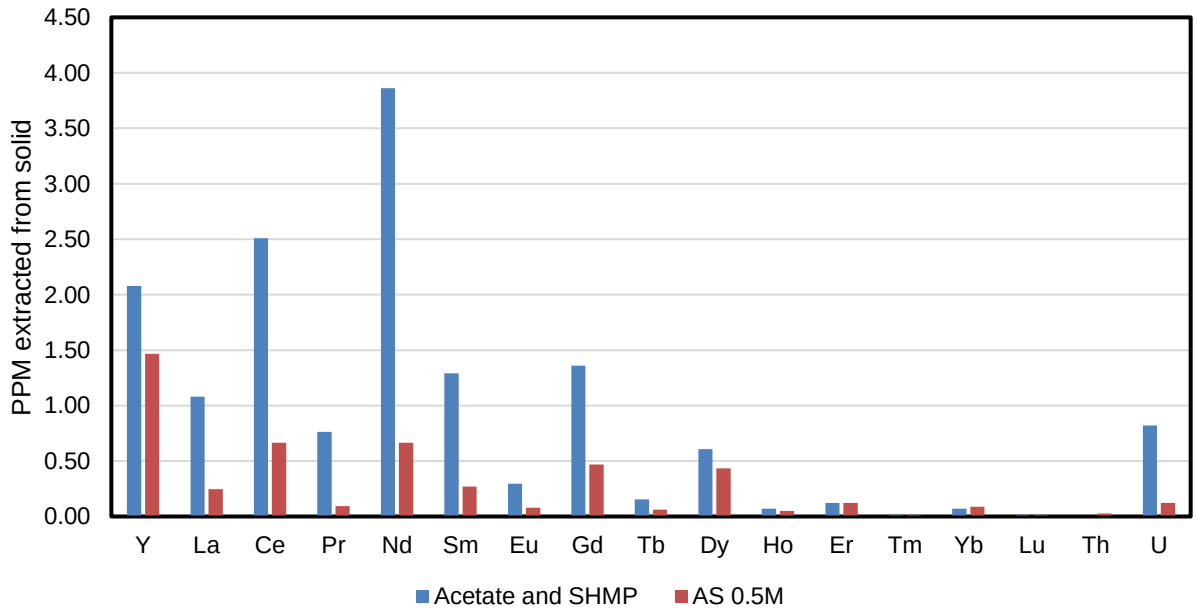

Figure 35. Comparison between AS 0.5M ion exchange at pH 4 and the two stage acetate and SHMP leaching. Note the Y-axis is in PPM not percent recovery.

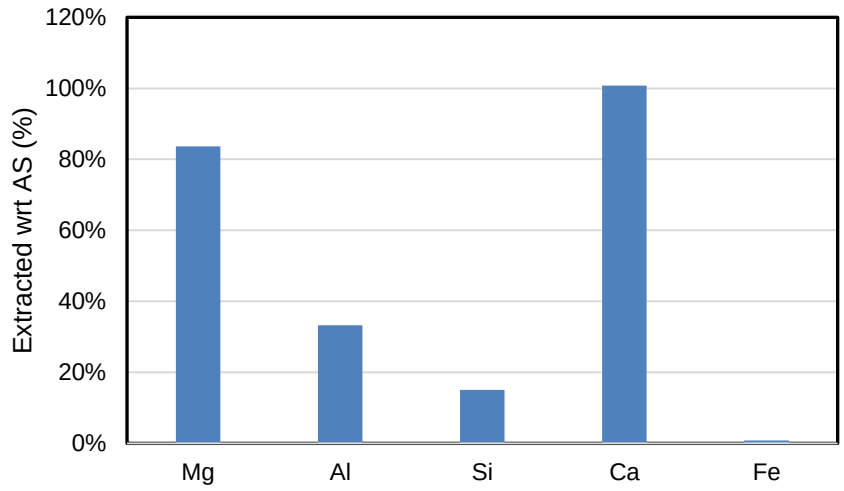

Figure 36. Differences in selected contaminants between AS and the two stage leaching process.

4.3.6. *Alkaline Pretreatment*

Figure 37 compares the effect of an 80°C NaOH treatment for 2 hours vs. an 80°C KOH exposure for 2 hours and a 180°C KOH treatment for 10 minutes. These results clearly show the impact of temperature on the final REE extraction efficiency. For the KOH treated samples, the 180°C solution was able to achieve a recovery nearly 3.5x higher than that of the 80°C solution. Note that the decrease in recovery for the sample pretreated with NaOH at 80°C was most likely caused by the pH climbing over 4.0 after the 3rd time point. Additionally, the aluminum dissolution caused by the 180°C solution was significantly greater, indicating that this condition is more efficient at breaking down the clay matrix and transforming the alumina into an exchangeable form (Figure 38). The results from these tests demonstrate the significant improvement that an alkaline pretreatment has on the recovery of REEs from the LWTUF. Based on the dramatic increase in recovery one can conclude that potentially upwards of 60% of the rare earth content is in a mineral form (Figure 39). The use of strong alkalis increasing recoveries is additional evidence for REE-phosphates being a significant fraction of the REEs in LWTUF.

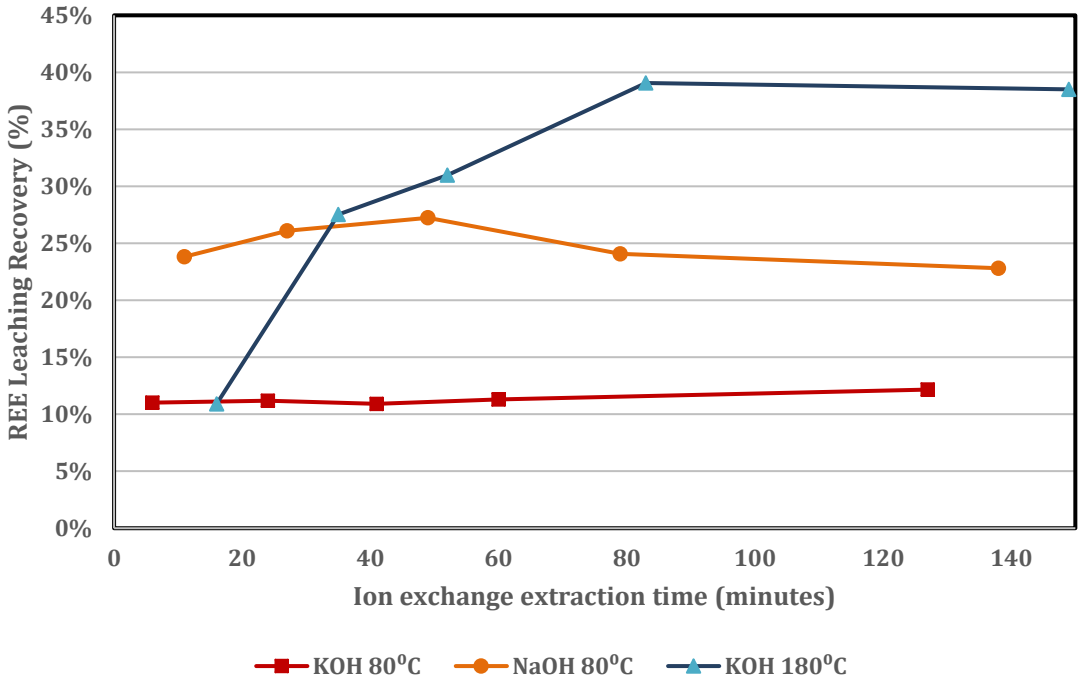

Figure 37. TREE extracted into the pregnant leach liquor solution (PLS, orange) over time after alkali pretreatment.

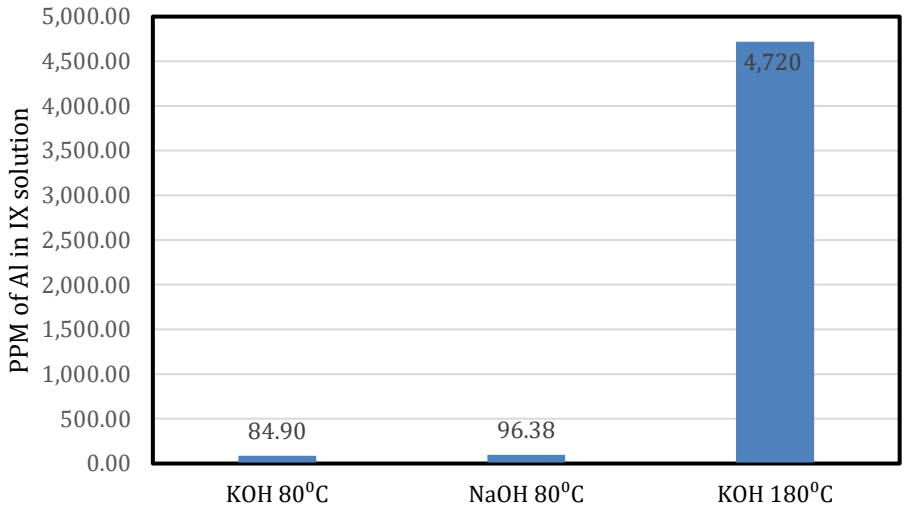

Figure 38. Total aluminum extracted during heated KOH and NaOH pretreatment tests. LWTUF sample.

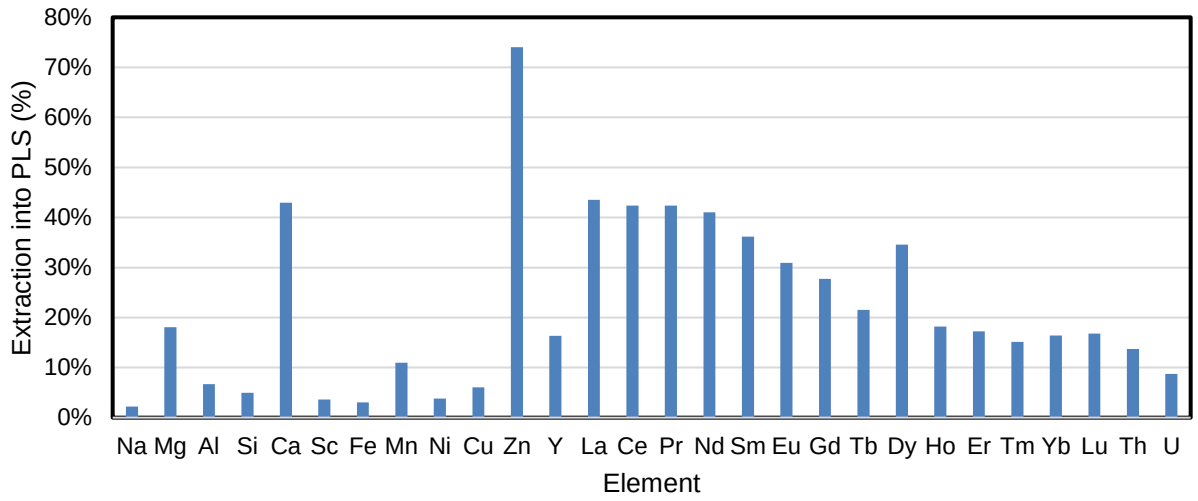

Figure 39. Elemental breakdown of ion-exchangeable fractions extracted from LWTUF based on the lithium meta-borate fusion feed assay.

4.3.7. *Solvent Extraction*

Figure 40 shows the flowsheet that was used for the solvent extraction tests along with the mass balance from the most favorable test result. Moreover, Figure 41 and Figure 42 show the element-by-element concentration ratios for REEs and gangue, respectively. On this plot, a value greater than 1.0 indicates that the element has been enriched through the process, while a number less than 1 indicates that the element has been rejected.

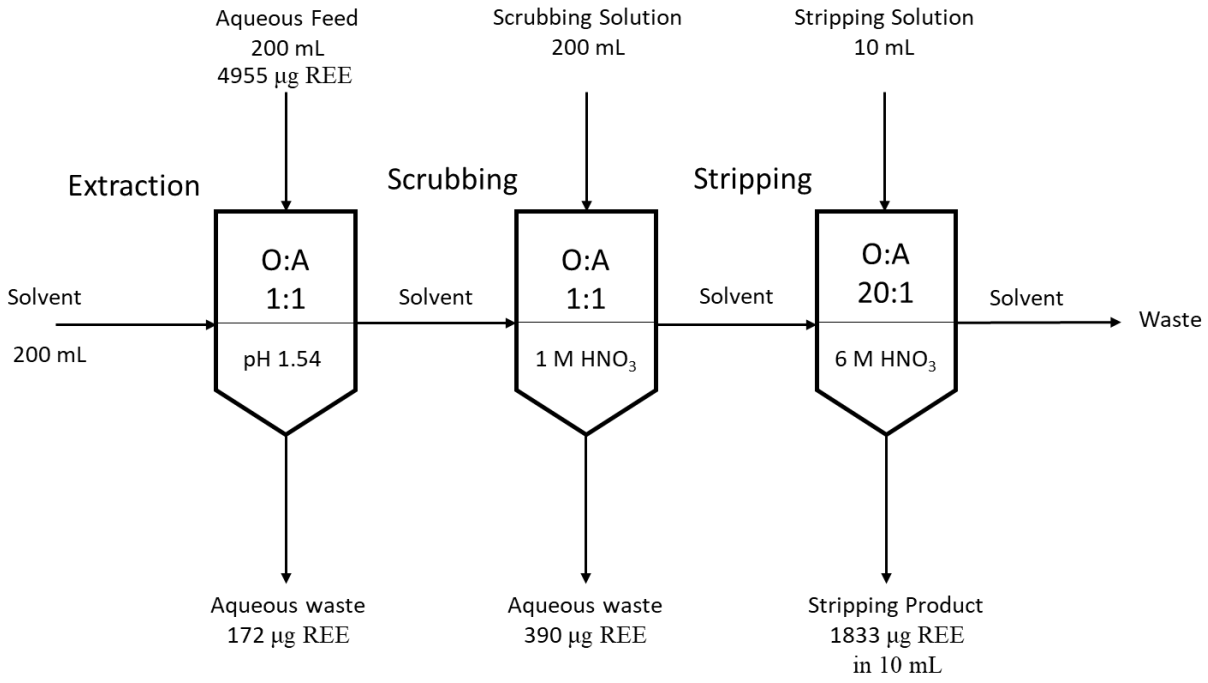

Figure 40. Solvent extraction process flowsheet.

As shown in Figure 41, a large portion of rare earths (particularly Yttrium and Scandium) were retained in the strip solution and not recovered to the concentrate. Nevertheless, the solvent extraction process showed strong selectivity of REEs over major gangue metals. All gangue elements except for Ca and Zn were successfully rejected, while the REEs, particularly LREEs were concentrated by a factor approaching 8.0. The ratio of REEs to total cations in the strip solution was determined to be 18%. Assuming full precipitation with oxalic acid and full conversion of oxalate to oxide in roasting, this value indicates that a final REE concentrate of 15 to 18% in TREE is achievable. Unfortunately, this value could not be validated as the small solution volumes did not produce sufficient solid mass needed for a solid-phase assay.

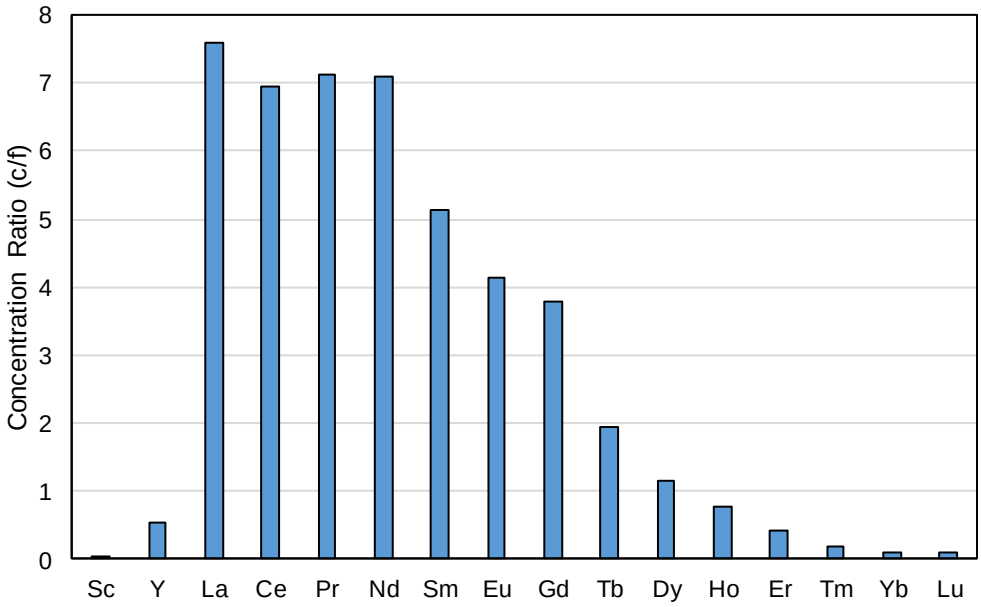

Figure 41. Element-by-element enrichment ratio of REEs for solvent extraction of BLAM leachate. 0.6M DEHPA and 0.4M TBP in kerosene. O:A = 1:1 extraction, 1:1 scrubbing with 1.0M HNO3, 20:1 stripping with 0.6M HNO3.

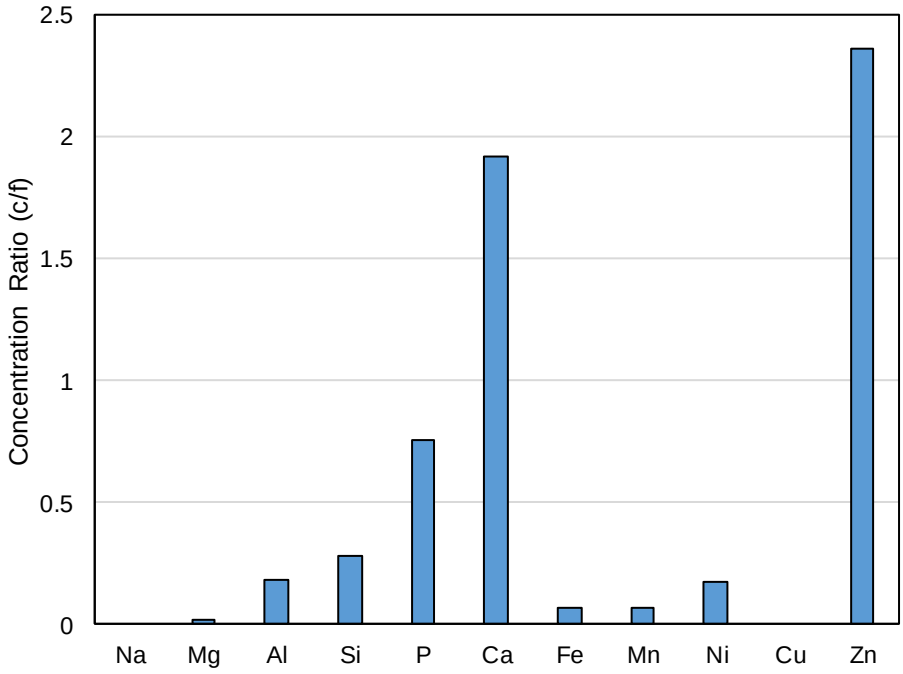

Figure 42. Element-by-element enrichment ratio of REEs for solvent extraction of BLAM leachate. 0.6M DEHPA and 0.4M TBP in kerosene. O:A = 1:1 extraction, 1:1 scrubbing with 1.0M HNO3, 20:1 stripping with 0.6M HNO3.

4.4. Summary and Conclusions

From the experimental work in this chapter, six key conclusions are derived:

- Standard ion exchange leaching using an ammonium sulfate lixiviant was shown to be ineffective at extracting REEs from the various thickener underflow samples evaluated in this study.
- The kinetics of the ion-exchange reactions evaluated in this study were found to be much slower than the reaction involving ion-adsorbed clays described in the literature.
- Alternative amine-based lixiviants were able to outperform ammonium sulfate as a leaching lixiviant by providing a similar extraction efficiency at a lower dose.
- Reductive leaching additives and purges gases showed only showed marginal improvement in REE extraction efficiencies when compared to baseline tests with ammonium sulfate.
- Alkaline pretreatment was found to be the best method to activate REEs and covert them to an ion-exchangeable phase.
- Solvent extraction tests confirmed that the leachates generated in this project can be successfully concentrated to produce high grade mixed rare earth oxide products. Results from an optimal test showed that a strip solution with a ratio of REEs to major metals of 18% was obtained.

Chapter 5. Summary and Conclusions

5.1. Summary

This research was conducted in the interest of exploring the potential of coal associated feed-stocks for economical rare-earth-element recovery by ion-exchange leaching. The samples selected for this project were obtained from a variety of locations but were focused on the northern, central, and southern Appalachian coal basins as the extensive presence of granite in close proximity to the coal seams could act as a source of detrital rare earth minerals. The majority of the obtained samples were obtained from thickener underflow streams as the material was already of a fine size which concentrates the clay fraction of the coal waste material. The testing progressed in the following manner: initial sample acquisition, exploratory ion-exchange leaching with various lixiviants, process improvement by organic acid addition, feed-stock improvement by dispersive liberation, and sample pretreatment by alkaline solutions.

At the inception of this research the first sample to be characterized and tested was the BLAM sample. Additional samples that were obtained and characterized during the initial phase of research include thickener underflow samples: LWTUF, MCMTUF, MCPTUF, TCATUF, TCBTUF, CMBTUF, and LTUF. During the course of this work further ALA was also included after it was received. The majority of the research focused on the LWTUF sample as it had the highest REE content of the originally received samples.

A dispersive liberation process was adapted from the clay industry to isolate and concentrate the clay minerals away from siliceous gangue. This process leads to an enriched REE content in the final fine clay product suggesting that the REEs are primarily associated with clay minerals. Of the five samples tested, all showed at least a 25% increase in feed REE concentration after dispersive liberation. The best result showed an increase of over 130%. SEM-EDS analysis of dispersed LWTUF samples identified REE-phosphate deposits associated with alumino-silicate particles.

The initial exploratory IX leaching tests were used to evaluate the influence of particle size, lixiviant type, and lixiviant concentration on extraction efficiency. Initial efforts in this series focused on the BLAM sample, and the REE extraction efficiencies were somewhat low, averaging only 11%, with a low of 0% and a high of 21%. All reagents performed better after grinding below 325 mesh and in the case of ammonium sulfate performed best at -10 micron. At -325 mesh TMAC and HTAC performed the best with recoveries close to 25% for certain

HREEs. Additionally, TMAC and HTAC were used at doses an order of magnitude less than ammonium sulfate.

To increase the recoveries a series of compounds were tested in conjunction with ammonium sulfate at lower pH ranges to improve the ability of the leach liquor to attack iron hydroxides that could potentially be encapsulating REEs. The compounds tested included both reducing agents and chelating agents. The addition of dithionite and citric or ascorbic acid did marginally improve recovery of rare earth elements from the LWTUF sample used in the test series but overall recoveries remained low.

The final series of extraction tests was performed using an alkaline pretreatment to both convert rhabdophane (hydrated REE phosphate) into rare earth hydroxide and also effectively disperse the clay in the samples. A set of tests were run with both KOH and NaOH at 80ºC and NaOH was shown to be the superior alkali for pretreatment with overall rare earth recoveries reaching approximately 27% on blunged LWTUF samples. At 180ºC this extraction could be improved to 39% at the cost of massively increasing the aluminum dissolved and therefore the alkali consumption. One unique characteristic of this extraction was that despite the low efficiency at extracting most HREEs dysprosium had a recovery more similar to the LREEs.

5.2. Conclusions

Based on the experimental results in this study, a number of general conclusions can be drawn:

1. Ammonium salt-based ion exchange leaching was ineffective at recovering REEs from fine coal refuse.
2. The dispersive liberation process was effective in removing siliceous gangue. The final product from the process was enriched in REEs and clays. All samples that underwent this process showed at least a 25% increase in REE concentration with the best result increasing the concentration to over 130%.
3. Reductive leaching and other leaching additives demonstrated only slight improvements over ammonium salt-based ion exchange leaching for the samples evaluated in this study.
4. Alkaline pretreatment of the feedstocks significantly improved the performance of ammonium salt-based ion-exchange leaching.

5. Solvent extraction tests confirmed that the leachates generated in this project can be successfully concentrated to produce high grade mixed rare earth oxide products.

5.3. Recommendations for future work

Based on the results from the above experiments there is potential in coal waste products as economical sources of REEs though further investigations are necessary.

1. A geological study to better understand the modes of occurrence of REEs in coal and associated processing waste streams.
2. Full scale parametric dispersive liberation testing of a high clay/ high REE feedstock with differing dispersants to identify optimal conditions for concentrating exchangeable or colloidal phase REEs.
3. Further optimization of the leaching process to either reduce the required concentration of alkaline materials or explore alternative pretreatment methods that reduce overall processing costs.

References

Akah, A. (2017). Application of rare earths in fluid catalytic cracking: A review. *Journal of Rare Earths*, *35*(10), 941–956. https://doi.org/10.1016/S1002-0721(17)60998-0

Alonso, E., Sherman, A. M., Wallington, T. J., Everson, M. P., Field, F. R., Roth, R., & Kirchain, R. E. (2012). Evaluating rare earth element availability: A case with revolutionary demand from clean technologies. *Environmental Science and Technology*. https://doi.org/10.1021/es203518d

Andersson, K., Dahlqvist, R., Turner, D., Stolpe, B., Larsson, T., Ingri, J., & Andersson, P. (2006). Colloidal rare earth elements in a boreal river: Changing sources and distributions during the spring flood. *Geochimica et Cosmochimica Acta*, *70*(13), 3261–3274. https://doi.org/https://doi.org/10.1016/j.gca.2006.04.021

Bao, Z., & Zhao, Z. (2008). Geochemistry of mineralization with exchangeable REY in the weathering crusts of granitic rocks in South China. *Ore Geology Reviews*, *33*(3–4), 519–535. https://doi.org/10.1016/j.oregeorev.2007.03.005

Bauer, D., Diamond, D., Li, J., McKittrick, M., Sandalow, D., & Telleen, P. (2011). Critical materials strategy. In *Critical Materials Strategy*.

Bentouhami, E., Bouet, G. M., Meullemeestre, J., Vierling, F., & Khan, M. A. (2004). Physicochemical study of the hydrolysis of Rare-Earth elements (III) and thorium (IV). *Comptes Rendus Chimie*, *7*(5), 537–545. https://doi.org/10.1016/j.crci.2004.01.008

Bohor, B. F., & Triplehorn, D. M. (1993). Tonsteins: altered volcanic-ash layers in coal-bearing sequences. *Tonsteins: Altered Volcanic-Ash Layers in Coal-Bearing Sequences*.

Bryan, R. C., Richers, D., & Ackman, T. (2015). *Study on the Utilization of Portable Hand-Held XRF Spectroscopy as a Screening Tool for Rare Earth Elements in Coal and Coal Waste Products*.

Bryan, R. C., Richers, D., Anderson, H. T., & Gray, T. (2015). Assessment of Rare Earth Elemental Contents in Select United States Coal Basins. *Tetra Tech*, *January*, 1–47. https://edx.netl.doe.gov/ree/?p=1385

Chang, P. (1995). Mineralogy and geology of rare earths in China. In *Science Press*. Science Press.

Chehreh Chelgani, S., & Hower, J. C. (2018). Estimating REY content of eastern Kentucky coal samples based on their associated ash elements. *Journal of Rare Earths*, *36*(11), 1234–1238. https://doi.org/10.1016/j.jre.2018.02.015

Chen, K., Pei, J., Yin, S., Li, S., Peng, J., & Zhang, L. (2018). Leaching behaviour of rare earth elements from low-grade weathered crust elution-deposited rare earth ore using magnesium sulfate. *Clay Minerals*. https://doi.org/10.1180/clm.2018.37

Chi, R., Li, Z., Peng, C., Zhu, G., & Xu, S. (2005). Partitioning properties of rare earth ores in China. *Rare Metals*.

Coppin, F., Berger, G., Bauer, A., Castet, S., & Loubet, M. (2002). Sorption of lanthanides on smectite and kaolinite. *Chemical Geology*. https://doi.org/10.1016/S0009-2541(01)00283-2

Dai, S., Graham, I. T., & Ward, C. R. (2016). A review of anomalous rare earth elements and yttrium in coal. In *International Journal of Coal Geology*. https://doi.org/10.1016/j.coal.2016.04.005

Drew, L. J., Qingrun, M., & Weijun, S. (1990). The Bayan Obo iron-rare-earth-niobium deposits, Inner Mongolia, China. *Lithos*, *26*(1–2), 43–65. https://doi.org/10.1016/0024-4937(90)90040-8

Foley, N., & Ayuso, R. (2015). REE enrichment in granite-derived regolith deposits of the Southeastern United States: Prospective source rocks and accumulation processes. *Strategic and Critical Materials Proceedings*.

Franus, W., Wiatros-Motyka, M. M., & Wdowin, M. (2015). Coal fly ash as a resource for rare earth elements. *Environmental Science and Pollution Research*. https://doi.org/10.1007/s11356-015-4111-9

Fuguo, L., Guohua, G., Li, H., Yanfei, X., Run, Y., & Kaizhong, L. (2018). Compound leaching of rare earth from the ion-adsorption type rare earth ore with magnesium sulfate and ascorbic acid. *Hydrometallurgy*, *179*(156), 25–35. https://doi.org/10.1016/j.hydromet.2018.05.027

Gallezot, P., Feron, B., Bourgogne, M., & Engelhard, P. (1989). Hydrothermal Aging of Cracking

Catalysts. IV – Destabilizing Effect of Vanadium on USY Zeolites and FCC Catalysts. *Studies in Surface Science and Catalysis*. https://doi.org/10.1016/S0167-2991(08)62013-3
Gambogi, J. (2018). Rare Earths - Mineral Commodity Summaries. *U.S. Geological Survey*.
Gambogi, J. (2020). RARE EARTHS: US Geological Survey, Mineral Commodity Summaries, January 2020. In *Mineral Commodity Summaries*.
Gupta, G. K., & Krishnamurthy, N. (1992). Extractive metallurgy of rare earths. *International Materials Reviews*. https://doi.org/10.1179/imr.1992.37.1.197
Harter, R. D., & Naidu, R. (2001). An Assessment of Environmental and Solution Parameter Impact on Trace-Metal Sorption by Soils. *Soil Science Society of America Journal*, *65*(3), 597–612. https://doi.org/10.2136/sssaj2001.653597x
Hatch, G. P. (2012). Dynamics in the global market for rare earths. *Elements*. https://doi.org/10.2113/gselements.8.5.341
Houot, R., Cuif, J.-P., Mottot, Y., & Samama, J.-C. (1991). Recovery of Rare Earth Minerals, with Emphasis on Flotation Process. *Materials Science Forum*. https://doi.org/10.4028/www.scientific.net/msf.70-72.301
Housecroft, C., & Sharpe, A. (2012). Inorganic Chemistry (Catherine E. Housecroft and Alan G. Sharpe). In *Pearson*.
Hower, J. C., Eble, C. F., Dai, S., & Belkin, H. E. (2016). Distribution of rare earth elements in eastern Kentucky coals: Indicators of multiple modes of enrichment? *International Journal of Coal Geology*. https://doi.org/10.1016/j.coal.2016.04.009
Hower, J. C., Qian, D., Briot, N. J., Henke, K. R., Hood, M. M., Taggart, R. K., & Hsu-Kim, H. (2018). Rare earth element associations in the Kentucky State University stoker ash. *International Journal of Coal Geology*. https://doi.org/10.1016/j.coal.2018.02.022
Hower, J. C., Ruppert, L. F., & Eble, C. F. (1999). Lanthanide, yttrium, and zirconium anomalies in the Fire Clay coal bed, Eastern Kentucky. *International Journal of Coal Geology*, *39*(1–3), 141–153. https://doi.org/10.1016/S0166-5162(98)00043-3
HU, G., FENG, Z., DONG, J., MENG, X., XIAO, Y., & LIU, X. (2017). Mineral properties and leaching characteristics of volcanic weathered crust elution-deposited rare earth ore. *Journal of Rare Earths*, *35*(9), 906–910. https://doi.org/10.1016/S1002-0721(17)60993-1
Ingri, J., Widerlund, A., Land, M., Gustafsson, Ö., Andersson, P., & Öhlander, B. (2000). Temporal variations in the fractionation of the rare earth elements in a boreal river; the role of colloidal particles. *Chemical Geology*, *166*(1), 23–45. https://doi.org/https://doi.org/10.1016/S0009-2541(99)00178-3
Jozanikohan, G., Sahabi, F., Norouzi, G. H., Memarian, H., & Moshiri, B. (2016). Quantitative analysis of the clay minerals in the Shurijeh Reservoir Formation using combined X-ray analytical techniques. *Russian Geology and Geophysics*. https://doi.org/10.1016/j.rgg.2016.06.005
Kao, H. C., Yen, P. S., & Juang, R. S. (2006). Solvent extraction of La(III) and Nd(III) from nitrate solutions with 2-ethylhexylphosphonic acid mono-2-ethylhexyl ester. *Chemical Engineering Journal*, *119*(2–3), 167–174. https://doi.org/10.1016/j.cej.2006.03.024
King, J. F., Taggart, R. K., Smith, R. C., Hower, J. C., & Hsu-Kim, H. (2018). Aqueous acid and alkaline extraction of rare earth elements from coal combustion ash. *International Journal of Coal Geology*. https://doi.org/10.1016/j.coal.2018.05.009
Kumari, A., Panda, R., Jha, M. K., Kumar, J. R., & Lee, J. Y. (2015). Process development to recover rare earth metals from monazite mineral: A review. *Minerals Engineering*, *79*, 102–115. https://doi.org/10.1016/j.mineng.2015.05.003
Land, L. S. (1984). Frio sandstone diagenesis, Texas Gulf Coast: a regional isotopic study. *Clastic Diagenesis*, 47–62.
Laudal, D. A., Benson, S. A., Addleman, R. S., & Palo, D. (2018). Leaching behavior of rare earth elements in Fort Union lignite coals of North America. *International Journal of Coal Geology*, *191*(March), 112–124. https://doi.org/10.1016/j.coal.2018.03.010
Long, K. R., Van Gosen, B. S., Foley, N. K., & Cordier, D. (2012). The principal rare earth elements

deposits of the United States: A summary of domestic deposits and a global perspective. *Non-Renewable Resource Issues: Geoscientific and Societal Challenges*, 131–155. https://doi.org/10.1007/978-90-481-8679-2_7

Luttrell, G. H., Kiser, M. J., Yoon, R. H., Noble, A., Rezaee, M., Bhagavatula, A., & Honaker, R. Q. (2019). A Field Survey of Rare Earth Element Concentrations in Process Streams Produced by Coal Preparation Plants in the Eastern USA. *Mining, Metallurgy and Exploration*. https://doi.org/10.1007/s42461-019-00124-5

Lyons, P. C. (1992). An Appalachian isochron: a kaolinized Carboniferous air-fall volcanic-ash deposit (tonstein). *Geological Society of America Bulletin*, *104*(11), 1515–1527. https://doi.org/10.1130/0016-7606(1992)104<1515:AAIAKC>2.3.CO;2

Mayfield, D. B., & Lewis, A. S. (2013). Environmental Review of Coal Ash as a Resource for Rare Earth and Strategic Elements. *2013 World of Coal Ash (WOCA) Conference*.

Meunier, A. (2005). Clays. In *Clays*. https://doi.org/10.1007/b138672

Moldoveanu, G. A., & Papangelakis, V. G. (2016). An overview of rare-earth recovery by ion-exchange leaching from ion-adsorption clays of various origins. *Mineralogical Magazine*, *80*(1), 63–76. https://doi.org/10.1180/minmag.2016.080.051

Moldoveanu, Georgiana A., & Papangelakis, V. G. (2012). Recovery of rare earth elements adsorbed on clay minerals: I. Desorption mechanism. *Hydrometallurgy*, *117–118*, 71–78. https://doi.org/10.1016/j.hydromet.2012.02.007

Moldoveanu, Georgiana A., & Papangelakis, V. G. (2013). Recovery of rare earth elements adsorbed on clay minerals: II. Leaching with ammonium sulfate. *Hydrometallurgy*. https://doi.org/10.1016/j.hydromet.2012.10.011

National Research Council (U.S.). Committee on Coal Waste Impoundments. (2002). *Coal waste impoundments : risks, responses, and alternatives* (NV-1 onl). National Academy Press. http://site.ebrary.com/id/10068515

Papangelakis, V. G., & Moldoveanu, G. A. (2014). Recovery of Rare Earth Elements From Clay Minerals. *ERES 2014:1st European Rare Earth Resources Conference*, 191–202.

Pradip, & Fuerstenau, D. W. (1991). The role of inorganic and organic reagents in the flotation separation of rare-earth ores. *International Journal of Mineral Processing*, *32*(1–2), 1–22. https://doi.org/10.1016/0301-7516(91)90016-C

Preston, J. S., Cole, P. M., Craig, W. M., & Feather, A. M. (1996). The recovery of rare earth oxides from a phosphoric acid by-product. Part 1: Leaching of rare earth values and recovery of a mixed rare earth oxide by solvent extraction. *Hydrometallurgy*. https://doi.org/10.1016/0304-386X(95)00051-H

Qiu, T., Yan, H., Li, J., Liu, Q., & Ai, G. (2018). Response surface method for optimization of leaching of a low-grade ionic rare earth ore. *Powder Technology*. https://doi.org/10.1016/j.powtec.2018.02.044

Ran, X., Ren, Z., Gao, H., Zheng, R., & Jin, J. (2017). Kinetics of rare earth and aluminum leaching from kaolin. *Minerals*. https://doi.org/10.3390/min7090152

Rebertus, R. A., Weed, S. B., & Buol, S. W. (1986). Transformations of Biotite to Kaolinite During Saprolite-Soil Weathering. *Soil Science Society of America Journal*, *50*(3), 810–819. https://doi.org/10.2136/sssaj1986.03615995005000030049x

Rozelle, P. L., Khadilkar, A. B., Pulati, N., Soundarrajan, N., Klima, M. S., Mosser, M. M., Miller, C. E., & Pisupati, S. V. (2016). A Study on Removal of Rare Earth Elements from U.S. Coal Byproducts by Ion Exchange. *Metallurgical and Materials Transactions E*, *3*(1), 6–17. https://doi.org/10.1007/s40553-015-0064-7

Scott, C., Deonarine, A., Kolker, A., Adams, M., & Holland, J. (2015). Size Distribution of Rare Earth Elements in Coal Ash. *World of Coal Ash*.

Seredin, V. V., & Dai, S. (2012). Coal deposits as potential alternative sources for lanthanides and yttrium. In *International Journal of Coal Geology*. https://doi.org/10.1016/j.coal.2011.11.001

Shan, X. quan, Lian, J., & Wen, B. (2002). Effect of organic acids on adsorption and desorption of rare earth elements. *Chemosphere*, *47*(7), 701–710. https://doi.org/10.1016/S0045-6535(02)00032-2

Shi, J., & Yordan, J. (1997). *United States Patent (19) 11 Patent Number: 5,348,136*.
Siebert, R. M., Moncure, G. K., & Lahann, R. W. (1984). *A Theory of Framework Grain Dissolution in Sandstones: Part 2. Aspects of Porosity Modification*. *59*, 163–175.
Steefel, C. I., & Van Cappellen, P. (1990). A new kinetic approach to modeling water-rock interaction: The role of nucleation, precursors, and Ostwald ripening. *Geochimica et Cosmochimica Acta*, *54*(10), 2657–2677. https://doi.org/10.1016/0016-7037(90)90003-4
Sulaiman, M. Y. (1991). An Overview of the Rare-Earth Mineral Processing Industry in Malaysia. *Materials Science Forum*. https://doi.org/10.4028/www.scientific.net/msf.70-72.389
Taggart, R. K., Hower, J. C., & Hsu-Kim, H. (2018). Effects of roasting additives and leaching parameters on the extraction of rare earth elements from coal fly ash. *International Journal of Coal Geology*. https://doi.org/10.1016/j.coal.2018.06.021
Teppen, B. J., & Miller, D. M. (2006). Hydration Energy Determines Isovalent Cation Exchange Selectivity by Clay Minerals. *Soil Science Society of America Journal*, *70*(1), 31–40. https://doi.org/10.2136/sssaj2004.0212
Van Gosen, Bradley S ; Philip L. Verplanck, R. R. S. I. K. R. L., & Gambogi, J. (2017). *Critical mineral resources of the United States— Economic and environmental geology and prospects for future supply:* https://doi.org/10.3133/pp1802O.
Wang, L., Liao, C., Yang, Y., Xu, H., Xiao, Y., & Yan, C. (2017). Effects of organic acids on the leaching process of ion-adsorption type rare earth ore. *Journal of Rare Earths*. https://doi.org/10.1016/j.jre.2017.07.001
Ward, C. R. (2002). Analysis and significance of mineral matter in coal seams. *International Journal of Coal Geology*. https://doi.org/10.1016/S0166-5162(02)00117-9
Xiao, Y., Huang, L., Long, Z., Feng, Z., & Wang, L. (2016). Adsorption ability of rare earth elements on clay minerals and its practical performance. *Journal of Rare Earths*. https://doi.org/10.1016/S1002-0721(16)60060-1
Xiao, Y., Liu, X., Feng, Z., Huang, X., Huang, L., Chen, Y., & Wu, W. (2015). Role of minerals properties on leaching process of weathered crust elution-deposited rare earth ore. *Journal of Rare Earths*. https://doi.org/10.1016/S1002-0721(14)60454-3
Xie, F., Zhang, T. A., Dreisinger, D., & Doyle, F. (2014). A critical review on solvent extraction of rare earths from aqueous solutions. In *Minerals Engineering*. https://doi.org/10.1016/j.mineng.2013.10.021
Yang, L., Li, C., Wang, D., Li, F., Liu, Y., Zhou, X., Liu, M., Wang, X., & Li, Y. (2019). Leaching ion adsorption rare earth by aluminum sulfate for increasing efficiency and lowering the environmental impact. *Journal of Rare Earths*, *37*(4). https://doi.org/10.1016/j.jre.2018.08.012
Zhang, W., Rezaee, M., Bhagavatula, A., Li, Y., Groppo, J., & Honaker, R. (2015). A review of the occurrence and promising recovery methods of rare earth elements from coal and coal by-products. *International Journal of Coal Preparation and Utilization*, *35*(6), 295–330. https://doi.org/10.1080/19392699.2015.1033097
Zhang, W., Yang, X., & Honaker, R. Q. (2018). Association characteristic study and preliminary recovery investigation of rare earth elements from Fire Clay seam coal middlings. *Fuel*. https://doi.org/10.1016/j.fuel.2017.11.075